NOAA TECHNICAL MEMORANDUM NWS CR-111

GLOBAL MODEL ERRORS ASSOCIATED WITH RAPID LOW TO HIGH ZONAL WAVE NUMBER TRANSITIONS

Edward K. Berry
National Weather Service
Central Region Headquarters
Scientific Services Division
Kansas City, Missouri

John A. McGinley and Paul Schultz
NOAA Forecast Systems Laboratory
Boulder, Colorado

March 1996

U.S DEPARTMENT OF Commerce / National Oceanic and Atmospheric Administration / National Weather Service

NOAA TECHNICAL MEMORANDA
National Weather Service, Central Region Subseries

The National Weather Service Central Region (CR) subseries provides an informal medium for the documentation and quick dissemination of results not appropriate, or not yet ready, for formal publication. The series is used to report on work in progress, to describe technical procedures and practices, or to relate progress to a limited audience. These Technical Memoranda report on investigations devoted primarily to regional and local problems of interest mainly to regional personnel, and hence will not be widely distributed.

Papers 1 through 15 are in the former series, ESSA Technical Memoranda, Central Region Technical Memoranda (CRTM); Papers 16 through 36 are in the former series, ESSA Technical Memoranda, Weather Bureau Technical Memoranda (WBTM). Beginning with Paper 37, the papers are part of the series, NOAA Technical Memoranda NWS.

Papers that have a PB or COM number are available from the National Technical Information Service, U. S. Department of Commerce, 5285 Port Royal Road, Springfield, VA 22151. Order by accession number shown in parenthesis at the end of each entry. Prices vary for all paper copies. Microfiche are $4.50. All other papers are available from the National Weather Service Central Region, Scientific Services, Room 1836, 601 East 12th Street, Kansas City, MO 64106.

ESSA Technical Memoranda

CRTM 1 Precipitation Probability Forecast Verification Summary Nov. 1965 - Mar. 1966, SSD Staff, WBCRH, May 1966.

CRTM 2 A Study of Summer Showers Over the Colorado Mountains. William G. Sullivan, Jr., and James O. Severson, June 1966.

CRTM 3 Areal Shower Distribution - Mountain Versus Valley Coverage. William G. Sullivan, Jr., and James O. Severson, June 1966.

CRTM 4 Heavy Rains in Colorado June 16 and 17, 1965. SSD Staff, WBCRH, July 1966.

CRTM 5 The Plum Fire. William G. Sullivan, Jr., August 1966.

CRTM 6 Precipitation Probability Forecast Verification Summary Nov. 1965 - July 1966. SSD Staff, WBCRH, September 1966.

CRTM 7 Effect of Diurnal Weather Variations on Soybean Harvest Efficiency. Leonard F. Hand, October 1966.

CRTM 8 Climatic Frequency of Precipitation at Central Region Stations. SSD Staff, WBCRH, November 1966.

CRTM 9 Heavy Snow or Glazing. Harry W. Waldheuser, December 1966.

CRTM 10 Detection of a Weak Front by WSR-57 Radar. G. W. Polensky, December 1966.

CRTM 11 Public Probability Forecasts. SSD Staff, WBCRH, January 1967.

CRTM 12 Heavy Snow Forecasting in the Central United States (an Interim Report). SSD Staff, January 1967.

CRTM 13 Diurnal Surface Geostrophic Wind Variations Over the Great Plains. Wayne E. Sangster, March 1967.

CRTM 14 Forecasting Probability of Summertime Precipitation at Denver. Wm. G. Sullivan, Jr., and James O. Severson, March 1967.

CRTM 15 Improving Precipitation Probability Forecasts Using the Central Region Verification Printout. Lawrence A. Hughes, May 1967.

WBTM CR 16 Small-Scale Circulations Associated with Radiational Cooling. Jack R. Cooley, June 1967.

WBTM CR 17 Probability Verification Results (6-month and 18-month). Lawrence A. Hughes, June 1967.

WBTM CR 18 On the Use and Misuse of the Brier Verification Score. Lawrence A. Hughes, August 1967 (PB 175 771).

WBTM CR 19 Probability Verification Results (24 months). Lawrence A. Hughes, February 1968.

WBTM CR 20 Radar Prediction of the Topeka Tornado. Norman E. Prosser, April 1968.

WBTM CR 21 Wind Waves on the Great Lakes. Lawrence A. Hughes, May 1968.

WBTM CR 22 Seasonal Aspects of Probability Forecasts: 1. Summer. Lawrence A. Hughes, June 1968 (PB 185 733).

WBTM CR 23 Seasonal Aspects of Probability Forecasts: 2. Fall. Lawrence A. Hughes, September 1968 (PB 185 734).

WBTM CR 24 The Importance of Areal Coverage in Precipitation Probability Forecasting. John T. Curran and Lawrence A. Hughes, September 1968.

WBTM CR 25 Meteorological Conditions as Related to Air Pollution, Chicago, Illinois, April 12-13, 1963. Charles H. Swan, October 1968.

WBTM CR 26 Seasonal Aspects of Probability Forecasts: 3. Winter. Lawrence A. Hughes, December 1968 (PB 185 735).

WBTM CR 27 Seasonal Aspects of Probability Forecasts: 4. Spring. Lawrence A. Hughes, February 1969 (PB 185 736).

WBTM CR 28 Minimum Temperature Forecasting During Possible Frost Periods at Agricultural Weather Stations in Western Michigan. Marshall E. Soderberg, March 1969.

WBTM CR 29 An Aid for Tornado Warnings. Harry W. Waldheuser and Lawrence A. Hughes, April 1969.

WBTM CR 30 An Aid in Forecasting Significant Lake Snows. H. J. Rothrock, November 1969.

WBTM CR 31 A Forecast Aid for Boulder Winds. Wayne E. Sangster, February 1970.

WBTM CR 32 An Objective Method for Estimating the Probability of Severe Thunderstorms. Clarence L. David, February 1970.

WBTM CR 33 Kentucky Air-Soil Temperature Climatology. Clyde B. Lee, February 1970.

WBTM CR 34 Effective Use of Non-Structural Methods in Water Management. Verne Alexander, March 1970.

WBTM CR 35 A Note on the Categorical Verification of Probability Forecasts. Lawrence A. Hughes and Wayne E. Sangster, August 1970.

WBTM CR 36 A Comparison of Observed and Calculated Urban Mixing Depths. Donald E. Wuerch, August 1970.

NOAA Technical Memoranda NWS

NWS CR 37 Forecasting Maximum and Minimum Surface Temperatures at Topeka, Kansas, Using Guidance from the PE Numerical Prediction Model (FOUS). Morris S. Webb, Jr., November 1970 (COM 71 00118).

NWS CR 38 Snow Forecasting for Southeastern Wisconsin. Rheinhart W. Harms, November 1970 (COM 71-00019).

NWS CR 39 A Synoptic Climatology of Blizzards on the North-Central Plains of the United States. Robert E. Black, February 1971 (COM 71-00369).

NWS CR 40 Forecasting the Spring 1969 Midwest Snowmelt Floods. Herman F. Mondschein, February 1971 (COM 71-00489).

NWS CR 41 The Temperature Cycle of Lake Michigan 1. (Spring and Summer). Lawrence A. Hughes, April 1971 (COM 71-00545).

NWS CR 42 Dust Devil Meteorology. Jack R. Cooley, May 1971 (COM 71-00628).

NWS CR 43 Summer Shower Probability in Colorado as Related to Altitude. Alois G. Topil, May 1971 (COM 71-00712).

NWS CR 44 An Investigation of the Resultant Transport Wind Within the Urban Complex. Donald E. Wuerch, June 1971 (COM 71- 00766).

NWS CR 45 The Relationship of Some Cirrus Formations to Severe Local Storms. William E. Williams, July 1971 (COM 71- 00844).

NWS CR 46 The Temperature Cycle of Lake Michigan 2. (Fall and Winter). Lawrence A. Hughes, September 1971 (COM 71-01039).

(Continued on Back Cover)

NOAA TECHNICAL MEMORANDUM NWS CR-111

GLOBAL MODEL ERRORS ASSOCIATED WITH RAPID LOW TO HIGH ZONAL WAVE NUMBER TRANSITIONS

Edward K. Berry
National Weather Service
Central Region Headquarters
Scientific Services Division
Kansas City, Missouri

John A. McGinley and Paul Schultz
NOAA Forecast Systems Laboratory
Boulder, Colorado

March 1996

UNITED STATES DEPARTMENT OF COMMERCE
Ronald H. Brown
Secretary

National Oceanic and Atmospheric Administration
D. James Baker
Under Secretary

National Weather Service
Elbert W. Friday, Jr.
Assistant Administrator

Table of Contents

GLOBAL MODEL ERRORS ASSOCIATED WITH RAPID LOW TO HIGH ZONAL WAVE NUMBER TRANSITIONS

Edward K. Berry
NOAA, National Weather Service
Central Region, Scientific Services Division
Kansas City, Missouri

John A. McGinley and Paul Schultz
NOAA Forecast Systems Laboratory
Boulder, Colorado

ABSTRACT

A very significant and energetic atmospheric behavior that is important to all meteorologists (including those doing operational forecasting) is northern hemispheric-scale low (waves 0-3) to high (5 or greater; wave 4 can act as either high or low) zonal wave number transitions (also called "breakdowns"). The breakdowns are most frequent during the spring and fall and least likely to occur in the summer.

Large forecast errors in the operational global models (MRF, ECMWF and UKMET) often occur during these transitions. The purpose of this report is to present an observationally formulated qualitative conceptual model of low to high zonal wave number transitions, then give statistical results to verify the forecast errors that do occur in the MRF model (version of this model before the October 1995 changes).

Forecasts from the other operational global medium-range NWP models were not available for this study (work is ongoing with the other models). The errors are believed to be related to the transitions.

Discussion is restricted to the northern hemisphere. In brief, a typical behavior of these transitions is the following. The westerlies start at a relatively high latitude either with a wave 0 or low amplitude wave 2 structure. The westerlies then come south, expand across the North Pacific Ocean Basin, favoring a positive phase of the PNA. At this stage, there is often a wave 3 structure of the westerlies.

Then, in no more than a matter of a few days, rapid amplification occurs. For the U.S., a deep mid and upper tropospheric trough often forms between 95° and 120°W, as part of a zonal wave 5 or higher regime (the locations of the "other troughs" are given in the conceptual model). Result can be destructive

severe weather of all types over a large portion of the U.S., especially in the Plains States, without much forecast lead-time. To stay within the scope of this paper, discussion back to low wave number is very limited (topic of future work).

Research is planned to quantify the dynamics of these wave number transitions including formulating several diagnostic and statistical tools, developing a climatology of the breakdowns and computing forecast error more completely (including other global models such as ECMWF and UKMET). Some preliminary results are given in the text. However, more conclusive evidence is planned to be reported in future publications. The goals of this work are not only to improve understanding and predictability, but also products and services to the users (public).

1. INTRODUCTION

A significant atmospheric mode of behavior that is important to all meteorologists (including those doing operational forecasting) is northern hemispheric-scale low (zonal wave numbers 0-3) to high zonal wave number (5 or greater; wave 4 can act as either high or low) transition events (also called "breakdowns" in this paper; Weng and Barcilon 1988). Besides these events being, at times, prolific significant and severe weather "producers" of all types, especially for the central United States, these low to high wave number transitions often lead to substantial errors and inconsistencies in the operational global medium-range numerical weather prediction (NWP) models (the transitions have low predictability).

The errors are for all forecast fields at all model levels, irrelevant of the vertical coordinates. Further, these errors can become quite large even after day 2, and thus certainly have an impact on any forecaster preparing a 3-5 or 4-7 day prediction. At the least, in these situations, forecaster confidence would be low for any medium-range prediction.

These models include the Global Spectral Medium Range Forecast (MRF) (White 1988a, b) model generated by the U.S. National Meteorological Center (NMC; currently NCEP, the National Centers for Environmental Prediction), the model produced by European Centre for Medium Range Weather Forecasts (ECMWF; Bengtsson 1985) and the one produced by the United Kingdom Meteorological Office (UKMET). "Short-range" models, like the operational NCEP NGM (Hoke et al. 1989) and ETA (Messinger et al. 1988) models, are not "immune" to the forecast errors caused by wave number transitions.

The purpose of this report is to present a qualitative conceptual model of the low to high zonal wave number transitions, based on observation, and then give statistical results to verify that this mode of atmospheric low frequency variability (LFV) can introduce forecast error in the MRF model. A goal is to

give operational forecasters signals to observe, a priori, when to expect relatively poor numerical model performance, due to wave number transitions. Although somewhat related, the concepts in this manuscript should not be confused with work done on predicting forecast skill (Wobus and Kalnay 1993, and references therein).

A few cases are given to illustrate wave number transitions. As will be seen, these events frequently involve zonal wave 3 to wave 5 but can include, for example, 2 to 5, 2 to 6, and 3 to 7. Model errors can occur from high to low transitions, but for the purposes and scope of this study, the focus is on the reverse.

Before going any farther, an important caveat needs to be addressed. Again, for simplicity, much of the discussion is restricted to zonal wave number space. This is so, because it is very difficult for many to visualize spherical harmonics of the northern hemispheric westerlies in real-time. However, in reality, it must be understood that two dimensional (total) wave number (zonal and meridional) thinking is more appropriate (and there is quantification work going on with total wave numbers).

Relatively speaking, very little information on low to high transitions can be found in the technical literature (Berry et al. 1993 for a brief treatment on this subject). *Therefore, this report is intended to serve as a vehicle to introduce this concept to the meteorological community, especially those involved with operations.*

It is emphasized that the motivation for this study is to both assist in the improvement and utilization of the very sophisticated operational NWP global models (for example, Tracton and Kalnay (1993) and references therein on ensemble forecasting) currently being generated in real-time at NCEP, and provide help to field forecasters in modifying the models when wave transitions are occurring. As will be shown, these events often lead to major baroclinic development from the Rocky Mountains to the Central states of the U.S. Often these breakdowns place an energetic mid/upper tropospheric trough in the height field west of the Mississippi River.

Even though a good understanding of planetary-wave theory is essential to more fully understanding the dynamics of low to high transitions, a review of this theory is not in the purpose of this report. Some of these ideas include baroclinic and barotropic dynamics (for example: Holton 1992), teleconnections (Glantz et al. 1991), and the physics of the low and high index phases of the Southern Oscillation (Trenberth 1991, Philander 1989, Horel and Wallace 1981). Also believed to be important are the dynamics of tropical-mid latitude interactions, including that due to the tropical 30- to 60-day oscillation (Weickmann 1983, Weickmann et al. 1985, 1990, Kiladis and Weickmann 1992a, 1992b), and energetics (Holton 1992, Chen 1982, Chen and Shukla 1983).

However, several easily accessible basic references (like was given above) relevant to the discussion will be cited during the course of the text. In addition, sufficient explanation will be given, where needed.

Section 2 presents a conceptual model of low-to-high breakdown, followed by Section 3 which addresses three case studies of these events. Also shown in Section 3, with the case studies, are the results from a very recently developed spectral and Hovmöller diagnostic package to help assess them.

In Section 4 statistical results are presented to show the correlation between MRF errors (before the October 1995 upgrade; TPB#128) and wave number transitions events. Finally, given in Section 5 are the conclusions drawn from this study.

2. CONCEPTUAL MODEL OF LOW TO HIGH WAVE NUMBER TRANSITIONS

A. Preliminaries

Low-to-high wave number transitions are believed to be just one of many modes of low-frequency variability (LFV; Holton 1992, Wallace and Blackmon 1983) operating in the atmosphere. These are variabilities that occur on time-scales longer than synoptic. Synoptic-scale variabilities, such as the high frequency behaviors due to transient eddies on the storm track associated with the polar jet stream, occur on a time-scale from about 2.5 to 6 days (Holopainen 1983). LFVs occur on time-scales ranging from about a week to a few months (Holton 1992, Wallace and Blackmon 1983).

Observationally, low to high transitions generally occur with intervals varying anywhere from a week to possibly three months. In general, the longer the period between breakdowns, the more significant that event will be, in terms of the amplitude of the high wave mode. The most energetic breakdowns on the northern hemispheric-scale (we will not consider the southern hemisphere in this report) may occur with a period that is compatible the intraseasonal time-scale, about 30- to 60-days. Whether this is the result of tropical-mid latitude coupling forced by the Madden-Julian Oscillation (MJO; Madden and Julian 1972) is open for debate and further research. Finally, low to high zonal wave number breakdowns are most likely to occur during the transition seasons of spring and fall, and least likely to happen during the summer.

The reader may, at this point ask, "how can there be any predictability of these transitions?". Diagnostic tools and ensemble forecasting techniques are believed to be helpful.

Diagnostic techniques include spectral analysis and energetics packages (above references), transformed Eulerian diagnostics (Pfeffer 1992), diagnostically

applying Rossby ray tracing theory (Hoskins and Karoly 1981), various forms of Hovmöller charts (Hovmöller 1949), etc. Ensemble forecasting (Tracton and Kalnay 1993) is a dynamical systems approach that treats the atmosphere just for what it is: nonlinear and chaotic. With the use of statistical tools, a most probable future state of the atmosphere may be realized by a cluster of ensemble members. The ensemble prediction technique may help predict when low to high breakdown will occur and where the locations of the troughs and ridges could become established.

However, during the course of the following text, the intent is to give the reader good observational signals to look for which are independent of the time scales. Recognition of low to high zonal wave number transitions a few days or so in advance can be an effective aid when utilizing the numerical guidance.

B. Discussion

An idealized conceptual model of a low-to-high wave number transition scenario is presented in Figures 1 through 4. These are streamline representations of the 500-mb constant pressure surface, and the flow is assumed to be in gradient wind balance. The intent of these diagrams is to give the reader an overall sense of the projection (or circulation pattern).

Figure 1 is a 500-mb wave number zero flow regime, with the westerlies contracted poleward. Put another way, the figure depicts an overly simplified representation of high-latitude zonal flow.

Considering the multiple time scales involved with these events, the following sequence is generally observed. First, the westerlies start to migrate southward. Then, as shown in Figure 2, a wave 2 flow structure typically evolves. For North America, there is usually a low amplitude full-latitude ridge over the western portion.

Now, a transition from wave 2 to wave 3 occurs, with amplification, shown in Figure 3. A key feature is the expansion of the westerlies longitudinally across the North Pacific Ocean Basin. We see that there is an amplified full-latitude ridge over western North America with a deep trough along the east coast of the U.S. Generally speaking, these features would have greater amplitude than climatology.

Looking at Figure 3 from another perspective, this would be an example of the positive phase of the Pacific North American Teleconnection (PNA; Wallace and Gutzler 1981). In addition, this is a phase of the PNA that can be observed during an El-Nino (Horel and Wallace 1981; also Barnston et al. 1992, and Livezey and Mo 1987 for an excellent discussion of this point, and the importance of the Tropical-Northern Hemisphere (TNH) and West Pacific Oscillation (WPO) "patterns"). The significance of these concepts is discussed below.

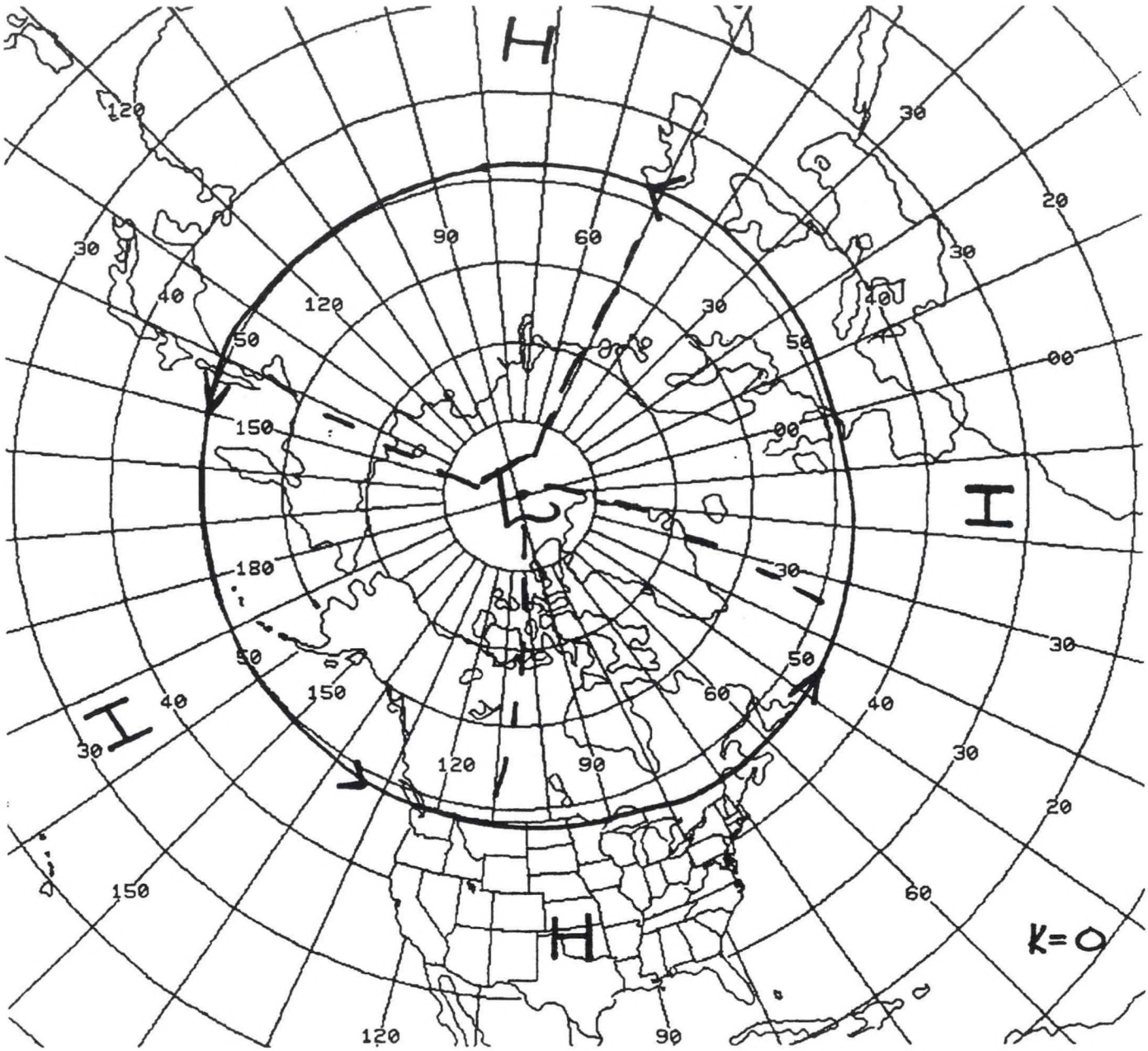

Figure 1. Streamline schematical representation of the 500-mb constant pressure surface, for wave number zero. H's and L's have their usual meanings, and the dashed lines denote low amplitude troughs at higher latitudes.

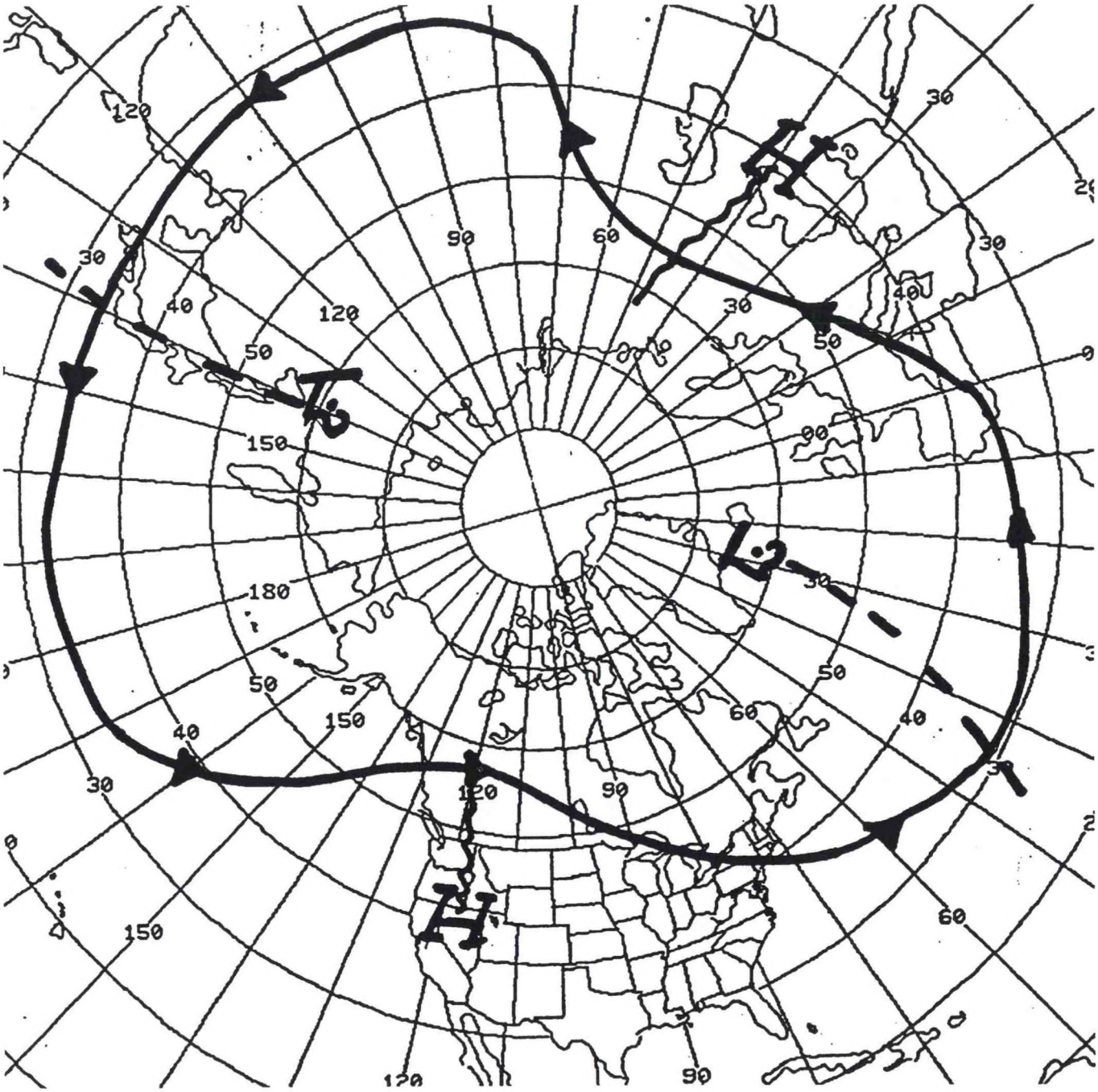

Figure 2. Same as Figure 1, but for wave number 2. "Zig-zag" line denotes a ridge in the 500-mb geopotential height field.

As a matter of note, recent studies by Haines et al. (1993) and Dole and Black (1993) present further examination of the dynamics and synoptic structure of the type of circulation regime depicted in Figure 3. The interested reader can refer to these papers and the references therein.

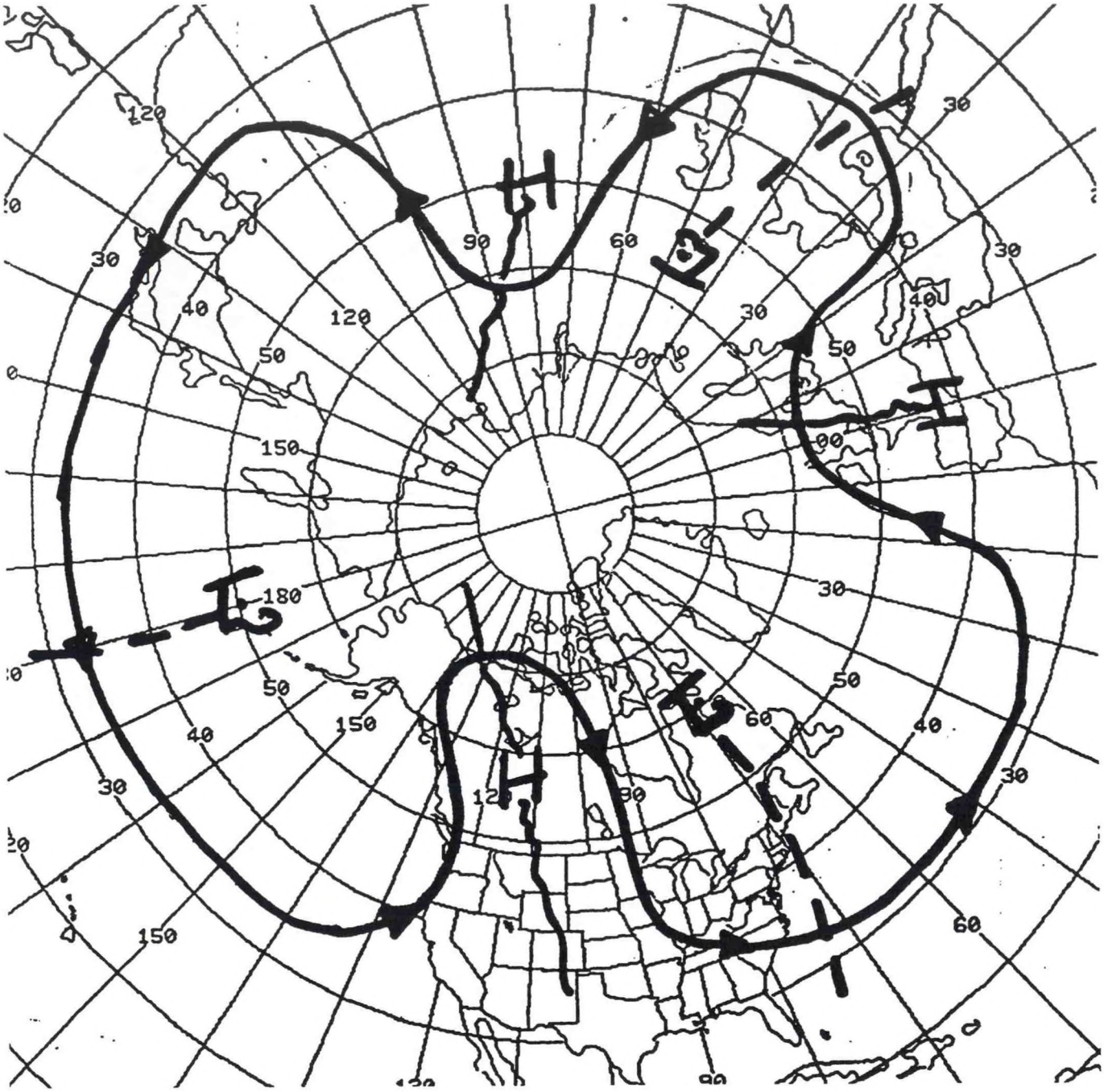

Figure 3. Same as Figure 1, but wave number 3.

Finally, a rapid (almost simultaneous at times) transition from zonal wave number 3 to zonal wave number 5 occurs, with the result being significant baroclinic development of wave 5 around the entire northern hemisphere (Figure 4). It is during the transition period (rapid downscale transfer of kinetic energy) when the greatest NWP errors and inconsistencies usually occur, including the planetary-scale. For the lower 48 states of the U.S., the result is often a deep mid and upper tropospheric trough in the height field across the west and central portions.

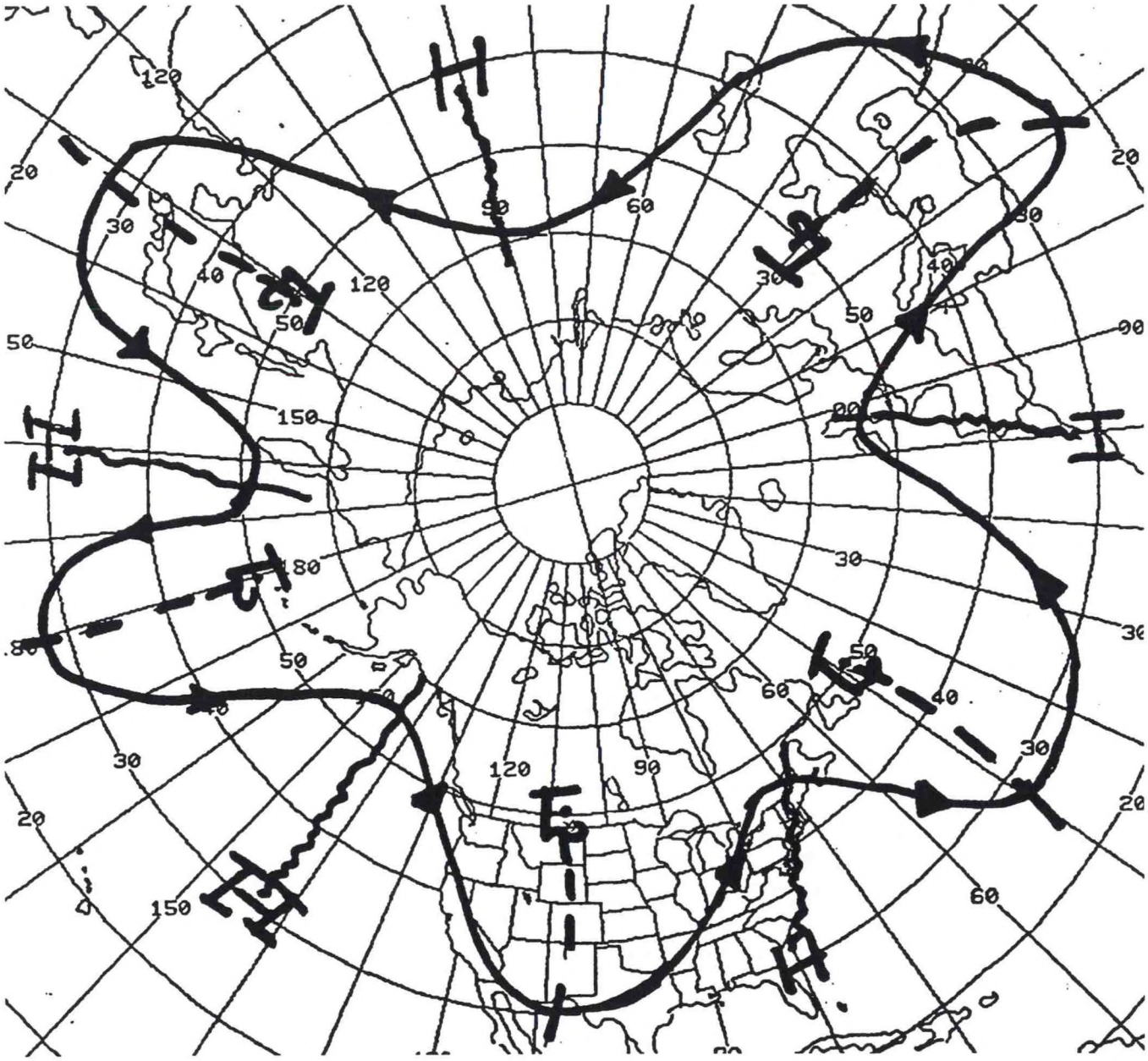

Figure 4. Same as Figure 1, but wave number 5.

More precisely, what often evolves are fully occluded vertically stacked closed lows at the southern end of the troughs. There may also be closed anticyclones in the northern portion of the ridges. At this time, baroclinic development, that is, the conversion of eddy available potential energy (APE) to eddy kinetic energy (KE; Holton 1992, chapters 8 and 10 for good discussion on baroclinic instability and basic energetics) has occurred.

The wave 5 regime then decays, often with the axes of the troughs and ridges becoming northeast to southwest oriented. The closed circulations become open waves during this process. More formally, at this stage, the eddies are

likely giving their KE back to the westerlies and there is a northward transport of westerly angular momentum occurring from the tropics (besides Holton, see Palmen and Newton 1969, on this latter point). Thus the westerlies contract poleward and start to intensify again.

At this stage, a regime (pattern) like that shown in Figures 1 or 2 may re-evolve, or an entirely different circulation structure may appear. For example, a wave 3 favoring an amplifying mid/upper tropospheric geopotential height trough across western North America could develop (a negative or reverse PNA).

Relatively few cases will "perfectly" fit the conceptual model of low to high wave number transitions, as given above. Also, it is not important, for the scope of this work to be concerned about preferred circulation types, trajectories from one state to the other, in phase space (Toth 1993, Kimoto and Ghil 1993a, 1993b), and regime transition. Observational signals of low-to-high wave number transitions are what is emphasized.

As already stated, there are multiple time scales involved with these wave number transitions. However, it is important to point out that when significant breakdowns occur, the event can proceed quickly from low wave to high wave in a matter of 1 to 3 days. Greatest forecast errors of the operational global models usually occur during this period of rapid downscale energy transfer.

The high wave mode may then persist for as long as 1 week, with 2 or 3 major cyclones moving through the western and central U.S. Forecast errors do remain large, but probably less in magnitude than would be seen during the actual transition. Often, each succeeding storm will be farther east. Also, it is not unusual to get significant cyclogenesis along the East coast of the U.S. from the last short-wave trough. In addition, there may, simultaneously, be a great deal of storminess at the locations of the other troughs around the northern hemisphere (Figure 4).

The cause of the multiple time scales is a complex problem. Papers by Weickmann et al. (1985, 1990), Kiladis and Weickmann (1992a and 1992b) and Lyons et al. (1992), which discuss tropical-mid latitude interactions, the 30- to 60-day oscillation and the zonal wind oscillation, present ideas that may be relevant to the dynamics of wave number transitions.

Some mention should also be made of the pioneering work done by Namias (1950). In his work, there was discussion of a 4 to 6 week index cycle. In this report, discussion of transitions from high (generally the low wave mode)-to-low index (the high wave mode), etc., on several time scales of varying magnitudes, are made. Furthermore, in Namias, no mention of specific wave number transitions, including the recurrent locations of features, and tropical-mid latitude interactions were given. Finally, the concepts reported here are only a first

step (of ongoing work) to quantifying a relationship between numerical model forecast error and scale-interaction processes, internal variability dynamics, circulation states, etc. (understanding that sensitivity to initial conditions is important; Toth and Kalnay (1993)). One goal is to be able to predict wave number transitions with at least 2 or 3 days lead time.

This paper should be viewed as a practical extension of the pioneering effort on extratropical vacillation/index cycles. Also, wave number transitions are not "cycles", and are not to be confused with wave number vacillation (Weng and Barcilon 1988).

Finally, before going on to actual cases, a brief hypothesis of low to high zonal wave transitions using some physical reasoning and further refinement of observational signals are given. Let us start by briefly mentioning climatology. That is important because significant departure from climatology occur during low to high breakdowns and these departures can be used as forecast tools.

Figure 5 is a depiction of the 500-mb geopotential height contours for January. Since most breakdowns occur during the cold season (roughly September through May), Figure 5 should be representative for our purposes. Because of the background forcing onto the northern hemispheric westerlies due to land-sea heating contrasts, orography, sea surface temperatures, etc., there is more or less a mean wave 3 distribution of geopotential height. There are full-latitude troughs at around 140°E, 80°W, and 30°E. Other features should be apparent to the reader.

Knowing that Figures 1 through 4 just showed streamlines, it can be seen that Figures 3 and 4 have significantly more amplitude than climatology. Figure 6 is a regime diagram derived from Fultz's annulus experiments (Holton 1992, 1979). See the caption for details. For the sake of argument, assume the vertical line is the Earth's rotation rate. Given a constant rotation rate, what is important to recognize is that the greater the zonally averaged meridional temperature gradient, the lower the zonal wave number of the dominant mode (ex. waves 1 through 3).

The greatest baroclinicity around the northern hemisphere is associated with the lowest zonal wave numbers. Now, as we progress through the evolution illustrated in Figures 1 through 4, the baroclinic mode most favored will be established by the ambient mean meridional temperature gradient (as shown in Figure 6). The wave 2 to 3 transition implies a reduction over time of mean baroclinicity due to "eddy" mixing.

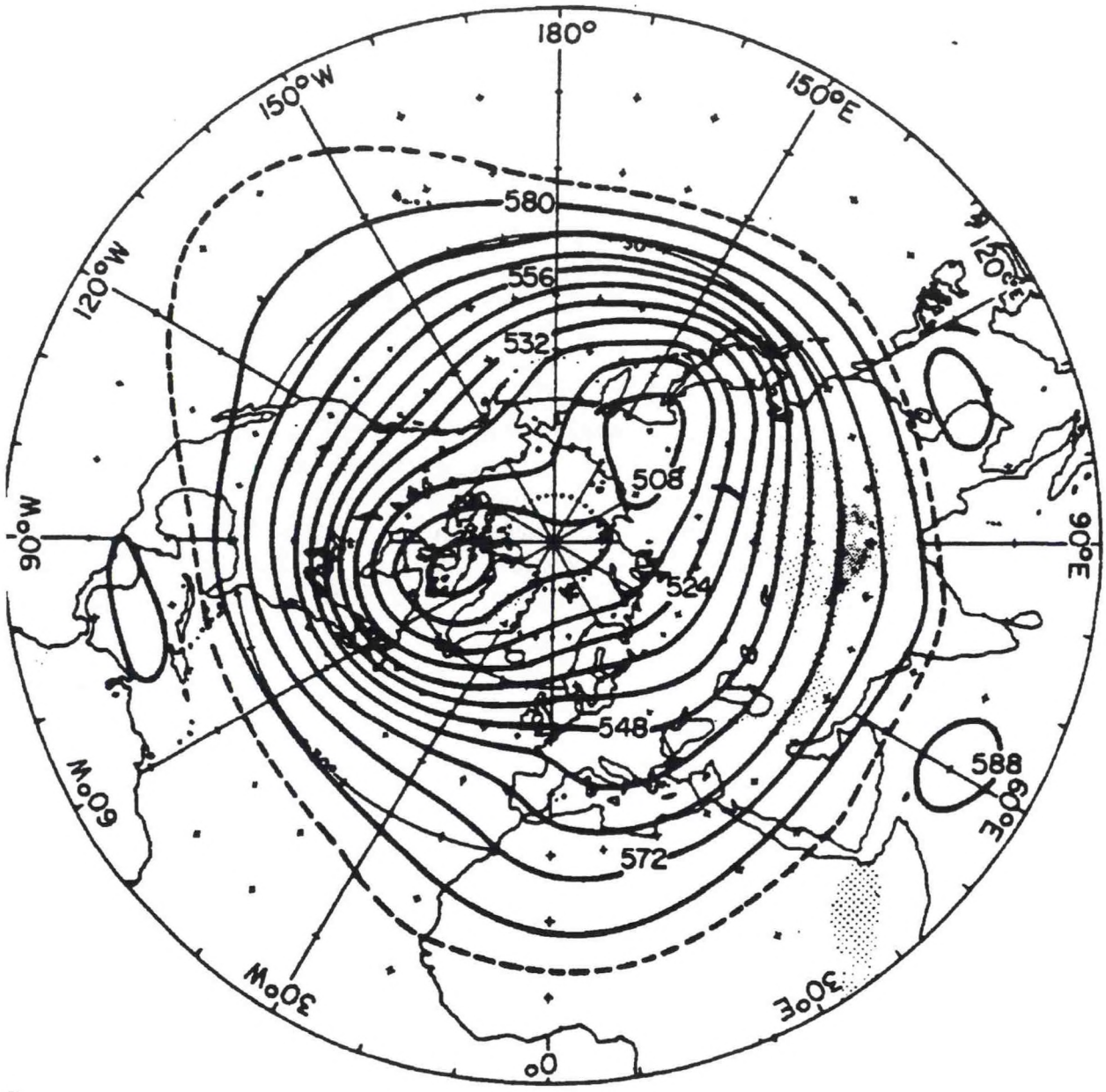

Figure 5. Mean 500-mb contours in January, northern hemisphere. Heights shown in tens of meters. (After Palmen and Newton 1969.) (Figure taken from Holton 1992.)

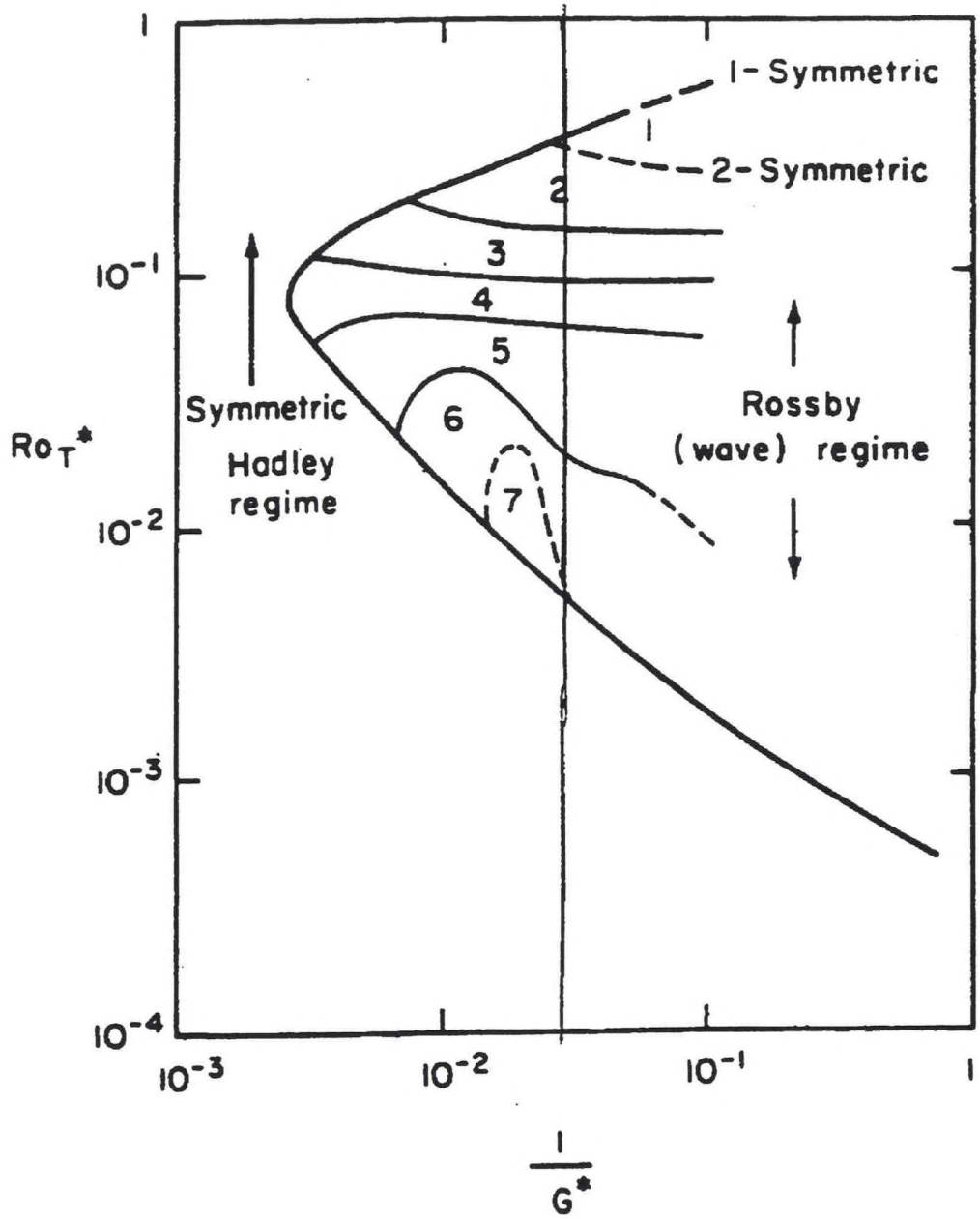

Figure 6. Regime diagram for Fultz's annulus experiments (after Phillips 1963.) (Figure taken from Holton 1992.). The abscissa can be thought of as a measure of the earth's rotation rate while the ordinate can be viewed as a measure of the meridional temperature gradient. The vertical line is drawn to represent the rotation rate of the earth, in the context of the annulus experiment. The numbers are non-dimensional.

Referring to Figure 3, let's suppose there is baroclinic development involving wave 3. That would imply a decrease in the temperature gradient. Hence, decrease north to south temperature gradient, increase the zonal wave number of the dominant wave. Based on observation only, often there is a transition from wave 3 to wave 5 after this development.

All of the above is one "simple minded" conceptual way to understand wave number transition. What about the growth rates of individual wave numbers?. Figure 7 is a diagram taken from a paper by Weng and Barcilon (1988). Here we see that the most unstable mode is highly influenced by static stability. As stability decreases maximum growth rates will occur at successively higher wave numbers allowing each to be the dominant mode.

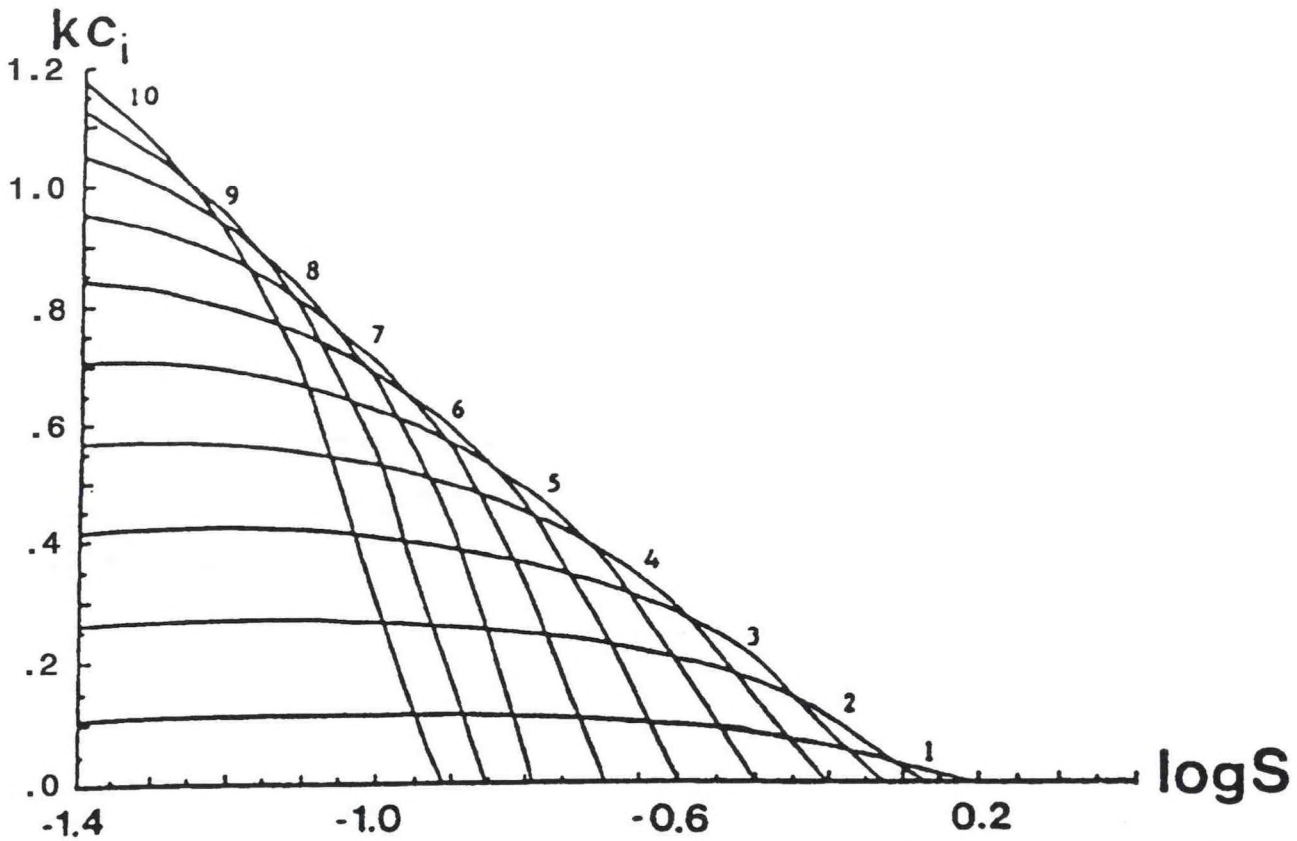

Figure 7. Growth rate diagram (from Weng and Barcilon 1987). The abscissa can be thought of as static stability and the ordinate represents growth rate. The numbers are non-dimensional.

Now, referring back to Figure 3, note that when the westerlies longitudinally expand across the Pacific, large expanses of cold continental air north of the polar jet will be advected over a relatively warm sea surface. The result is destablization of the lower and mid troposphere due to the fluxes of sensible and diabatic heat, including moisture.

Putting the concepts shown in Figures 6 and 7 together, what results are that the higher wave numbers end up with the fastest growth rates. The "jump" from 3 to 5, instead of a nice progression of 3 to 4 to 5, may be due to the sudden destablization of the troposphere as discussed above. Based on these observations, and other considerations that are topics of future work, the most

energy efficient zonal wave numbers vary from 4 through 7, with 5 and 6 perhaps the most common (Cai 1992 for a more complete treatment of energetically efficient vs. the most baroclinically unstable wave).

For the sake of completeness, some mention should be made of the concept of group velocity and the downstream propagation of baroclinic energy. Much has been published in the literature on this topic (for example: Simmons and Hoskins 1979, Krishnamurti et al. 1977, Clark 1979) and forms the basis of utilizing Hovmöller diagrams ("Hovs") (Hovmöller 1949). Suffice to say that the dynamics of low to high wave number transitions are believed to be far more complicated than downstream (or upstream) propagation. It is believed that dynamical processes such as Rossby wave energy dispersion on a sphere (Hoskins and Karoly 1981), which involve at least two dimensional wave numbers (zonal and meridional), are involved with low to high breakdowns. Since that may be the case, Hovs (at least for 2-dimensional Hovs, time - longitude (t-x) sections; 3-dimensional Hovs may give signals of Rossby ray traces) may not useful for "forecasting" the low zonal to high zonal wave number transitions (Wallace and Blackmon 1983).

Finally, there has been some "hint" of tropical-mid latitude interactions as being important for the breakdowns. There is evidence to support that hypothesis.

Figure 8 is taken from a paper by Kiladis and Weickmann (1992b). See the caption for the details. What is important to note is that by observing the negative anomalies of outgoing longwave radiation (due to enhanced convection), there is a two-way interaction of first, the extratropics forcing enhanced tropical convection, then feedback to the northern extratropics. The end result are negative stream function anomalies across the western U.S. Put another way, there would generally be a mid and upper tropospheric trough (with negative height anomalies) in the geopotential height field over the western U.S. resulting from the extensive convection as depicted.

Integrating all the above ideas, the operational forecaster should observe the following signals as precursors of low-to-high wave number transitions. First, using full disk satellite imagery, look for persistent, say 5 to 7 days (Weickmann 1992, personal communication) of tropical convection across the Pacific Ocean Basin. Further, observe it's movement. If that convection is moving slowly eastward, say from west of the dateline to around 160°W (southwest of Hawaii), watch for eastward expansion of the extratropical westerlies. Secondly, if the westerlies do expand across the Pacific, like shown in Figure 3, that maybe a precursor to a low to high breakdown.

Third, using, say, the water vapor imagery, observe deepening of a mid Pacific trough, and enhancement of tropical convection just southeast of it. If this occurs, a breakdown is likely in progress, with the result being a western (or central) U.S. mid and upper tropospheric trough, like shown in Figure 4.

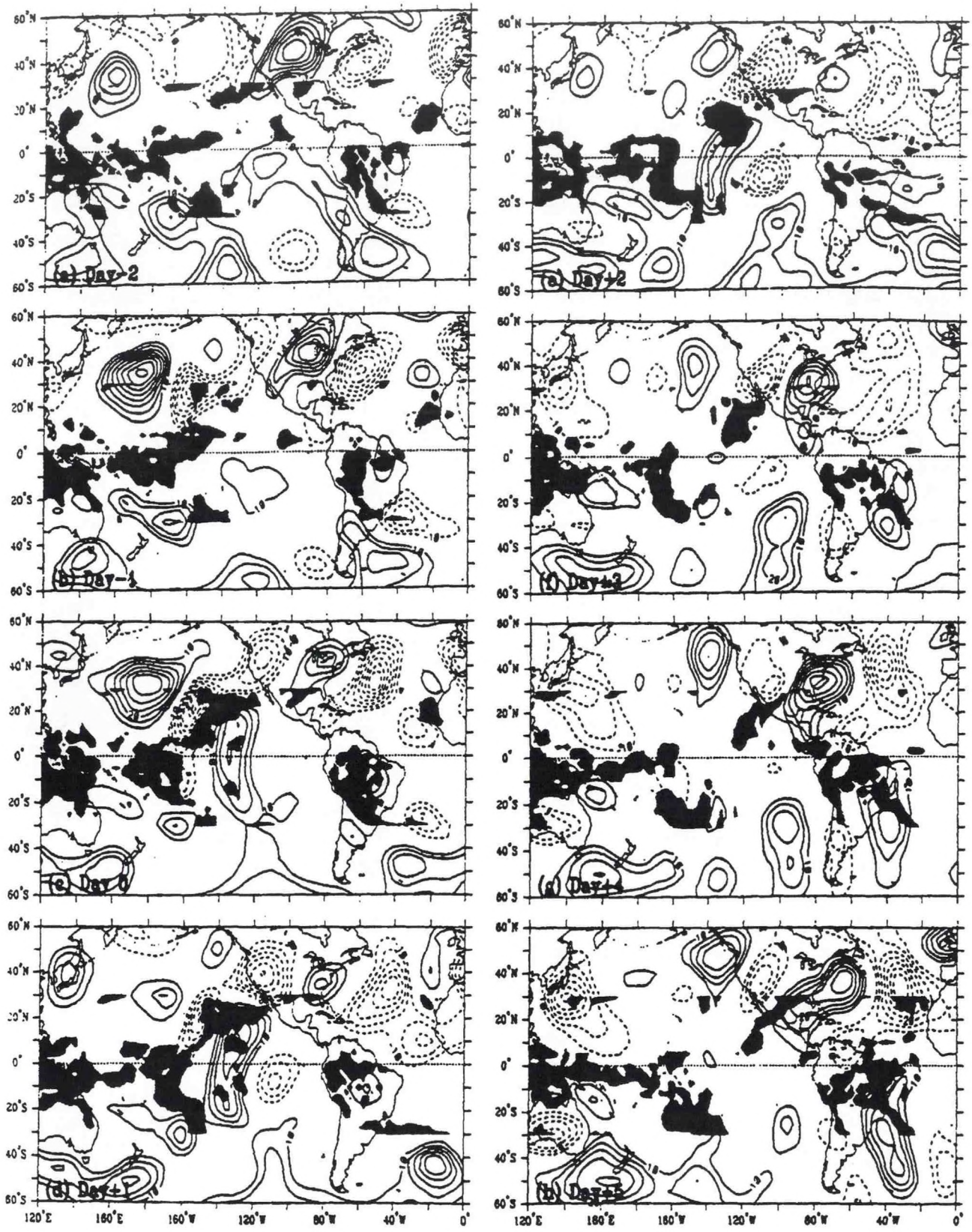

Figure 8. Figure taken from Kiladis and Weickmann (1992) depicting 200-mb stream function anomalies as a function of time. Dashed lines denote negative anomalies while solid denotes positive anomalies. Dark shading indicates the spatial coverage by negative OLR anomalies. For further details, see the caption in the cited paper.

Earlier, some brief mention of made of El Nino. More precisely, events that involve anomalously warm waters in the equatorial Pacific Ocean Basin, and can result in a low index phase of the Southern Oscillation. When both the ocean and the atmosphere are coupled, these are called ENSO (El-Nino/Southern Oscillation) events (Trenberth 1991; Rasmussen and Carpenter 1982). During ENSO's, low to high breakdowns tend to be relatively frequent, with periods of about 7 to 10 days. However, observationally, there is generally less baroclinic development (and therefore, less amplitude in the high wave mode).

In all the above discussion, no mention was made of the other ocean basins and extratropical processes away from the Pacific North American sector. That was deliberate, to keep the text simple. The basic concepts revealed up to this point should allow forecasters to use low to high breakdown as a tool for periods through at least 6 to 10 days. In the next section on case studies, a diagnostic tool will be presented that also gives a good precursor for these breakdowns.

3. CASE STUDIES OF LOW TO HIGH ZONAL WAVE NUMBER TRANSITIONS

A. Preliminaries

Three cases of low to high zonal wave number transitions will be illustrated. These are the periods of 13-15 March 1990, 15-21 April 1992 and 25 October-6 November 1992.

For each case, the ideal presentation would be to show a 500-mb northern hemispheric analyses, a spectral analysis diagnostic package (discussed below) and numerical model solutions. However, due to limitations this complete package cannot be given. That includes graphical numerical model output for the first two cases. Nevertheless, enough information is given to stress important concepts of wave number transitions.

Finally, the stages depicted in Figures 3 and 4 are emphasized for each case. That is because those observational signals are believed to be the most useful in regard to anticipating a wave number transition. Furthermore, it is quite likely that the most significant forecast errors of the operational numerical weather prediction models occur during the transition from the state depicted in Figure 3 to that of Figure 4.

B. Case 1: March 13-15, 1990

Though numerical model output was not available, this case is shown because of its "explosive" nature. Figure 9 is the zonal wave-zero to five wave 500-mb analysis valid 0000 UTC 13 March 1990. This type of analysis is gener-

ated by running a spectral analysis on the 500-mb height field and retaining zonal wave numbers 5 or less. The planetary-scale waves (Blackmon 1976) can be more easily observed. This product is routinely processed at NCEP and distributed.

From Figure 9, observe the dominant zonal wave 3 structure of the 500-mb height field. Note how the westerlies are longitudinally expanded across the Pacific Ocean Basin and the similarity to Figure 3. Although not shown, the actual unfiltered 500-mb northern hemispheric analysis also indicated a dominate wave 3 structure. However, the wave zero-to-five chart, for this case, makes that structure easier to see and thus eliminates confusion. Often, the wave 3 is easier to observe with the filtered chart and the wave 5 is more obvious with the unfiltered version.

Figure 10 is the actual unfiltered 500-mb northern hemispheric geopotential height analysis valid 1200 UTC 15 March 1990. A very rapid transition to zonal wave 5 has occurred, with a relatively energetic cyclonic baroclinic development event in the central U.S. This wave 5 structure is 10° to 20° farther east than shown in Figure 4.

Suffice to say that the errors in the operational numerical prediction models in the 3- to 5-day period were quite significant. There was a lack of model run to run continuity, and large differences between the individual members (time and space). Some forecast problems included storm track position, and the depth and intensity of the Great Plains cyclone. Stated another way, with respect to the storm in the nation's mid section, this was a case of rapid baroclinic development, and the numerical models (including some "short range") did not capture the feature until "it practically happened". It is certainly possible that a contribution to the forecast errors was caused by improper modeling of the complex terrain due to the Rocky Mountains.

Additionally, there was a considerable amount of both wintertime and springtime-type severe weather. The latter included severe and tornadic deep moist convection and substantial snowfall, in the appropriate air masses (National Severe Storms Forecast Center (NSSFC) 1990).

C. Case 2: 25 October-6 November 1992

This case is a bit more complex than Case 1. As will be seen, the wave number transition was more of a 3 to 7 than 3 to 5. However, the event is shown because the transition was captured with a spectral analysis diagnostic package developed at the Environmental Research Laboratories/Forecast Systems Laboratory (ERL/FSL) in Boulder, Colorado. However, graphical displays of operational global numerical models (MRF, ECMWF and UKMET) were again not available for this case.

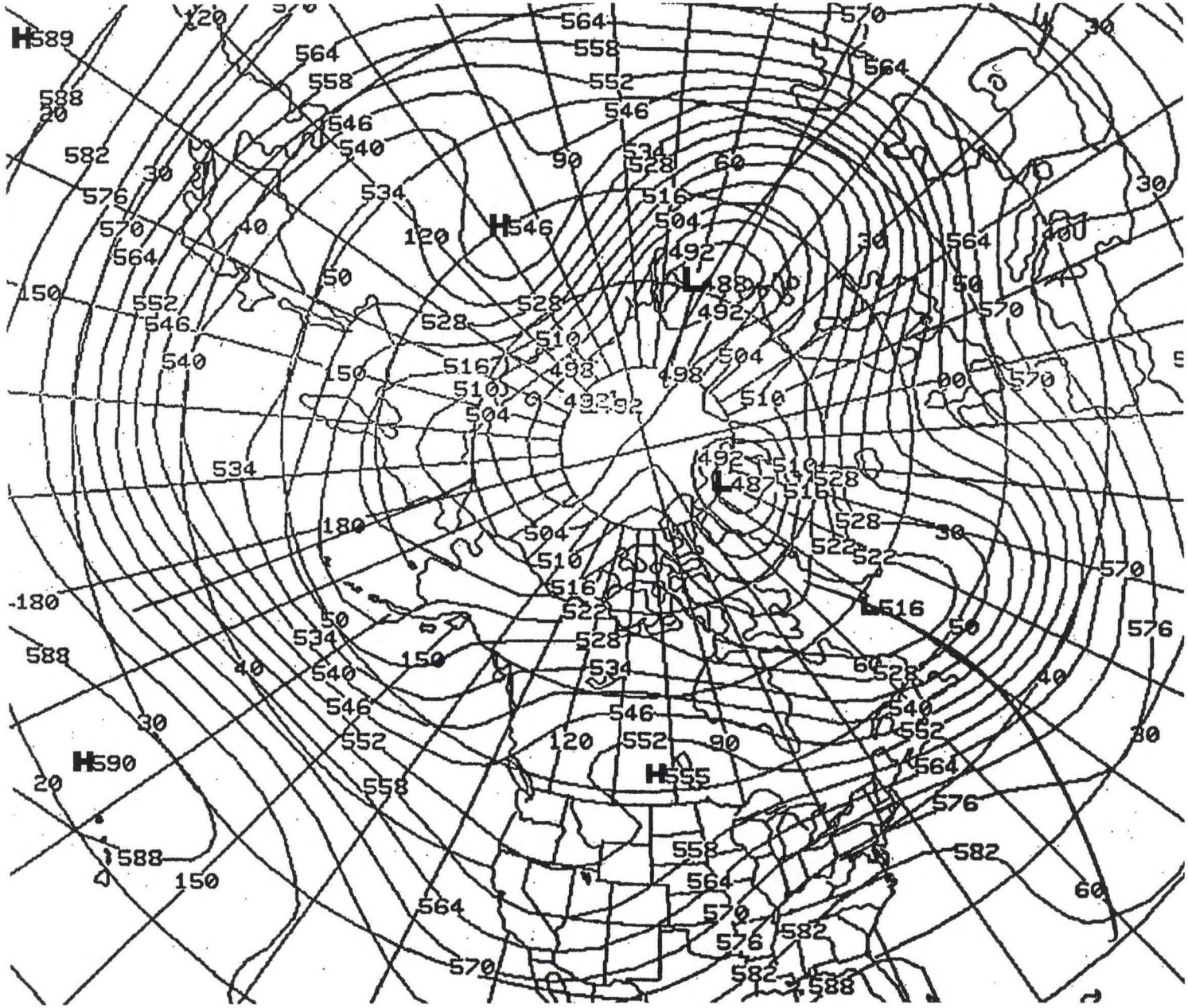

Figure 9. 500-mb zero-to-five wave chart valid 0000 UTC 13 March 1990. Heights are analyzed every 6 gpdm.

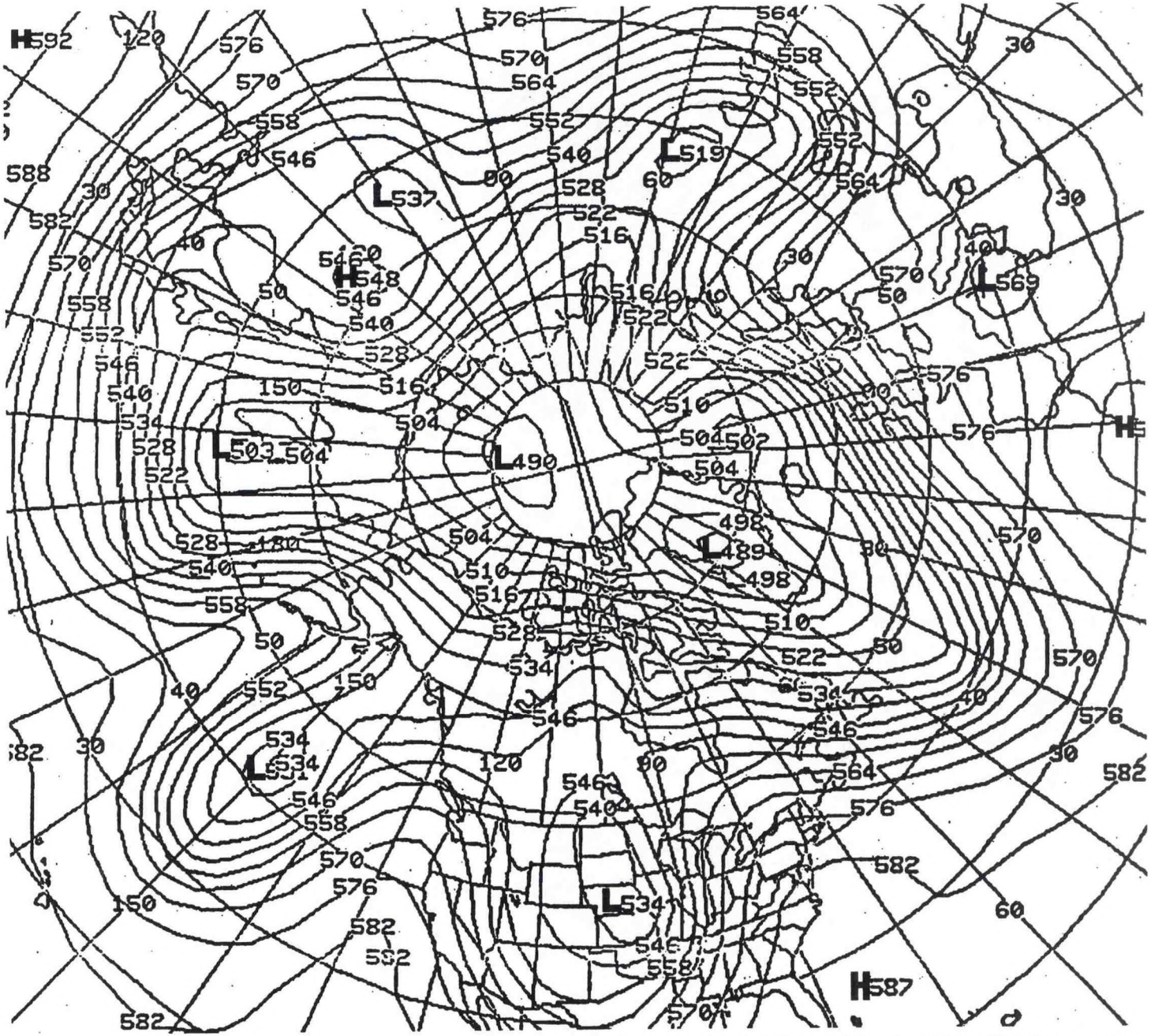

Figure 10. 500-mb northern hemispheric constant pressure analysis valid 0000 UTC 15 March 1990. Heights are in gpdm, with the analysis interval every 60 gpdm.

Figures 11 through 16 are the 500-mb northern hemispheric geopotential height analyses from 1200 UTC 25 October through 0000 UTC 6 November 1992. The times for the individual maps are shown on the captions.

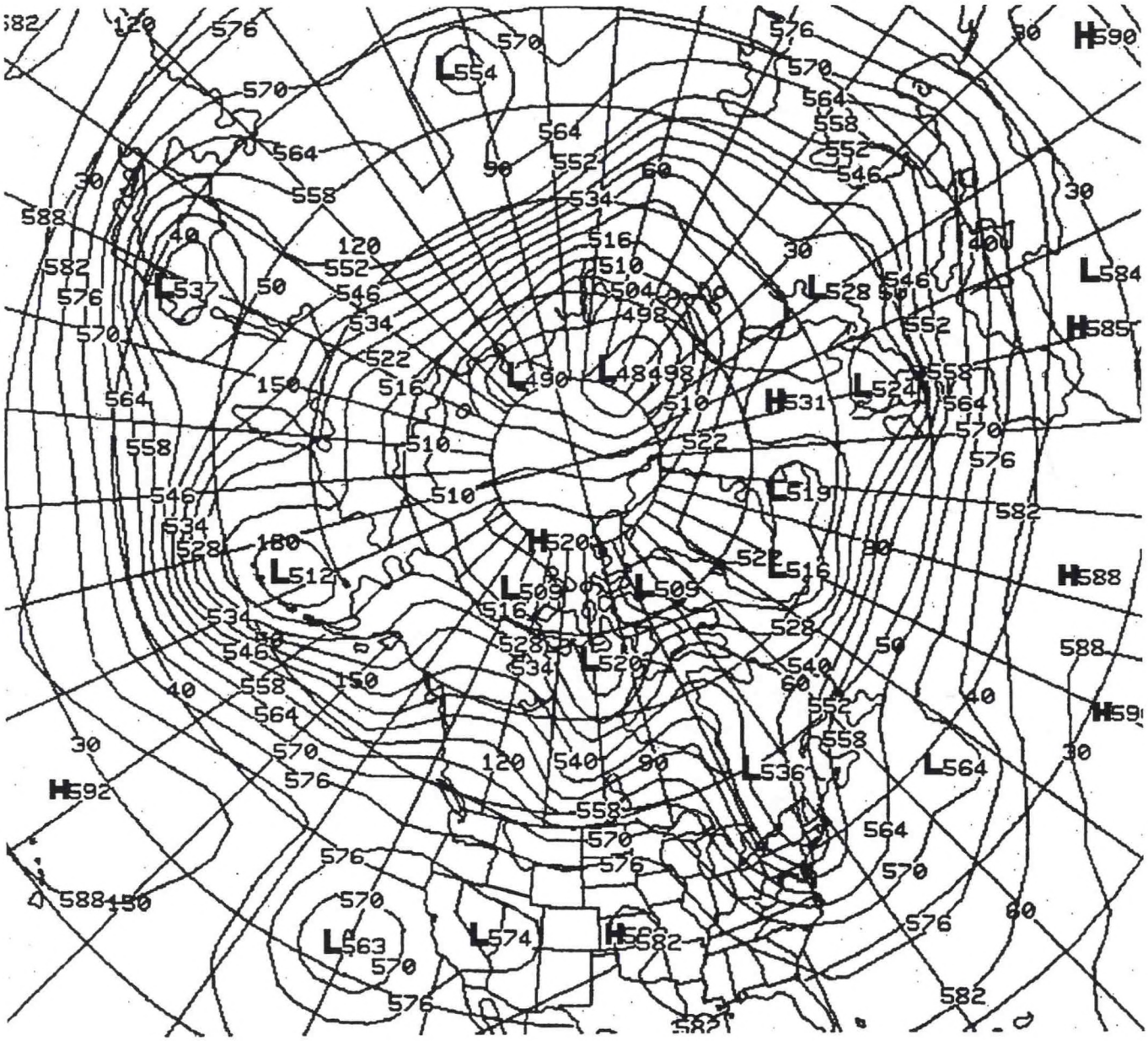

Figure 11. Same as Figure 10, but valid 1200 UTC 25 October 1992.

From Figure 11, observe the wave 3 structure of the westerlies, especially at the higher latitudes. There are relatively low amplitude troughs at the dateline, 70°W and about 30°E. Ridges can be observed between the troughs in the height field.

Seventy-two hours later, Figure 12, observe how the westerlies had expanded equatorward, with an increase in the zonal wave number. Note also the eastward extension of the westerlies across the central North Pacific Ocean Basin. Figure 12 has similarities to Figure 3, and, observationally, a low wave to high zonal wave number transition event was in progress at this time.

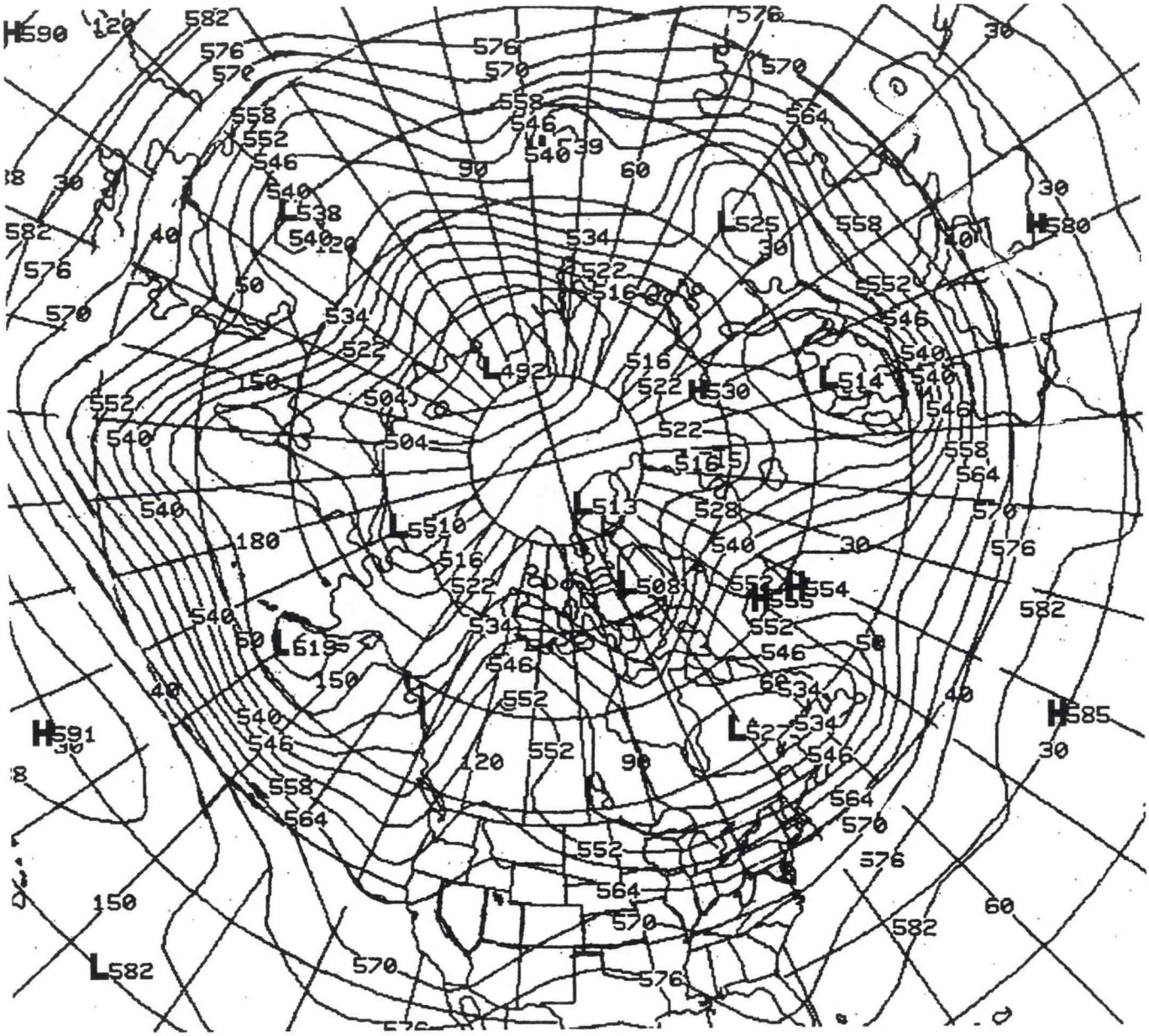

Figure 12. Same as Figure 10, valid 1200 UTC 28 October 1992.

As the reader studies the rest of the analyses (Figures 13 -15), amplification is apparent, with an increased meridional component of the flow. Maximum amplification seems to have occurred by the time shown in Figure 15.

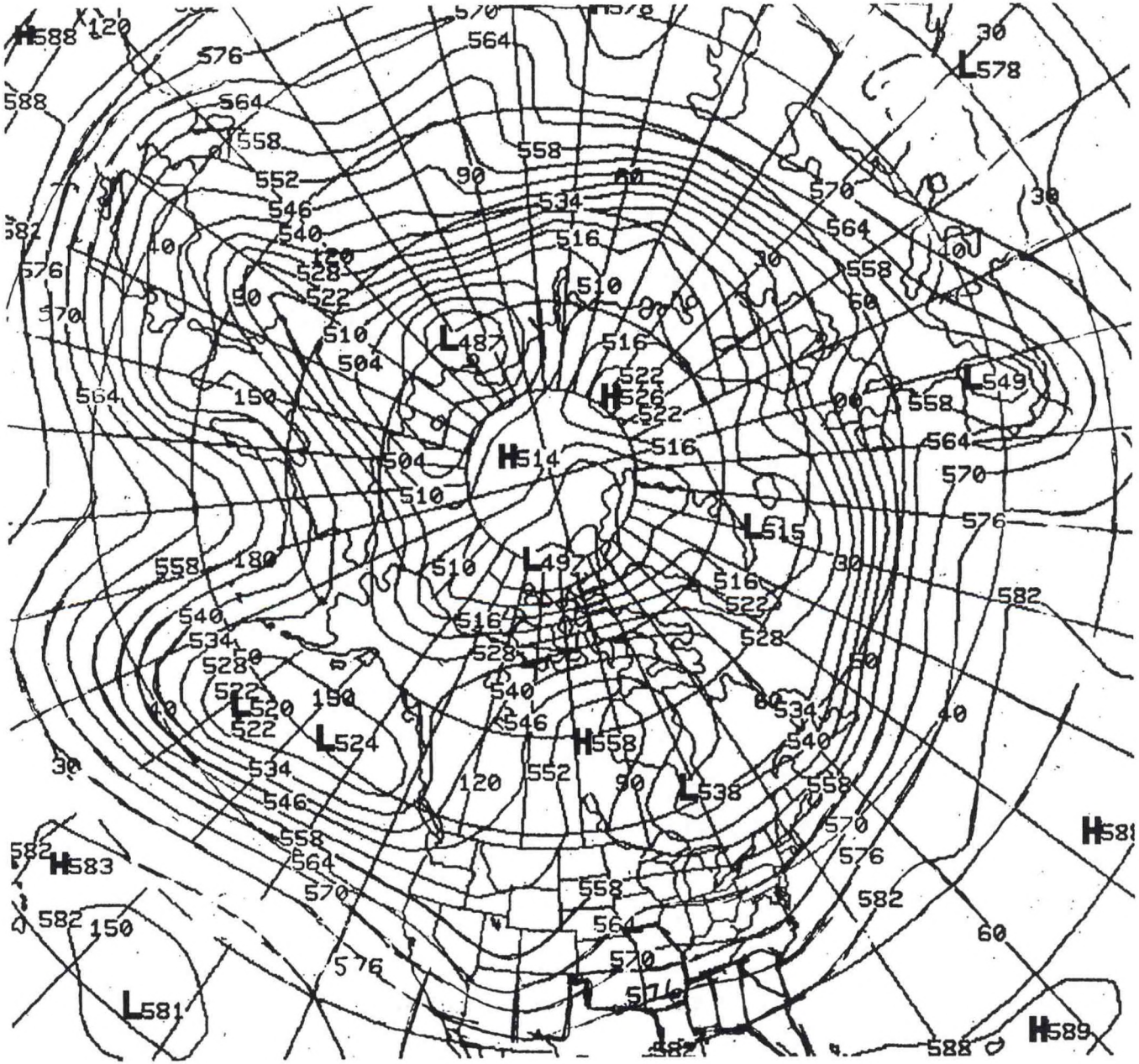

Figure 13. Same as Figure 10, valid 1200 UTC 31 October 1992.

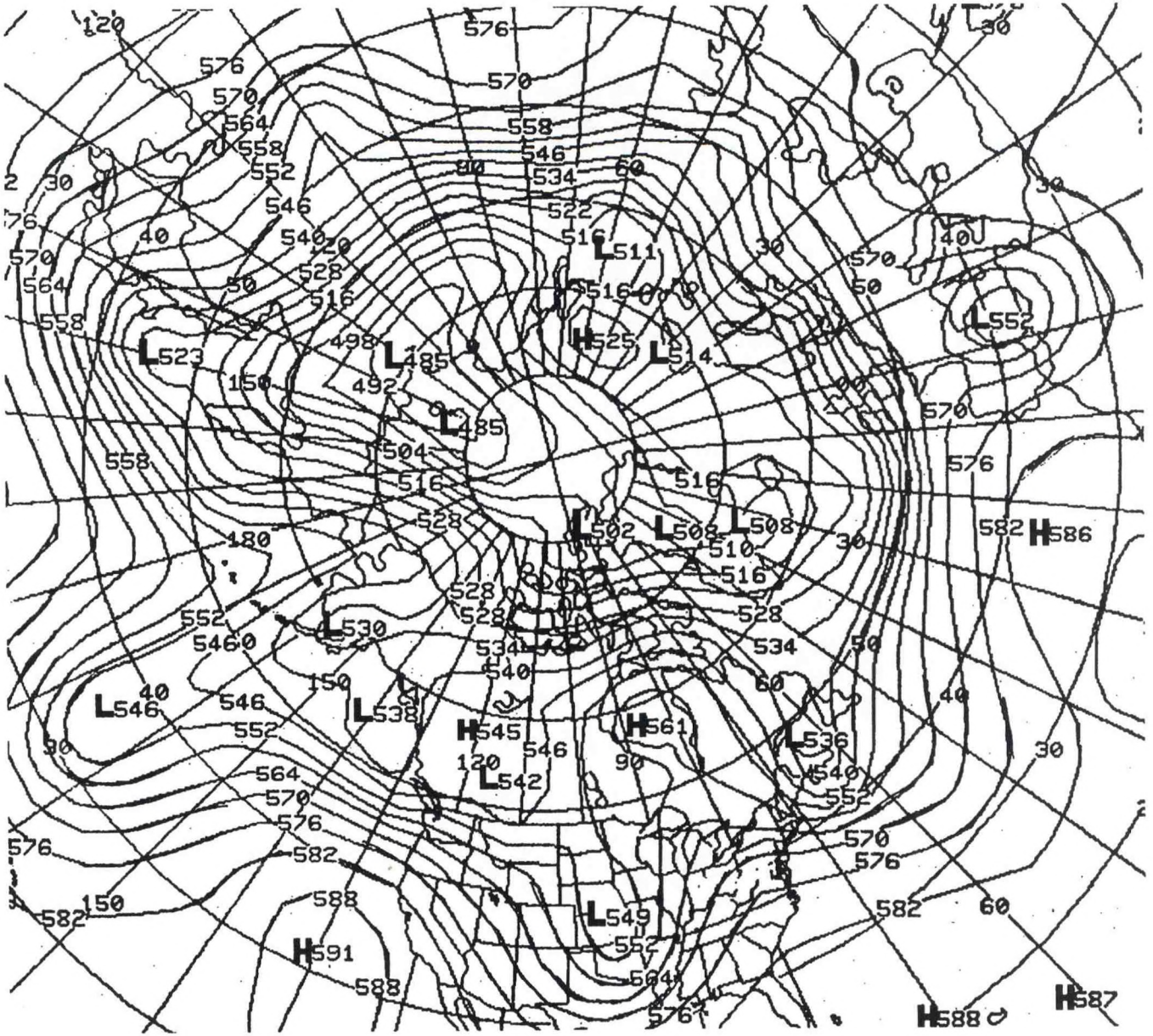

Figure 14. Same as Figure 10, valid 0000 UTC 02 November 1992.

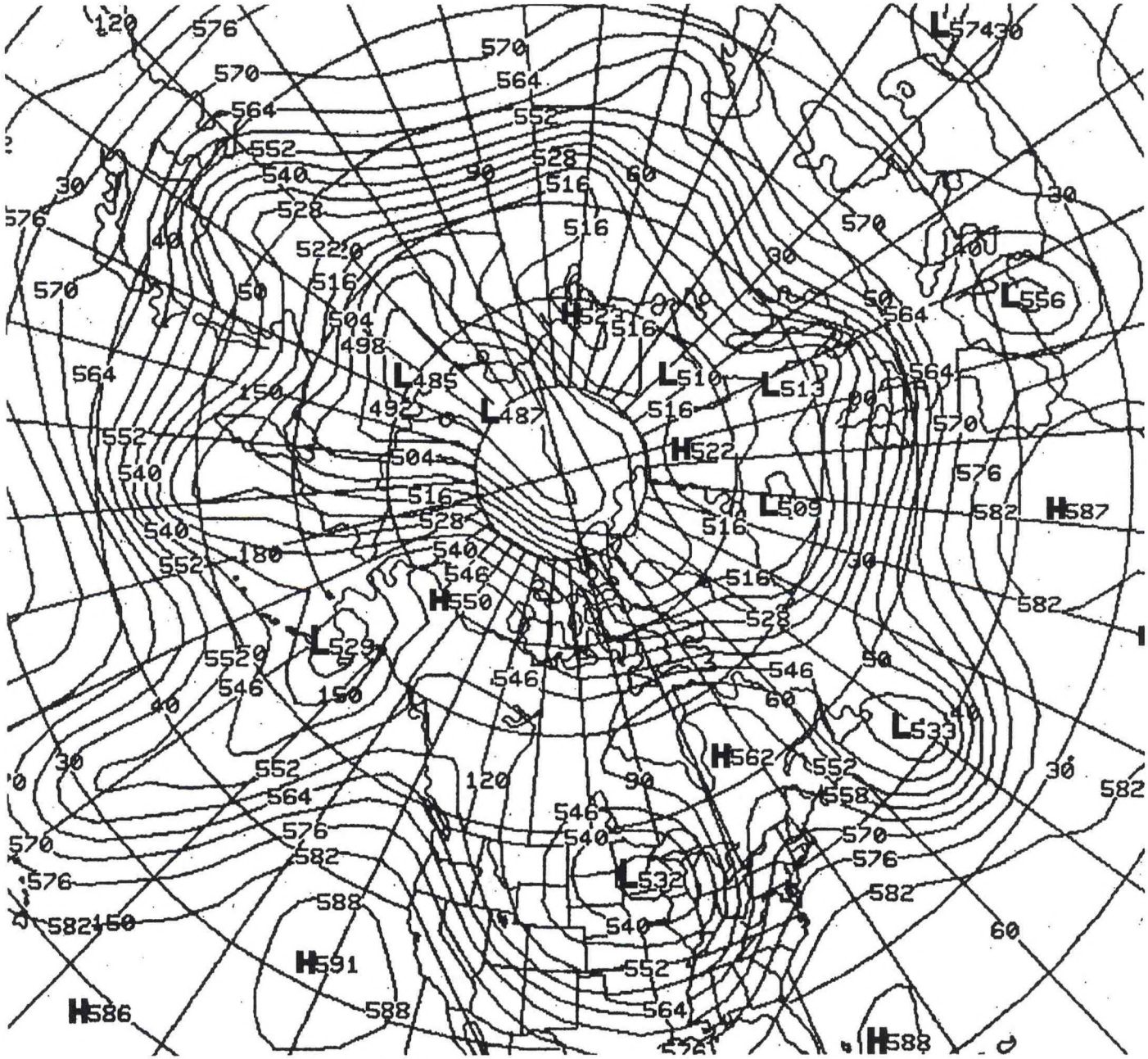

Figure 15. Same as Figure 10, valid 0000 UTC 03 November 1992.

occurred across the western hemisphere. Further, the polar vortex became displaced toward eastern Asia. That was partially the result of a high latitude wave 1 retrogression process. Wave 1 and wave 2 can create significant asymmetries in how these breakdowns occur (Lanzante 1990, and references therein, for discussion of wave 1 and wave 2).

Continuing with Figure 15, the large cyclonic circulation centered over southwest Minnesota is quite apparent. Performance of the operational global medium-range numerical models (MRF, ECMWF and UKMET) with respect to forecasting this large cyclone was relatively poor. There were inconsistencies from cycle to cycle in each global model and large disagreement between the models.

Finally, at the time of Figure 15, an asymmetric wave 7 can be observed. There are troughs at 155°W, 95°W, 50°W, 10°E, 60°E, 125°E, and 160°E. Ridges are roughly between the trough positions.

At the time of Figure 16, the wave 7 regime can be seen to be decaying, back to a wave 3 structure similar to Figure 3. Note the large amount of northeast to southwest tilt of the troughs and ridges. That is a signature of the northward transport of westerly angular momentum from the tropics (Palmen and Newton 1969, Holton 1992). All of this is fairly typical after a wave number transition.

Figures 17 through 21 depict one objective way to verify the above observations for this case. Figure 17 is a time series plot of the zonally averaged analyzed 500-mb height as a function of time. The time series is done in 10° wide latitude bands, as shown on the figure.

A signature of the equatorward migration of the westerlies can be seen. At the latitude band of 50° to 60°N, observe the rapid mean height falls starting about 18 October 1992. Farther south, 40° to 50°N, note that there are slight mean height rises simultaneously. That is indicative of increasing westerlies at the relatively high latitudes. Approximately 26 October 1992, the same signature can be seen at 40° to 50°N. That is an indication that the westerlies are expanding southward.

Finally, note the lesser mean height falls at 30° to 40° N. At this time, the breakdown was maturing. The height falls at this latitude band are not as dramatic as farther north.

From the foregoing discussion and Figure 17, a slow forward progression in time of southward moving height falls can be seen starting at around 18 October. The point to be made here is that the signature shown in Figure 17 is typical of low to high wave number transitions.

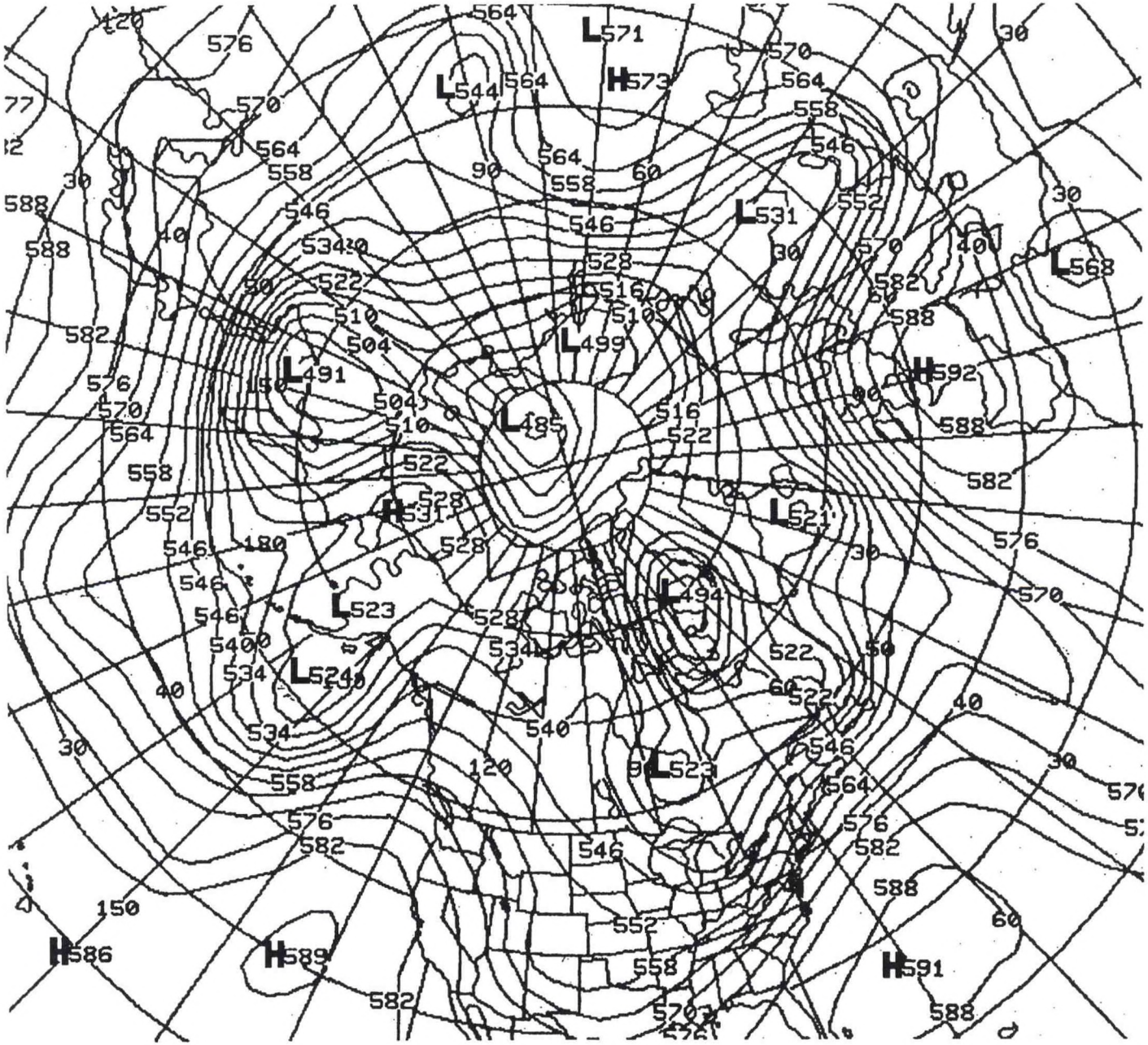

Figure 16. Same as Figure 10, valid 0000 UTC 06 November 1992.

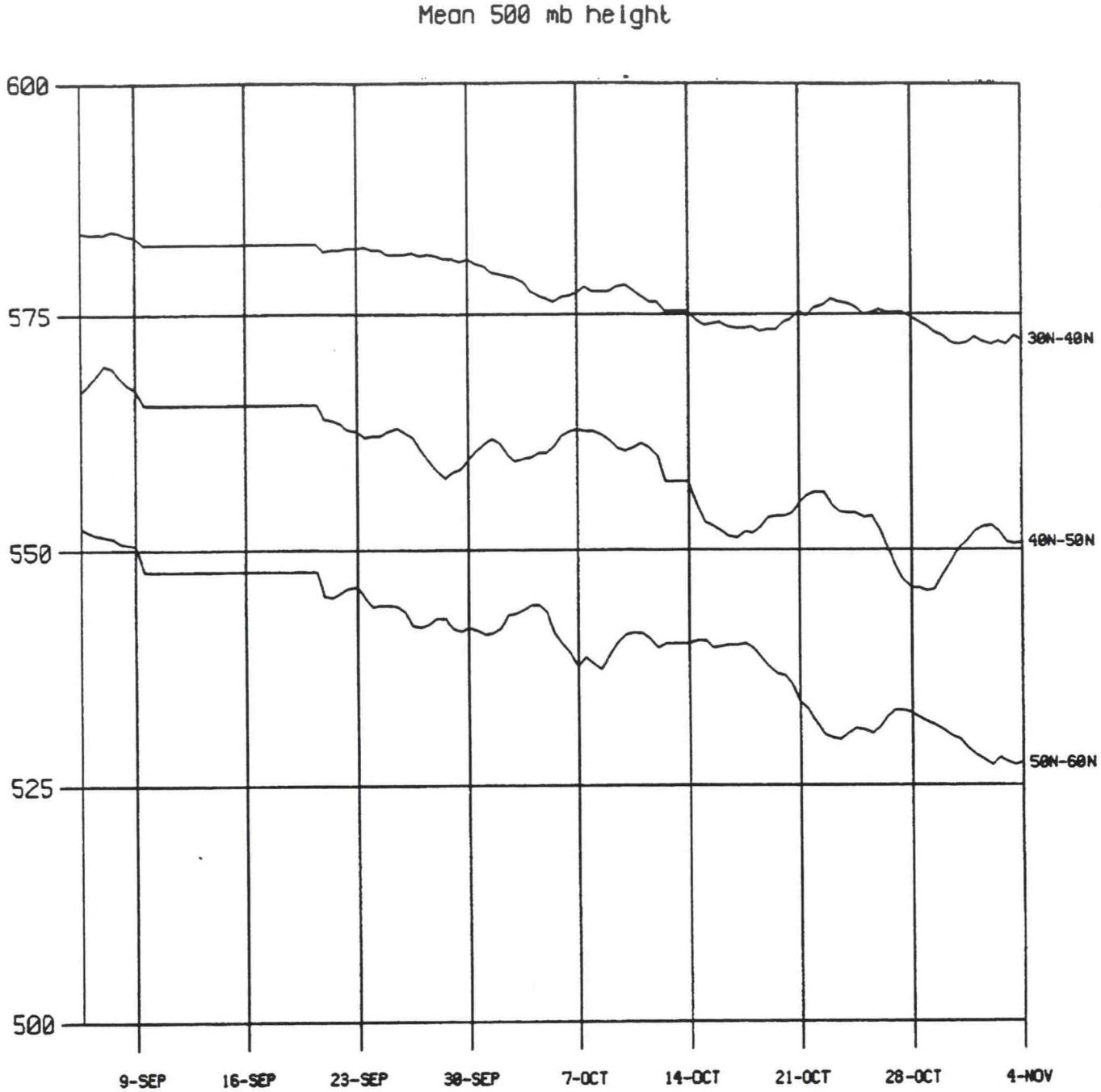

Figure 17. Time series analyses of mean 500-mb height, as a function of the indicated latitude bands. Units are in gpdm (ordinate), with time in day-month format (abscissa). The year is 1992.

Figures 18 through 21 are also in time series format as a function of latitude band. However, what is plotted are the actual harmonics for two dimensional wave numbers 2 through 6.

These plots are produced by looking at global geopotential data in latitudinal bands. Harmonics are obtained through spectral decomposition, with waves

1 through 6 retained. The horizontal axis is height amplitude and the solid or dashed lines indicate the waves. Thus, the dominant planetary wave can be determined as a function of time (the vertical axis).

From Figure 18, observe the dominance of waves 2 and 3 from roughly 9 October to 15 October, then a slight peak of spectral power around 22 October 1992. Going to Figure 19, note the spike of wave 2 power at around 22 October. From comparing the above two Figures, one can see the low wave number energy propagating southward.

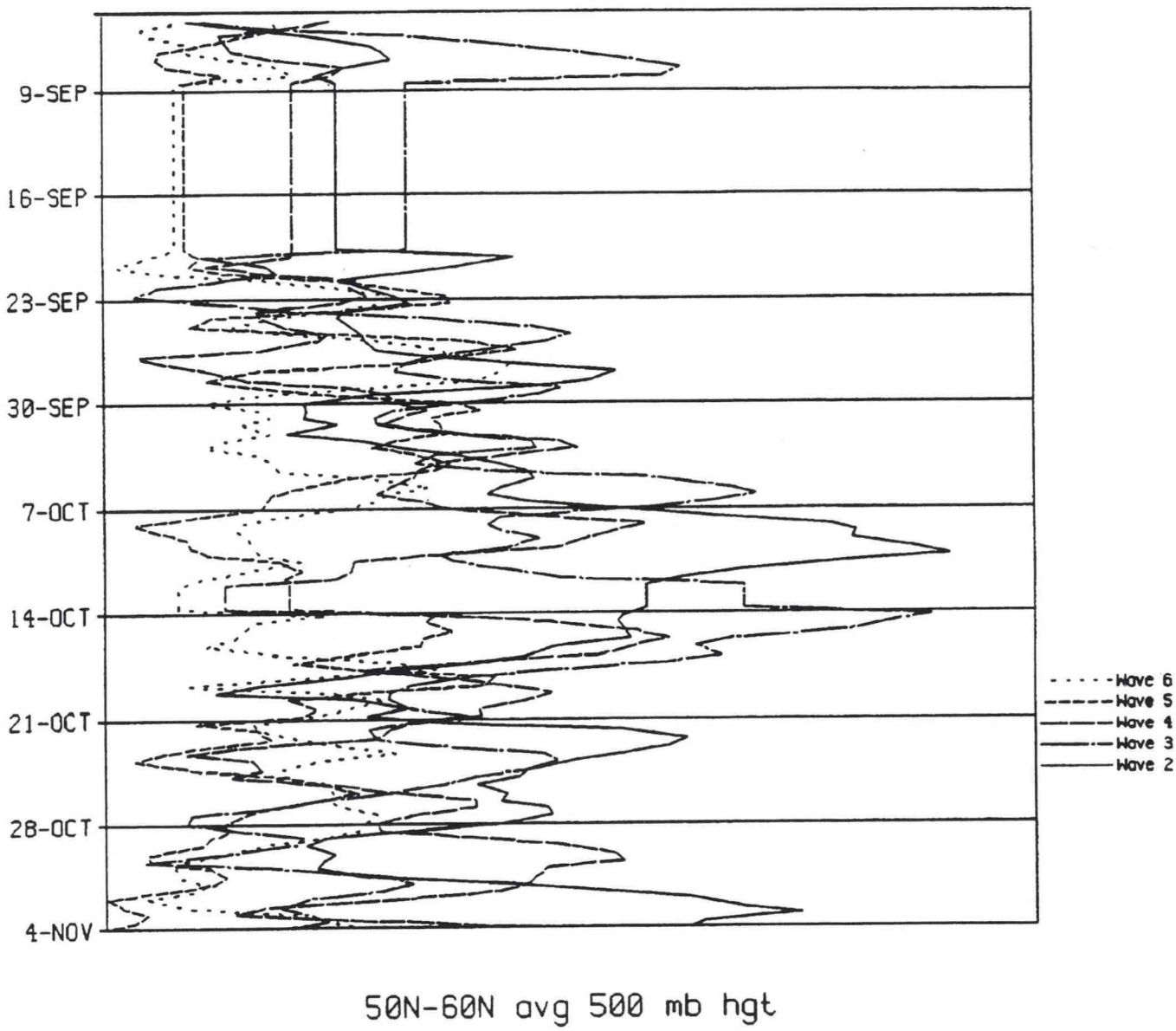

Figure 18. Time series analysis of total wave number spectral power, for the latitude band of 50° to 60°N. The abscissa are the dates, for 1992, while the ordinate is dimensionless. What is important to observe are the relative strengths the wave numbers to each other, with the wave numbers indicated by the key.

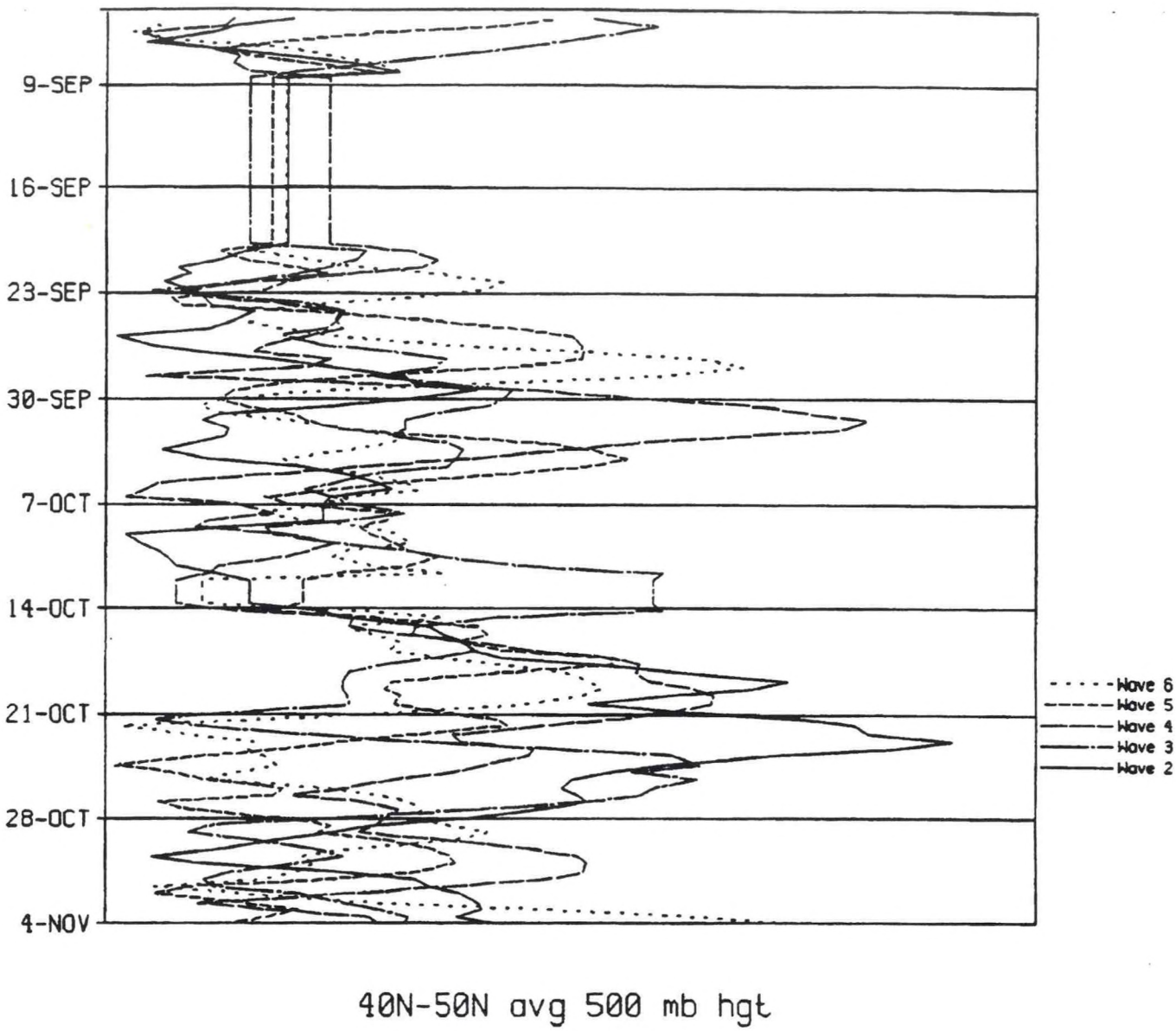

Figure 19. Same as Figure 18, but for 40° to 50°N.

Finally, from Figure 20, observe the increase in spectral power of waves 4 through 6, with wave 6 having the greatest amplitude, after 28 October (wave 7 was not computed; the point, again, is low to high transition). Referring to Figures 18 and 19, for the same times, note the relatively low power for waves 2 and 3. The exception is the peak in wave 2 for 50° to 60°N.

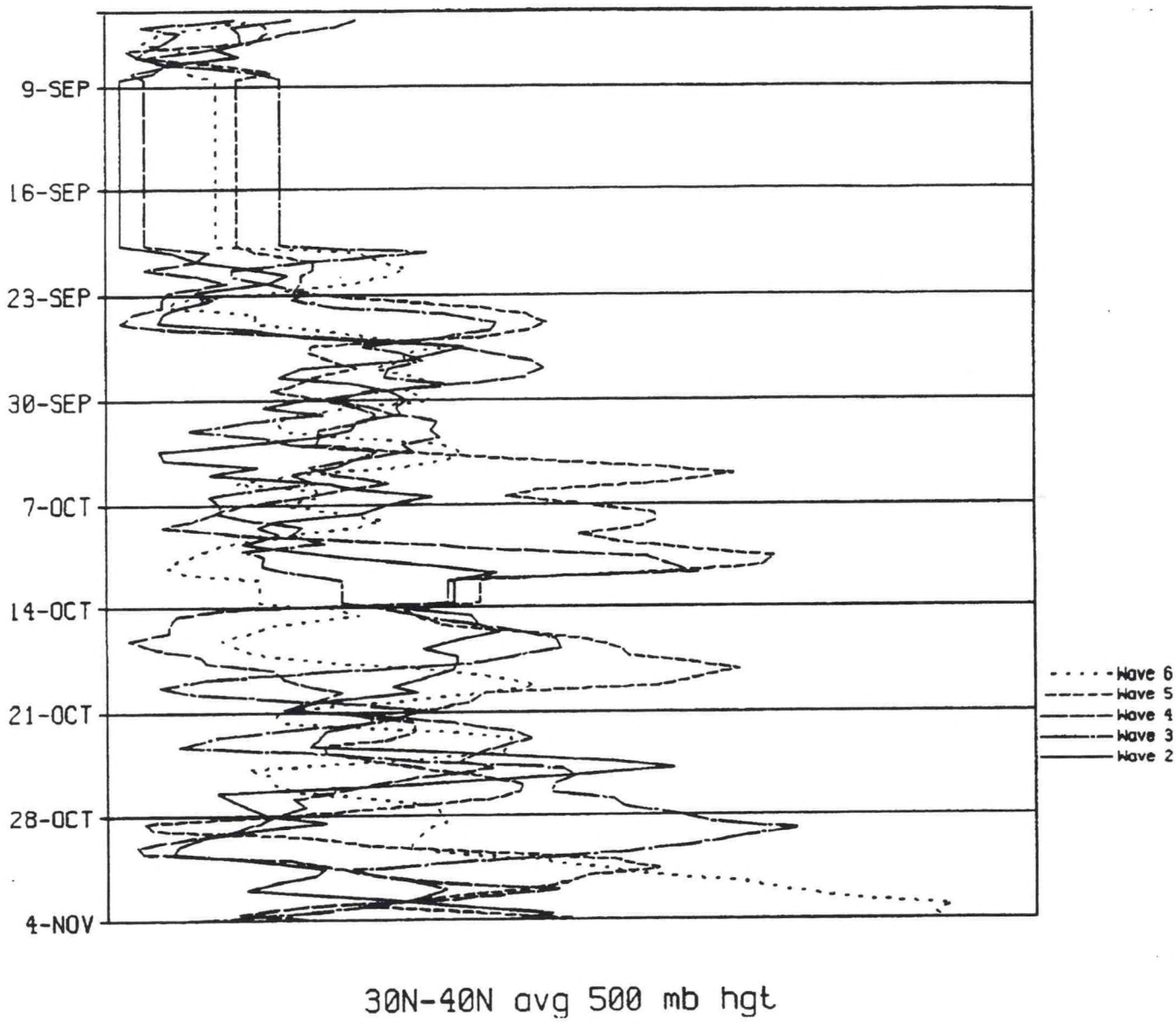

Figure 20. Same as Figure 18, but for 30° to 40°N.

Figure 21 is taken over a 30 degree band from 30° to 60°N. This is almost an average of the above processes isolated in their various bands. However, this wide latitude band can provide a "quick look" at wave number behavior. What is depicted in Figure 21 is consistent with Figures 18 through 20.

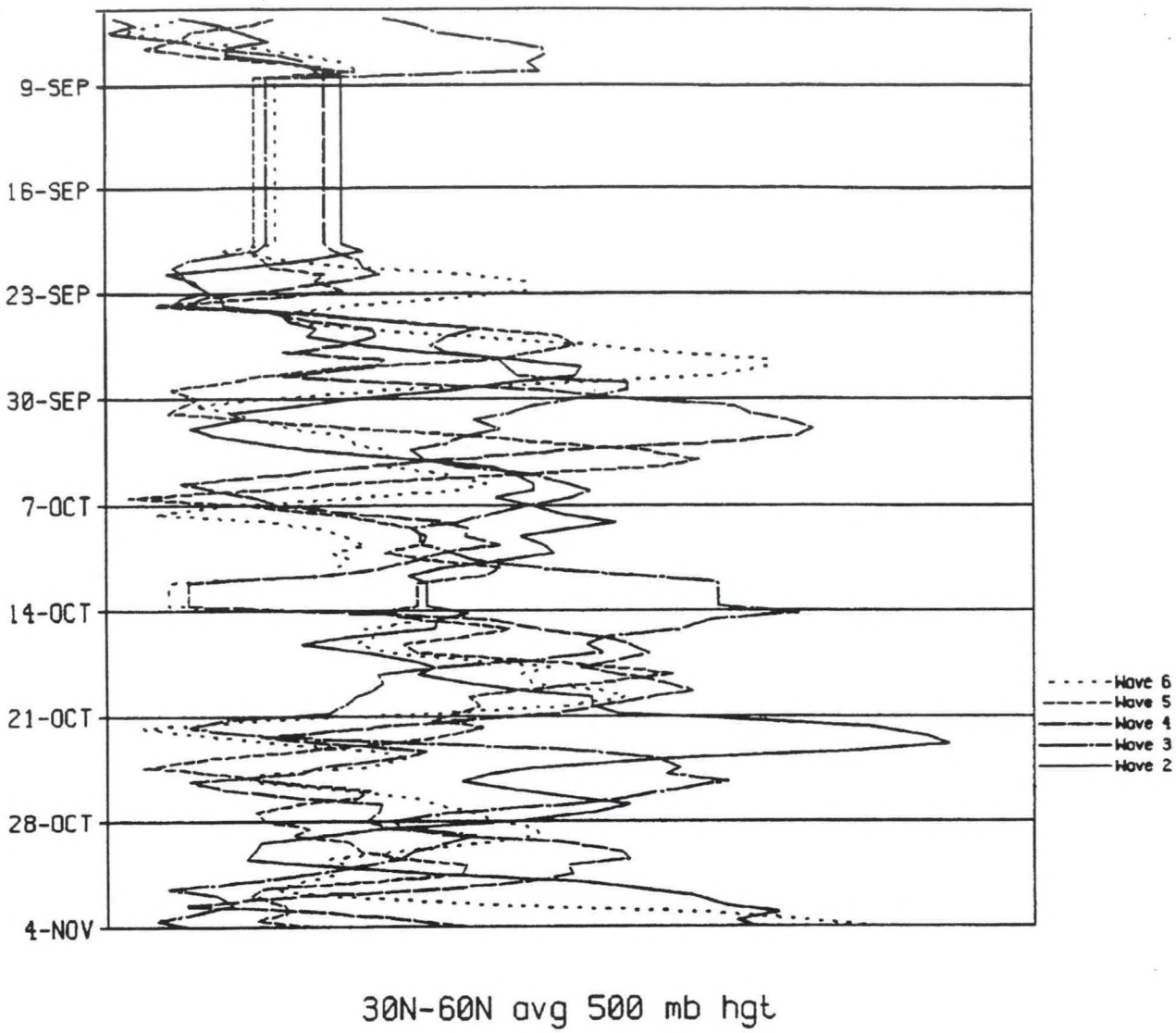

Figure 21. Same as Figure 18, but for 30° to 60° N.

In summary, the most important observation to be made from Figures 17 through 21 is that, as the westerlies came south, there was a transition from a low wave number to a high wave number projection, especially south of 50°N. For this case, from waves 2 and 3 to at least wave 6. Observationally, this behavior is consistent with other wave number transition events.

D. Case 3: April 15-21, 1992

This was a case of a significant late-season snowstorm and severe weather outbreak (Berry 1993 for details) in the mid section of the U.S. What was very interesting about this event is that there were two baroclinic cyclonic developments forced by the middle and upper tropospheric long wave trough, as the latter progressed through the Rockies and Northern Plains.

Figure 22a depicts the tracks of the sea-level lows observed. Figure 22b depicts the movements of lows and vorticity centers at 500-mb. The second, or southernmost development, was seemingly more energetic. Again, that mode of baroclinic development behavior is not unusual for low to high wave breakdowns and again, forecast errors in the operational numerical models are usually very significant. The latter point is the main motivation for showing this case, since numerical model output was available.

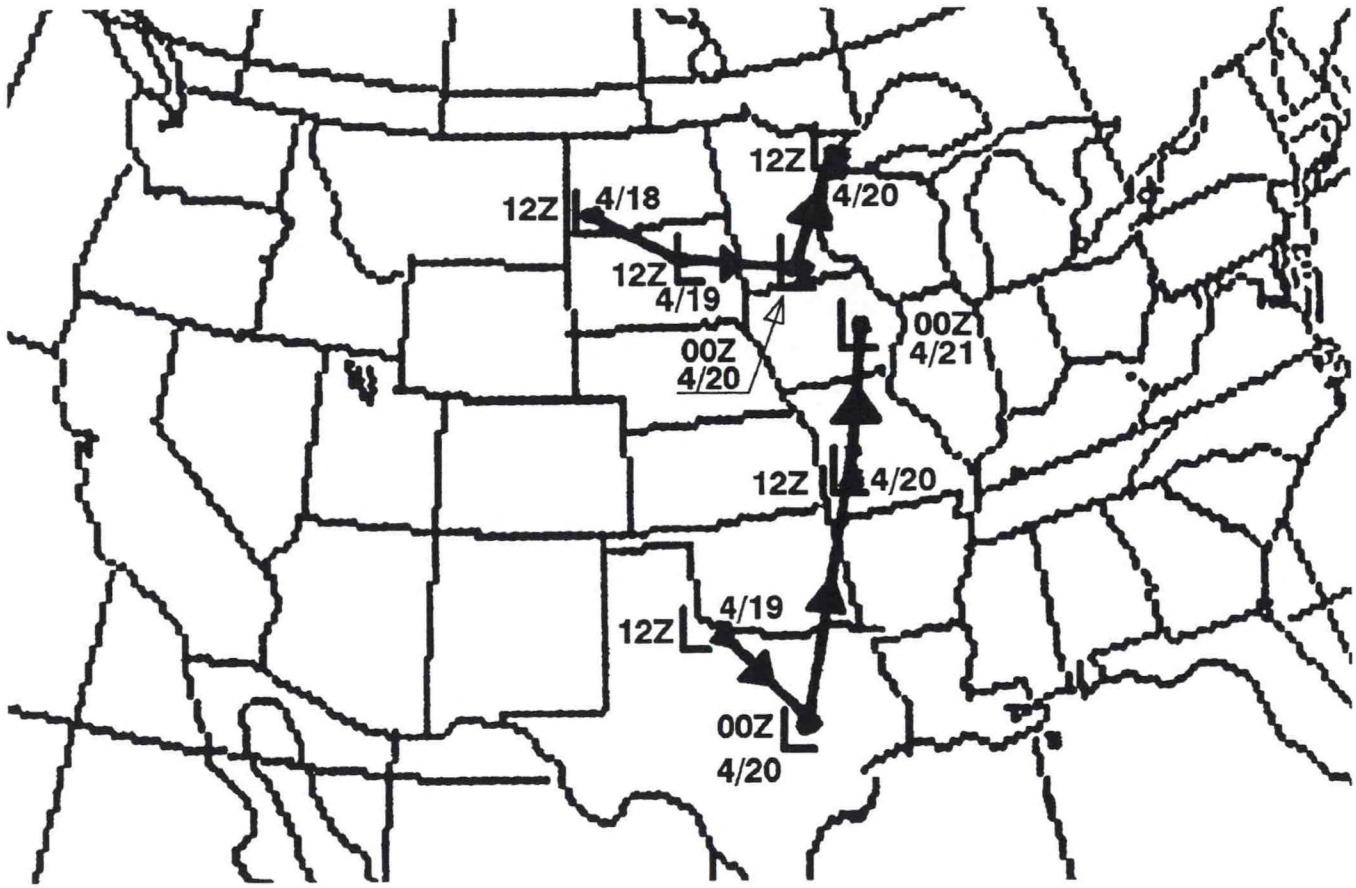

Figure 22(a). Plots of the actual mean sea-level cyclone (L) positions from 1200 UTC 18 April to 1200 UTC 21 April 1992.

To help illustrate the forecast errors in the operational numerical models for this case. The former depicts the forecasts for the 500-mb lows and vorticity centers and the latter for the sea-level lows. The forecasts are taken from the 1200 UTC 17 April 1992 cycle, and the track from a particular numerical model is given in the figure legends. Note the scatter of the forecast tracks.

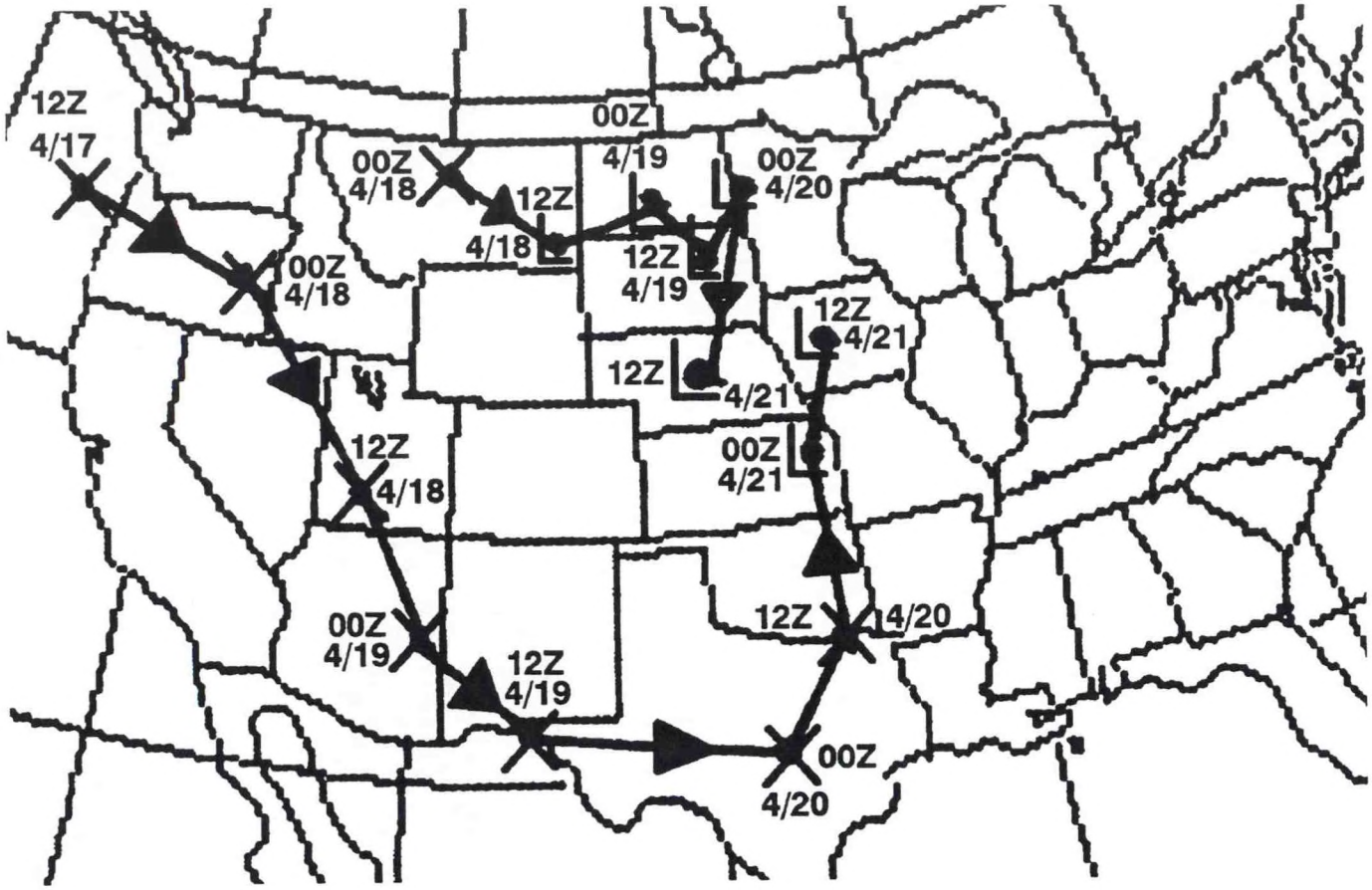

Figure 22(b). Plots of the actual positions of the cyclone (L) and vorticity centers (x) at 500-mb. The period was from 1200 UTC 17 April to 1200 UTC 20 April 1992.

Figures 23a and b are taken from the initial analysis of the ETA (Mesinger et al. 1988, Janic 1990) model. For all intents and purposes, these figures can be used as verification for 1200 UTC 19 April 1992.

Figure 24a-h are presented to illustrate the actual 48-hour heights/ vorticity and sea-level pressure/1000 to 500-mb thickness forecast fields valid 1200 UTC 19 April 1992 (again, based on the 1200 UTC 17 April 1992 data). By comparing these Figures with Figures 23a and b, the differences between the individual members (of what could be considered a small ensemble) and the real atmosphere is apparent.

Figures 25a-c are the actual northern hemispheric geopotential height analyses for the 500-mb constant pressure surface. See the captions for details. Based on all previous discussion, the "3/5 breakdown" should be more obvious to the reader. Maximum baroclinic development of the southern low occurred about 24 hours after the time of Figure 25c, 0000 UTC 21 April 1992.

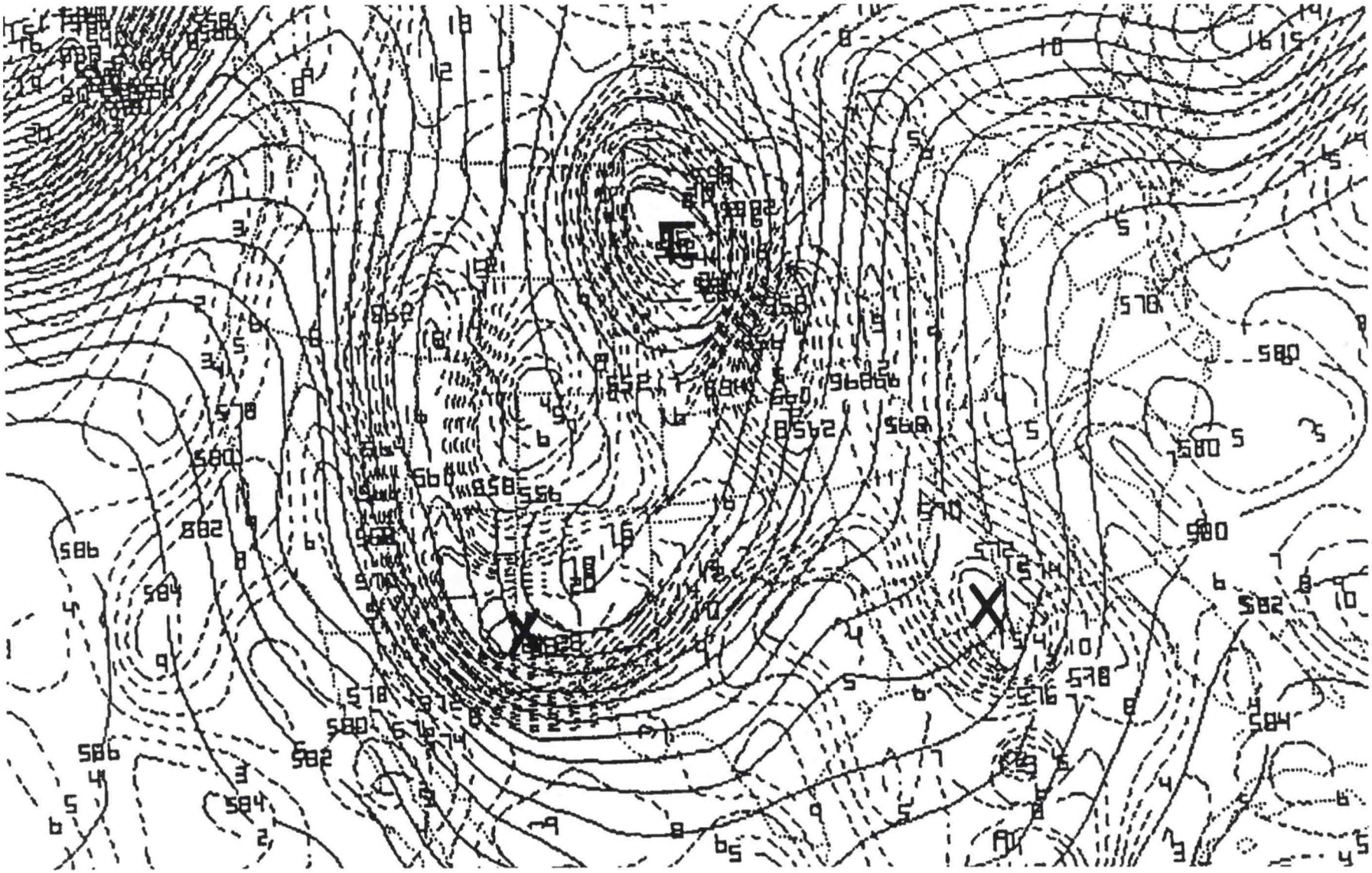

Figure 23(a). Eta model initial analysis valid 1200 UTC 19 April 1992, for 500-mb geopotential heights (solid) and absolute vorticity (dashed). Units are gpdm for heights and $10^{-5}s^{-1}$ for absolute vorticity. Contour interval for heights are every 2 gpdm and every $10^{-5}s^{-1}$ for the absolute vorticity. Both figures (a & b) were obtained from the gridded model initial fields utilizing the PCGRIDDS software package.

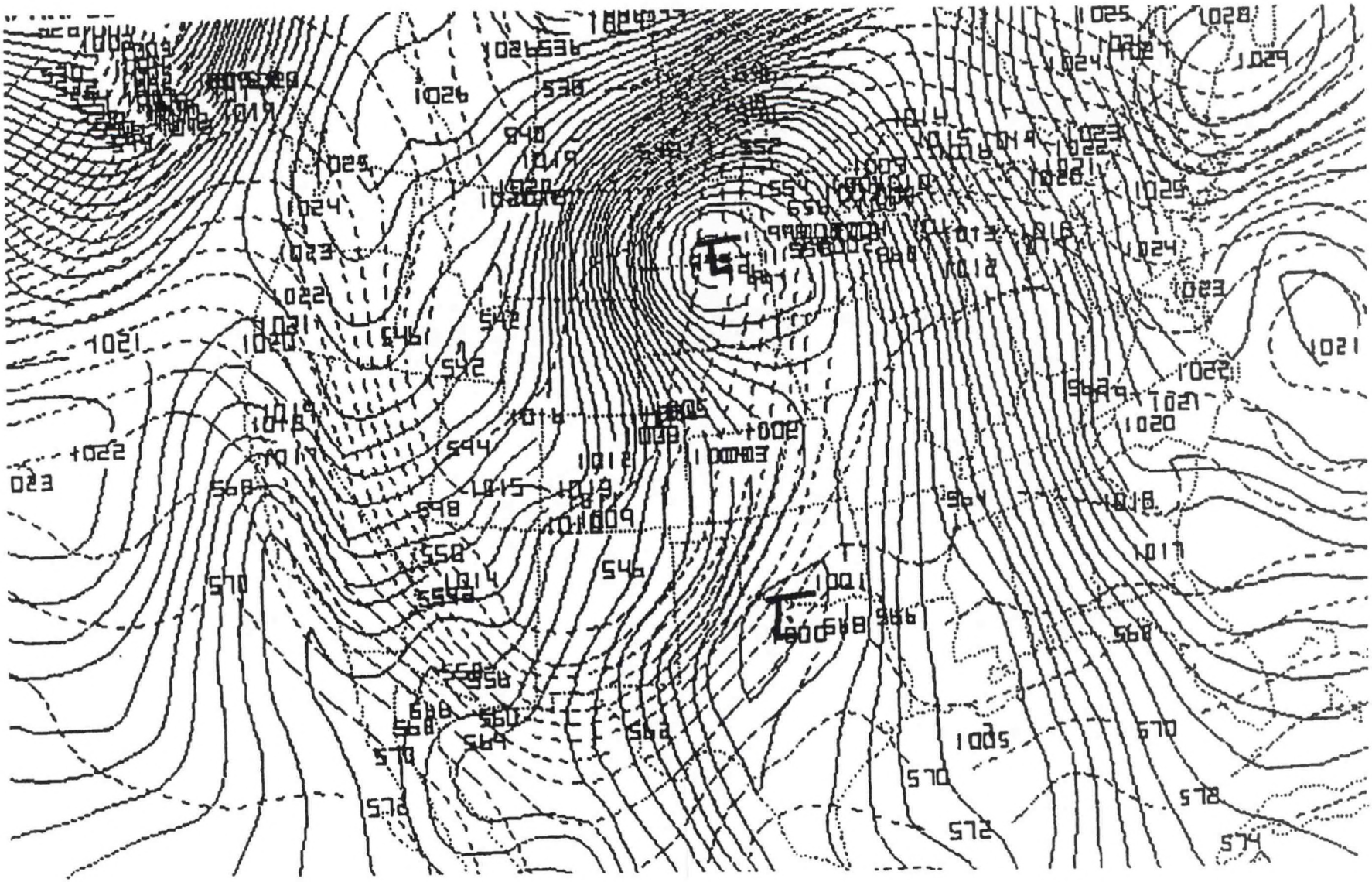

Figure 23(b). Same as (a), except 1000 to 500-mb thicknesses (dashed) and sea-level isobars (solid). Units are gpdm for thickness and mb for isobars. Contour interval is every 2 gpdm for thickness and every mb for isobars. Both figures (a & b) were obtained from the gridded model initial fields utilizing the PCGRIDDS software package.

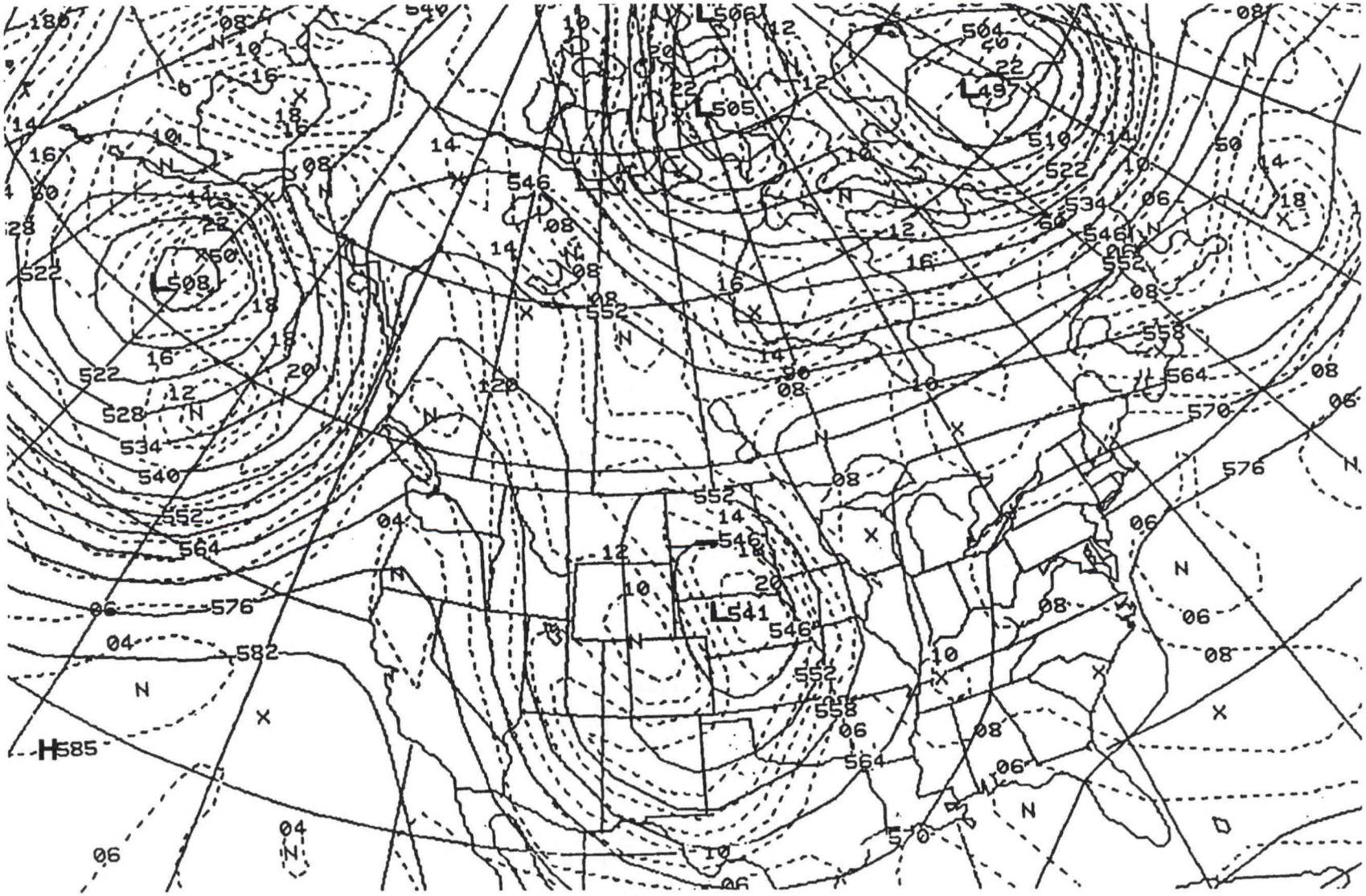

Figure 24(a). Same as Figure 23 (a), except 48-hour AVN model forecast obtained from AFOS. Contour intervals: every $2*10^{-5}s^{-1}$ for absolute vorticity and 6 gpdm for 500-mb height.

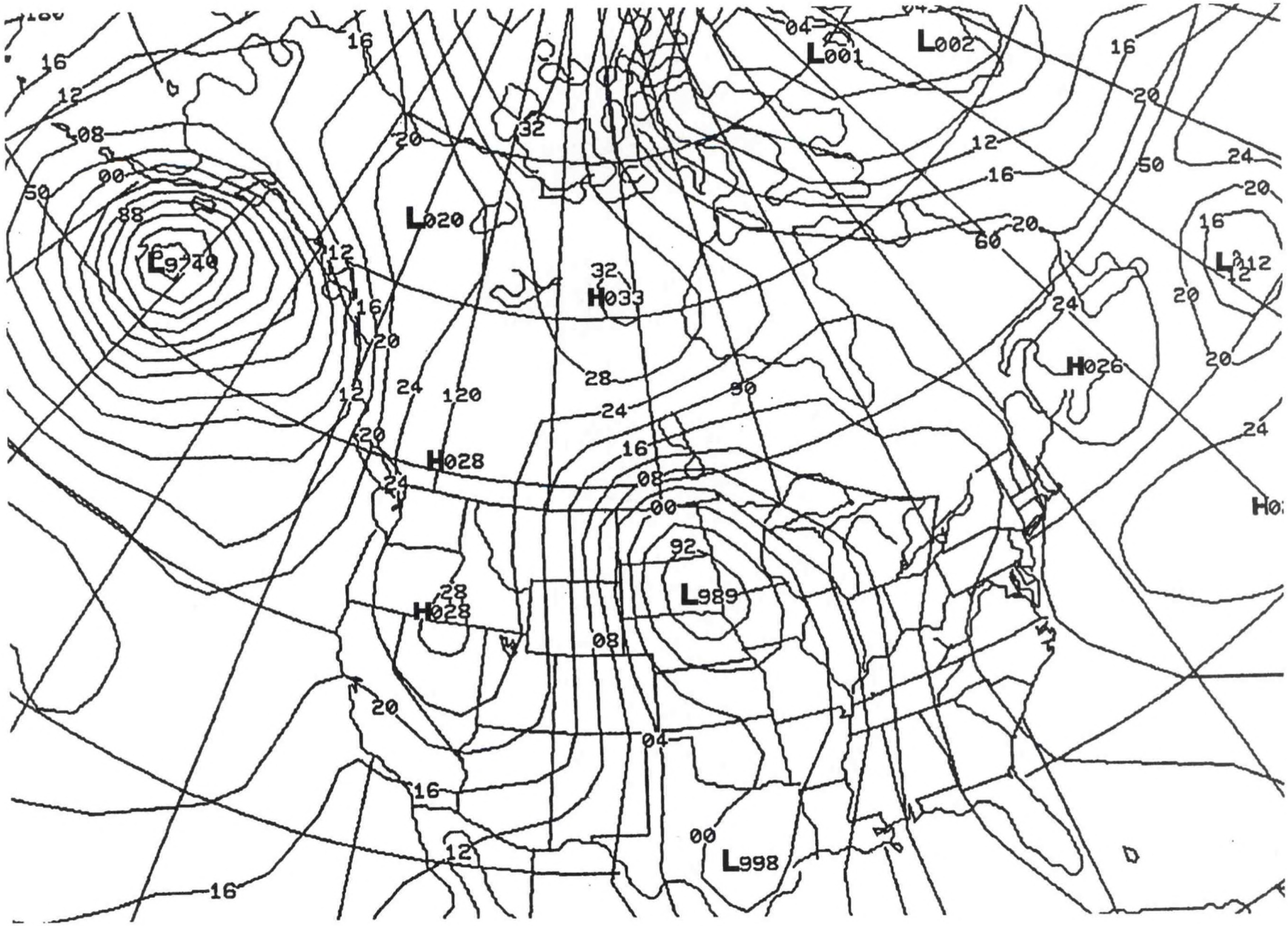

Figure 24(b). AVN model forecast for mean sea-level isobars valid 1200 UTC 19 April 1992. Contour interval every 4 mb.

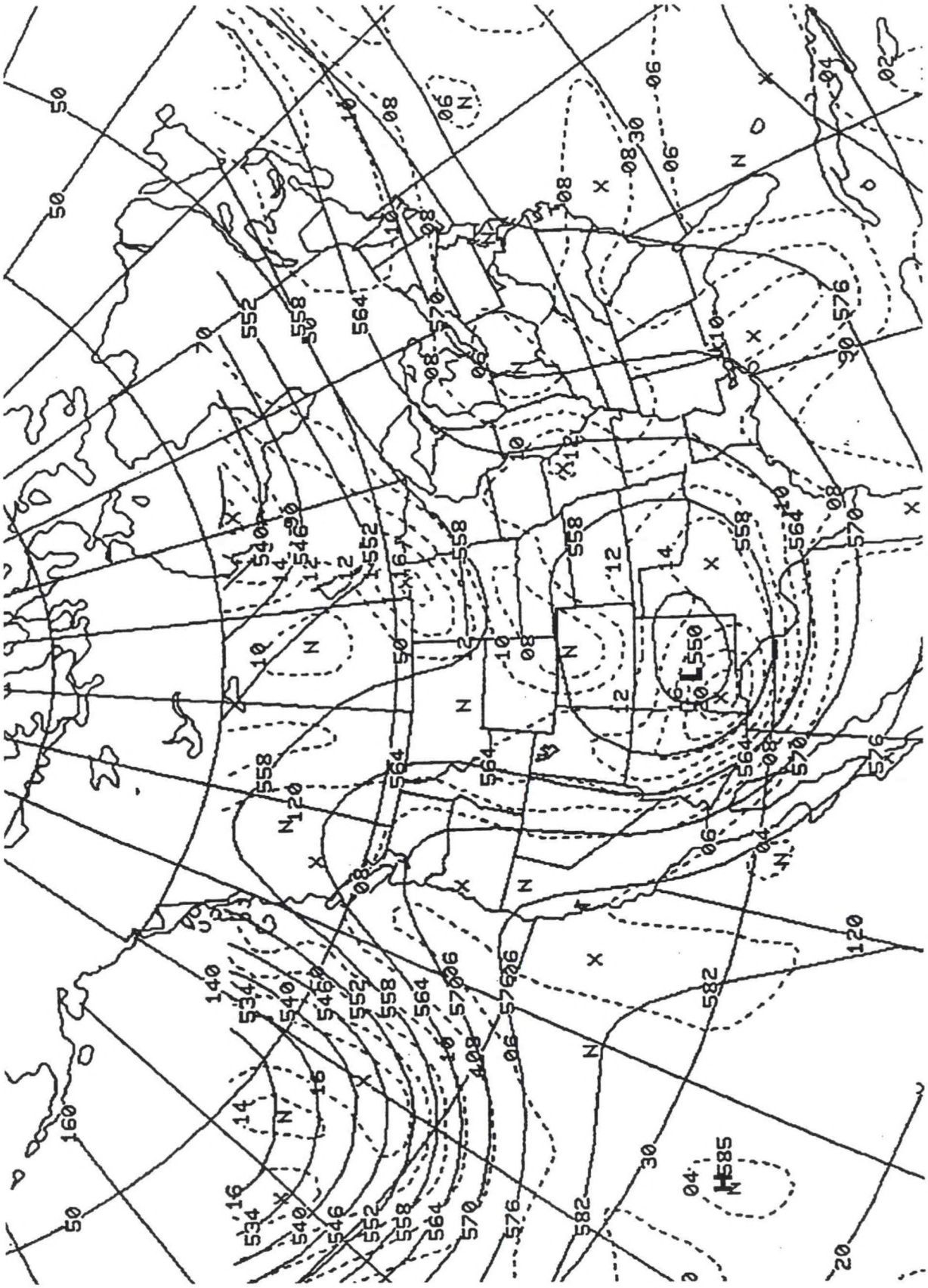

Figure 24(c). Same as (a), except the LFM model.

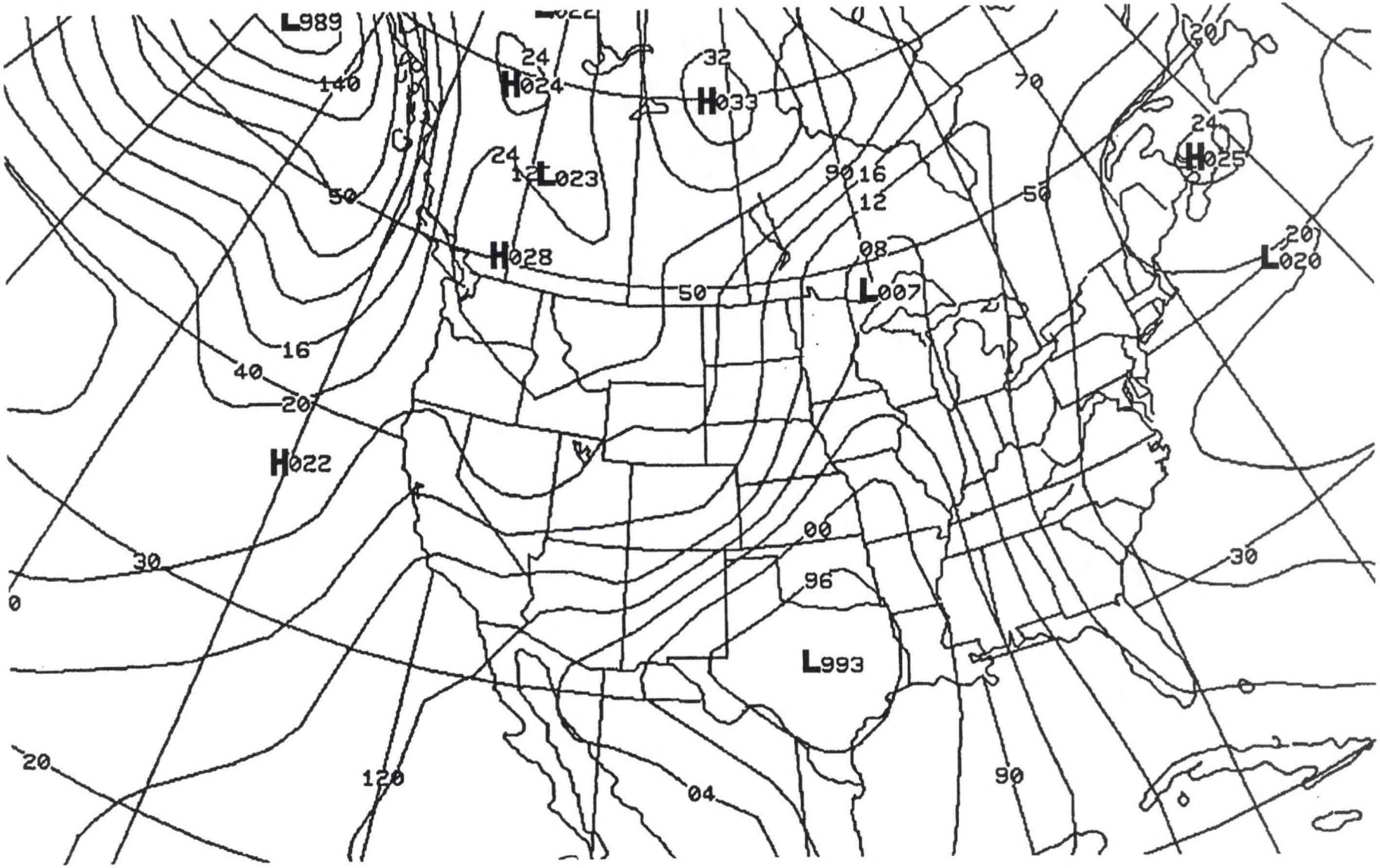

Figure 24(d). Same as (b), except the LFM model.

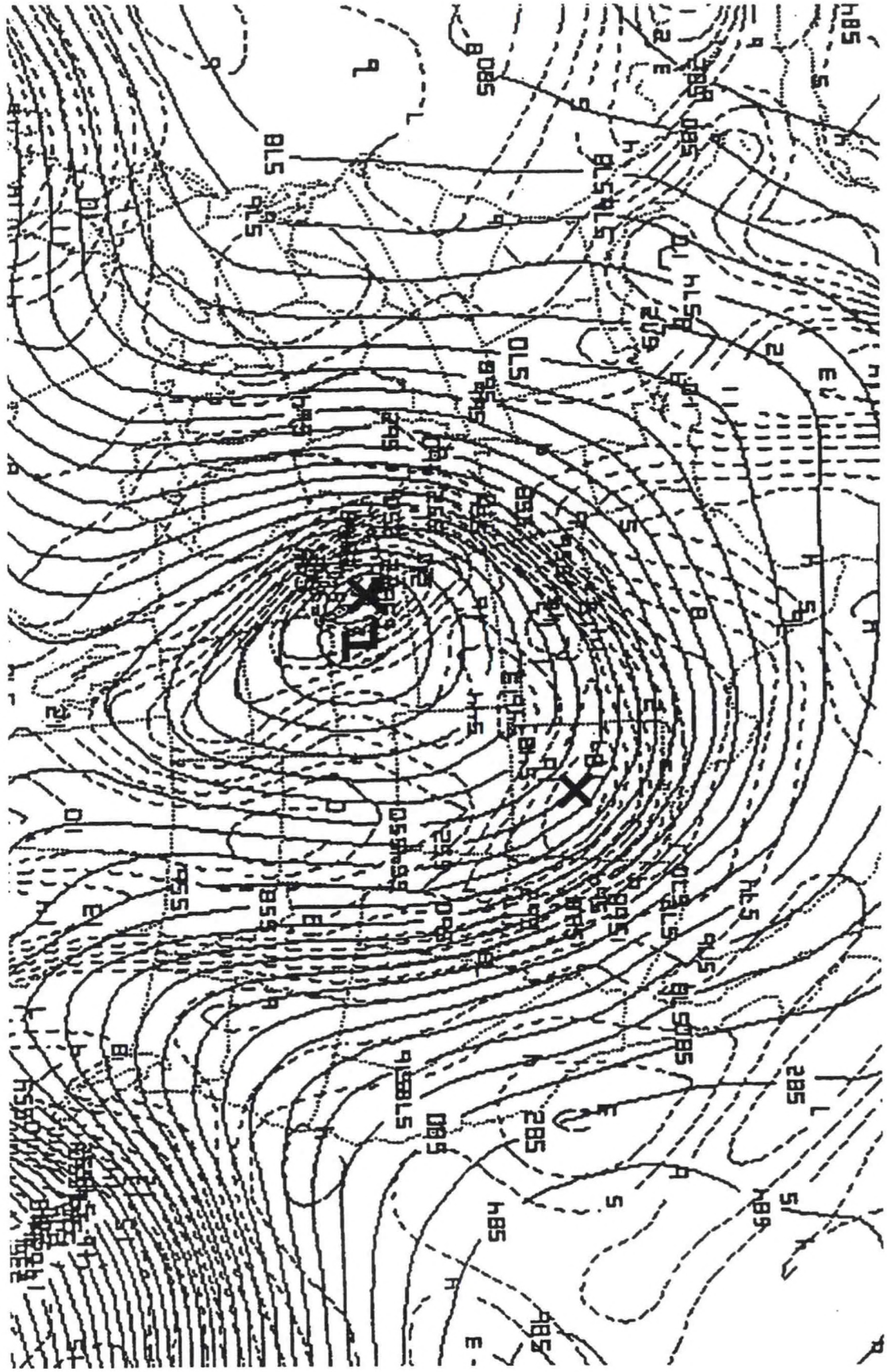

Figure 24(e). Same as Figure 23(a), but for the 48-hour NGM forecast.

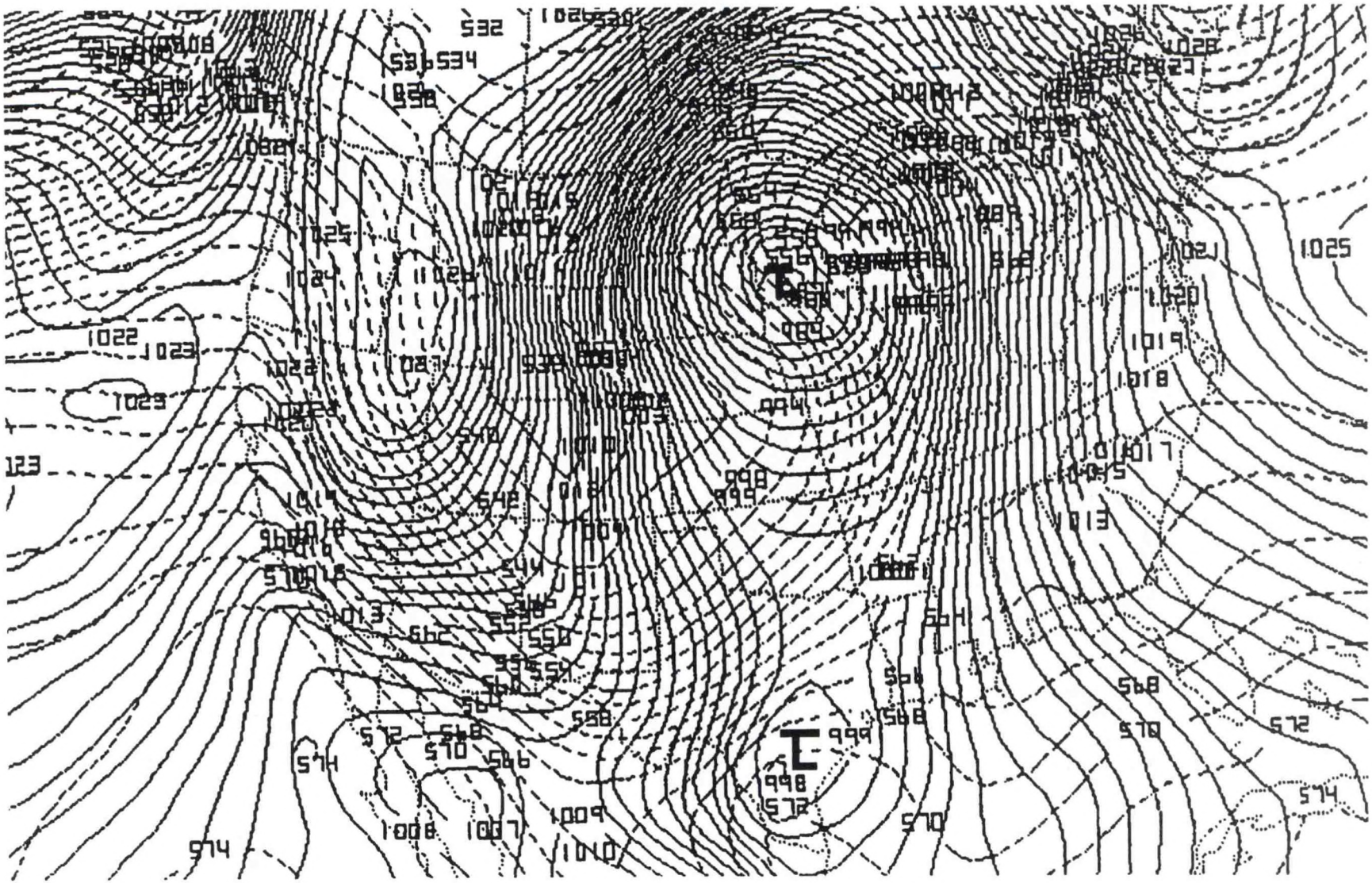

Figure 24(f). Same as Figure 23 (b), except 48-hour NGM forecast.

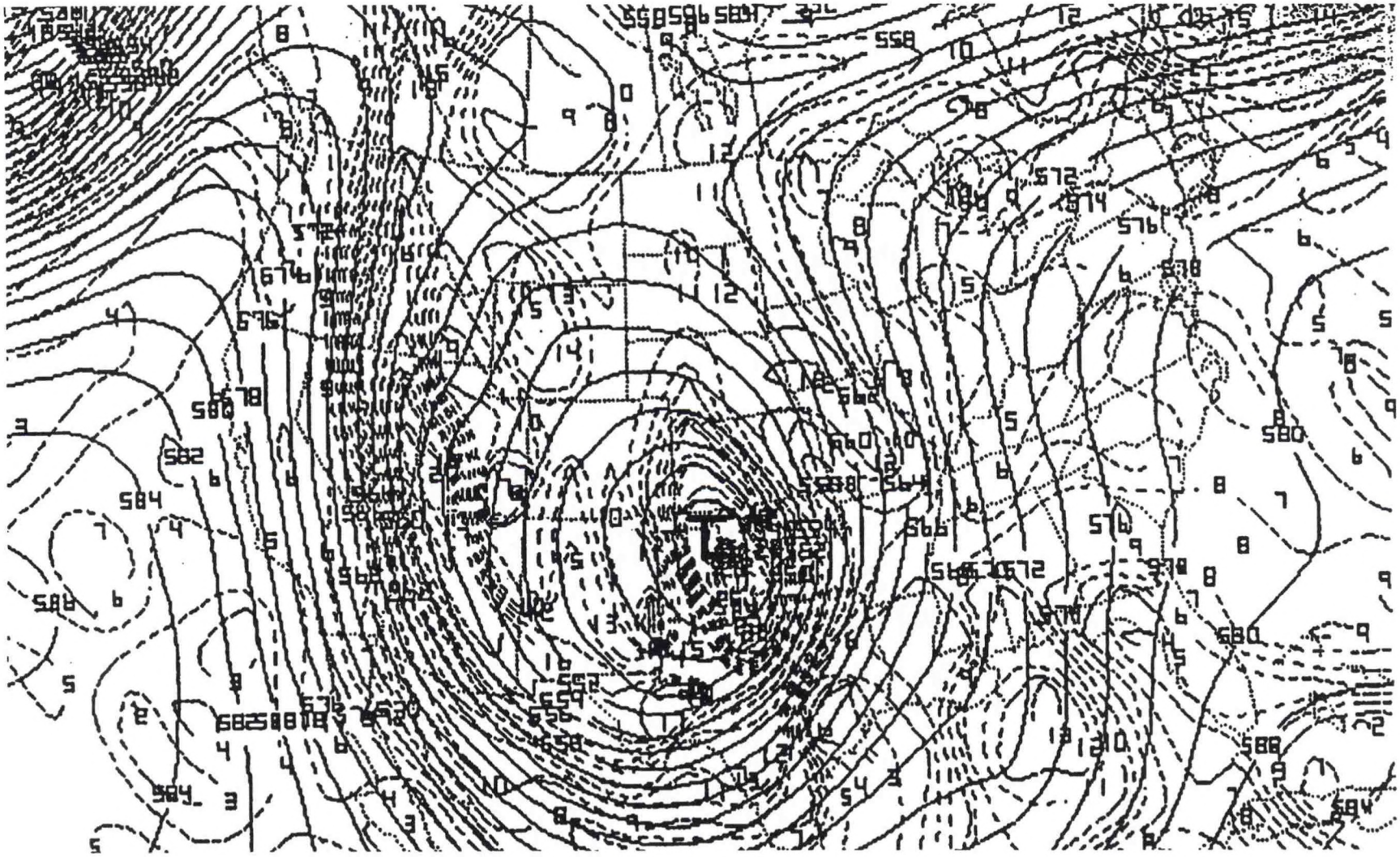

Figure 24(g). Same as Figure 23 (a), but for the 48-hour Eta model forecast.

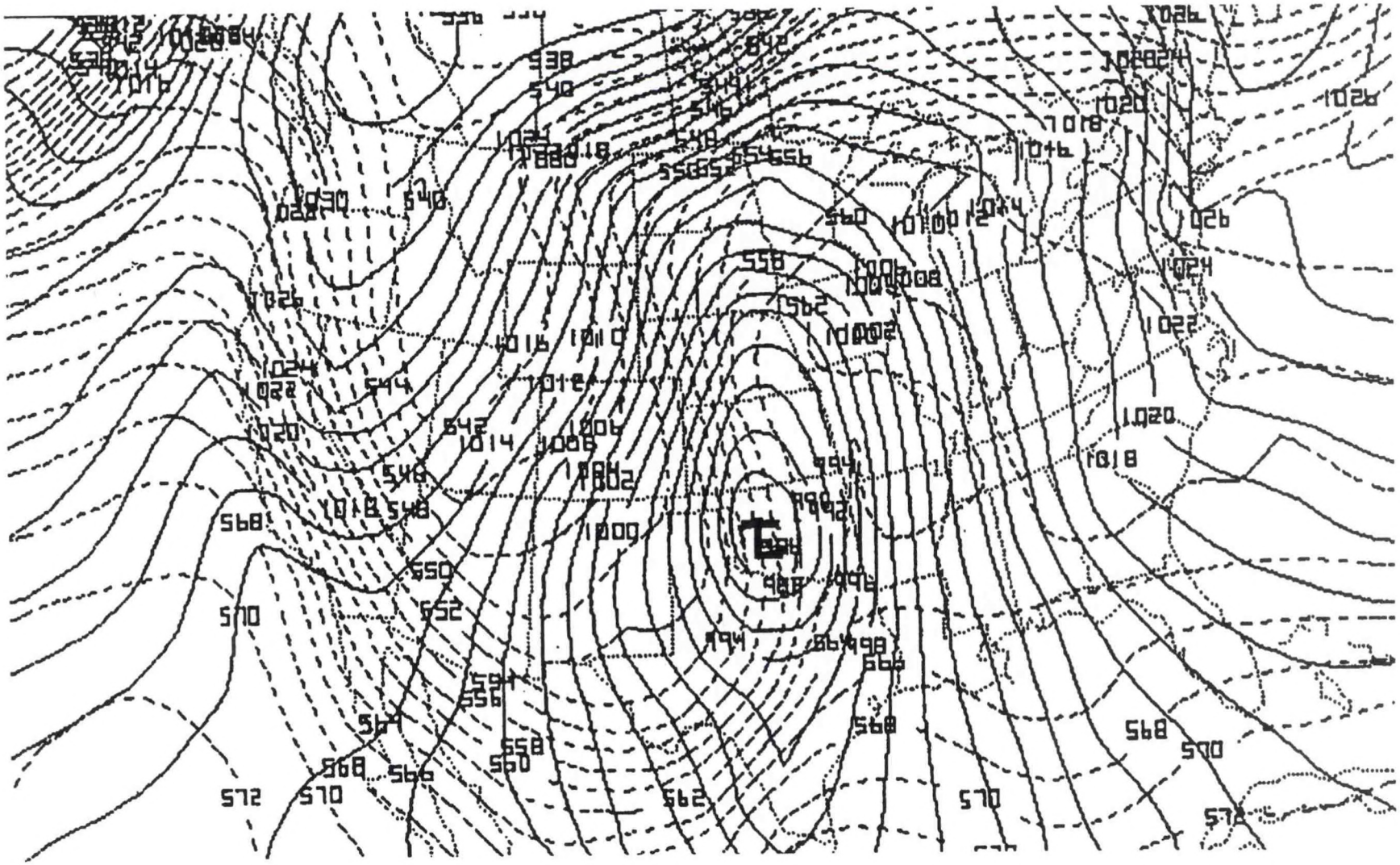

Figure 24(h). Same as Figure 23(b), but for the Eta model forecast.

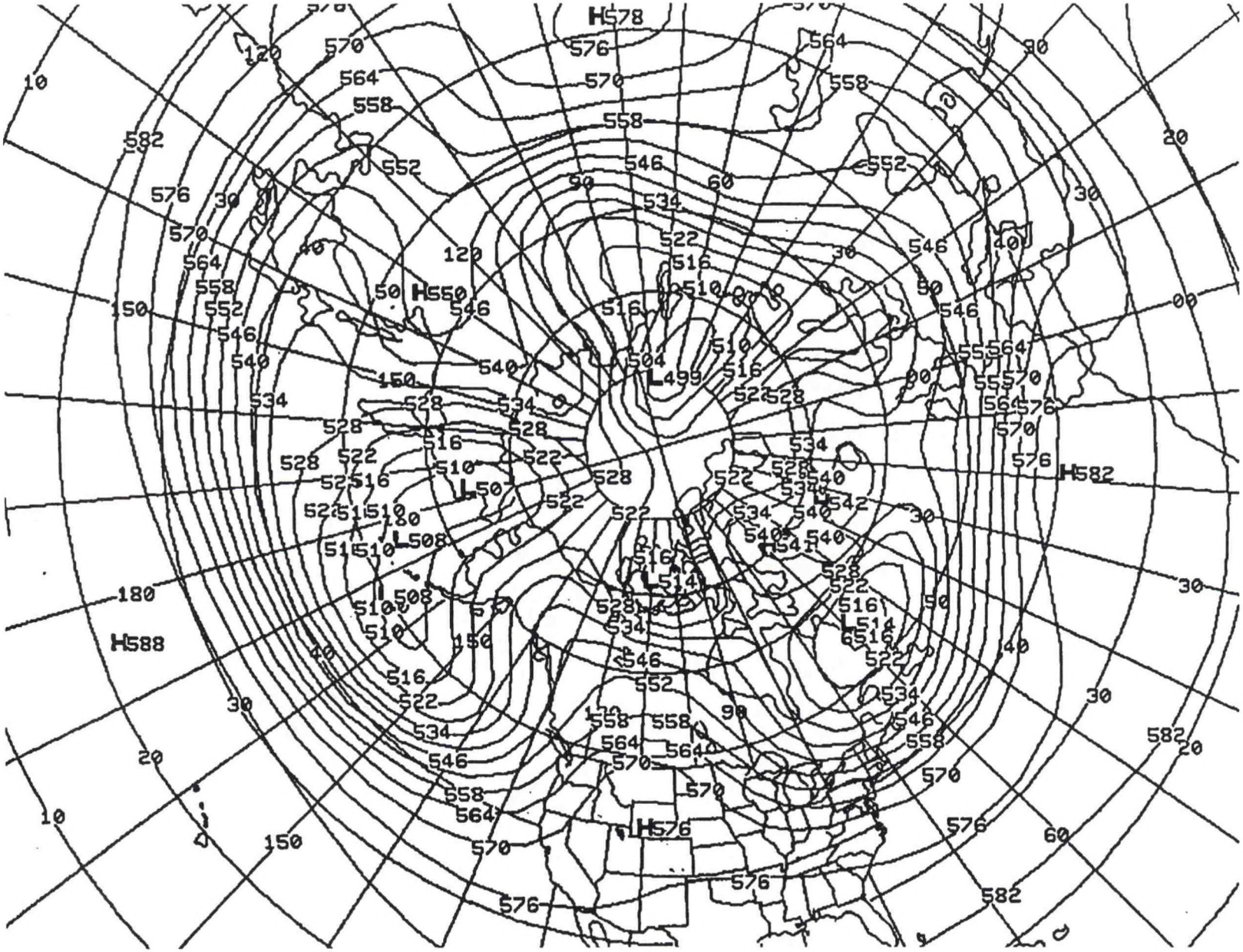

Figure 25(a). Same as Figure 9, but valid 0000 UTC 15 April 1992.

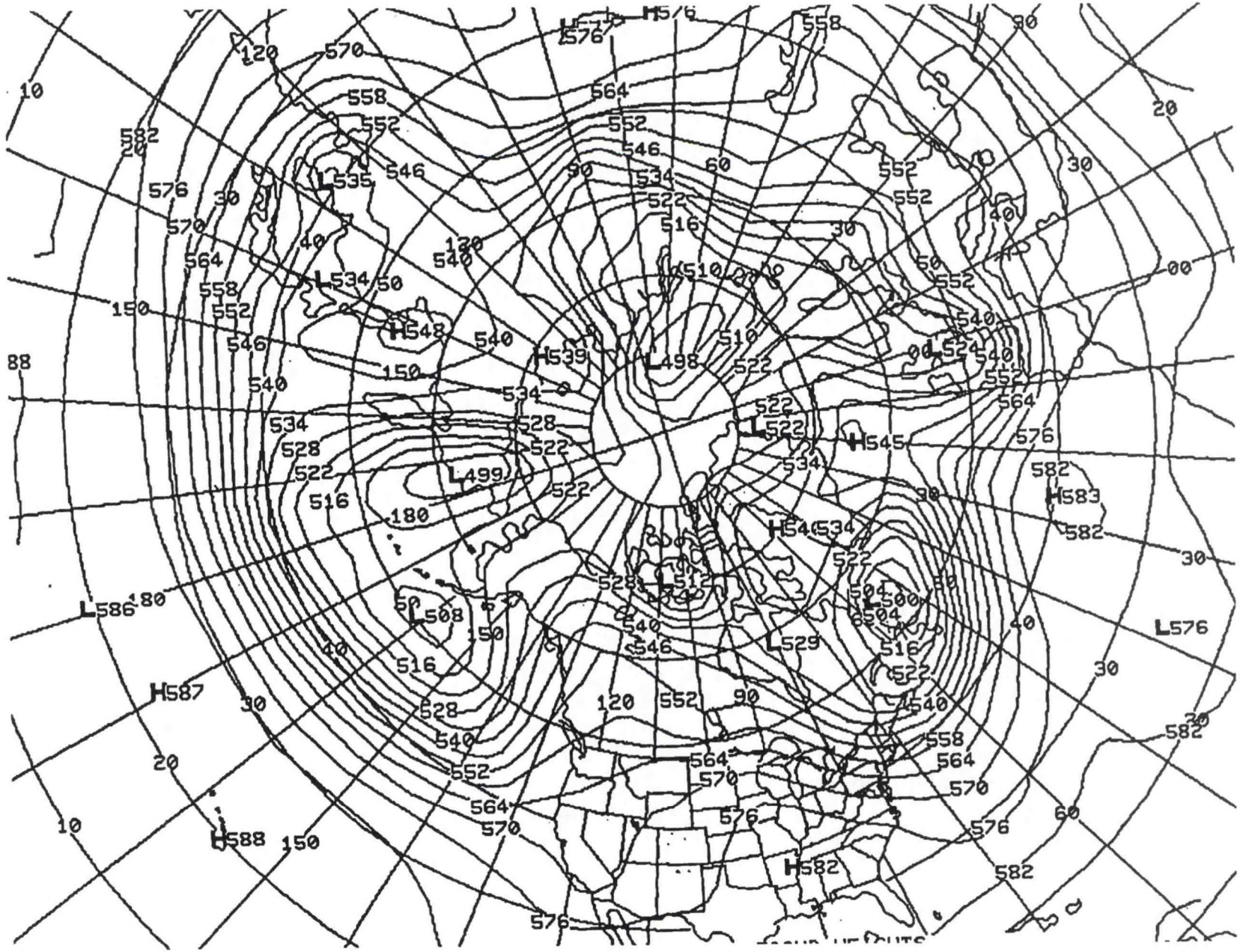

Figure 25(b). Same as Figure 10, except valid at 0000 UTC 15 April 1992.

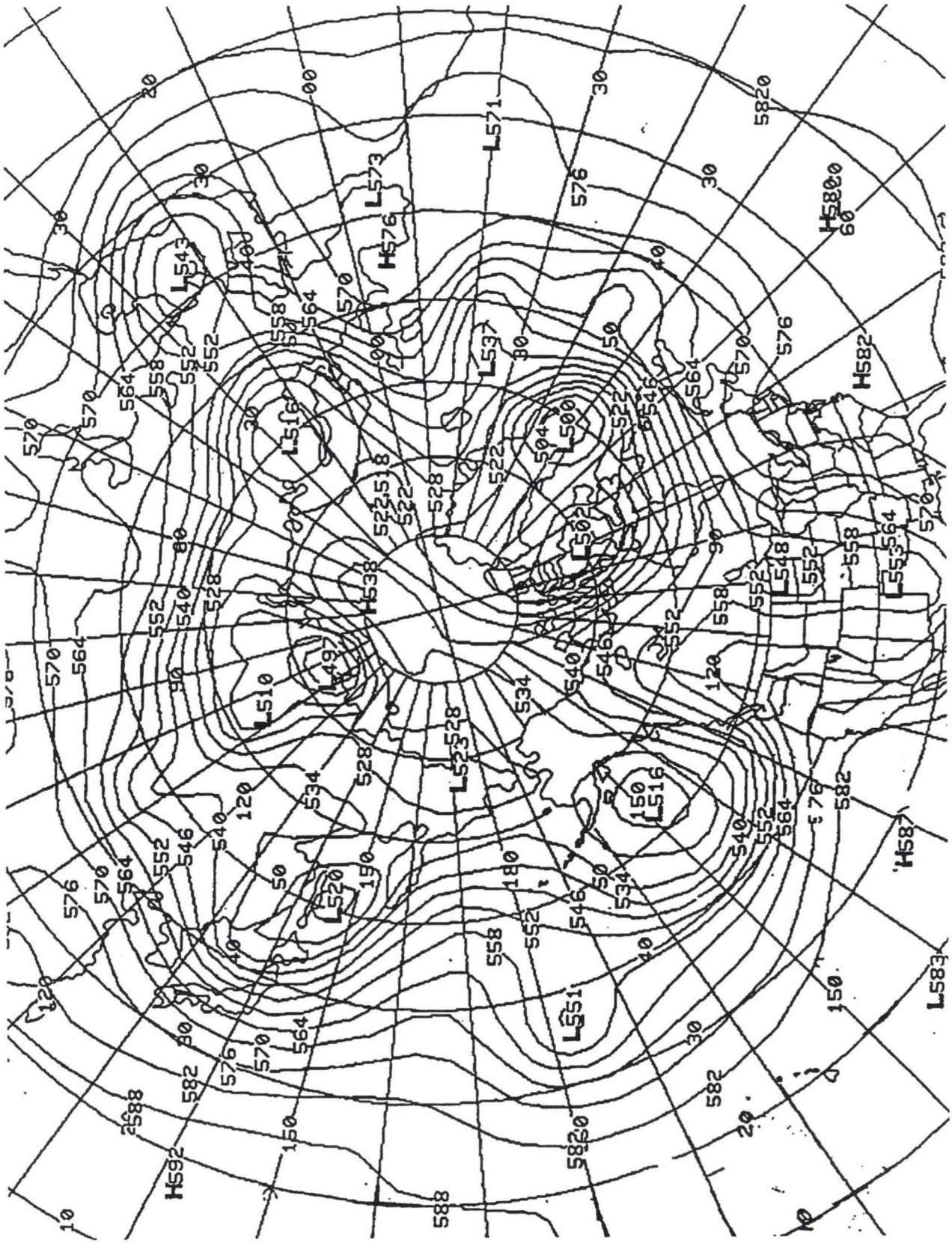

Figure 25(c). Same as (b) except valid at 0000 UTC 20 April 1992.

4. STATISTICAL RESULTS

While global model error of the NCEP medium-range forecast model (MRF), in association with low to high zonal wave number transitions, has been observed, a statistical study was warranted. The latter was necessary to confirm a relationship between MRF error and wave number transitions.

As stated, a spectral package that decomposes global height data into Fourier components has been developed. Since the focus of this paper is the middle latitudes, data was processed over the 30° to 60° N band. The spectral package outputs amplitude (A) and phase (Φ) for each wave number (K) in the band from 1 to 8. This process is performed for both the 0000 and 1200 UTC cycles on the 00-hour (analysis) and 72-hour forecasts. Since interest was in how well the MRF forecasts the amplitude and phase of these planetary waves, total model error (E) was defined as a difference of the first 8 wave components of the forecasts and analyses corresponding to the same valid time. E is given by:

$$E = \frac{1}{N} \sum_{l=1}^{N} \sum_{k=1}^{8} \left[A_{72,k} \cos\left(\frac{2\pi lk}{N} - \Phi_{72,k} \right) - A_{00,k} \cos\left(\frac{2\pi lk}{N} - \Phi_{00,k} \right) \right]$$

where subscript "72" and "00" define the 72-hour forecast and analysis, respectively, l is the latitude (computed in increments of 1°) and K is the zonal wave number.

Figure 26 illustrates the spectral decomposition (left) and model error (right). From this 138-day sample (from 12 Feb 93 to 1 Jul 93), periods with obvious hemispheric transitions from low to high wave number are identified. These are indicated on the chart with heavy bars. During this period there were 17 breakdown events and 19 periods of no breakdowns (the periods between events). Identification of these periods was based on a combination of observing the 500-mb height analysis, utilizing the conceptual model given in Figures 1-4, and the left side of Figure 26.

The mean duration of the breakdown periods (from the peak amplitude of the low wave number to the peak of the high wave number) was 3 days, with a standard deviation of 18 hours. Total error as defined, was computed for each 12-hour cycle and plotted. To identify periods of significant error, it was arbitrarily defined as a 1.5-standard deviation limit above the mean. "Significant" error was identified by dotted peaks on the error curve - above a trend line. This quantity was computed by identifying 1.5 standard deviation error for the center point in time, and sloping it accordingly to a linear regression of E. As one would expect, model error falls off as the warm season approaches. Note those 20 significant MRF error events occurred during the 4.5 month period (missing data periods were not included).

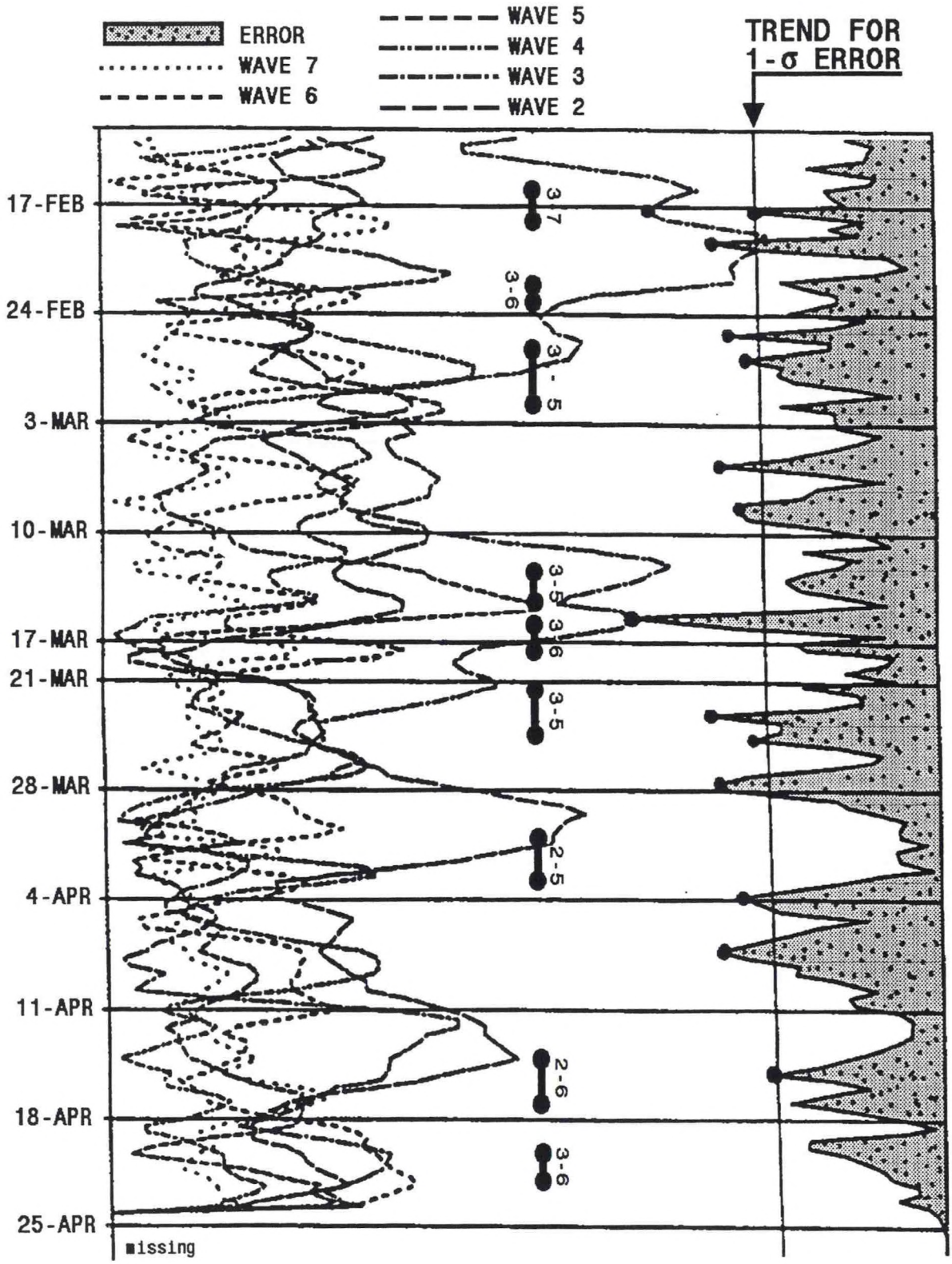
ERROR
WAVE 7
WAVE 6
WAVE 5
WAVE 4
WAVE 3
WAVE 2
TREND FOR
1-σ ERROR
17-FEB
24-FEB
3-MAR
10-MAR
17-MAR
21-MAR
28-MAR
4-APR
11-APR
18-APR
25-APR
3-7
3-6
3-5
3-5
3-6
3-5
2-5
2-6
3-6
missing

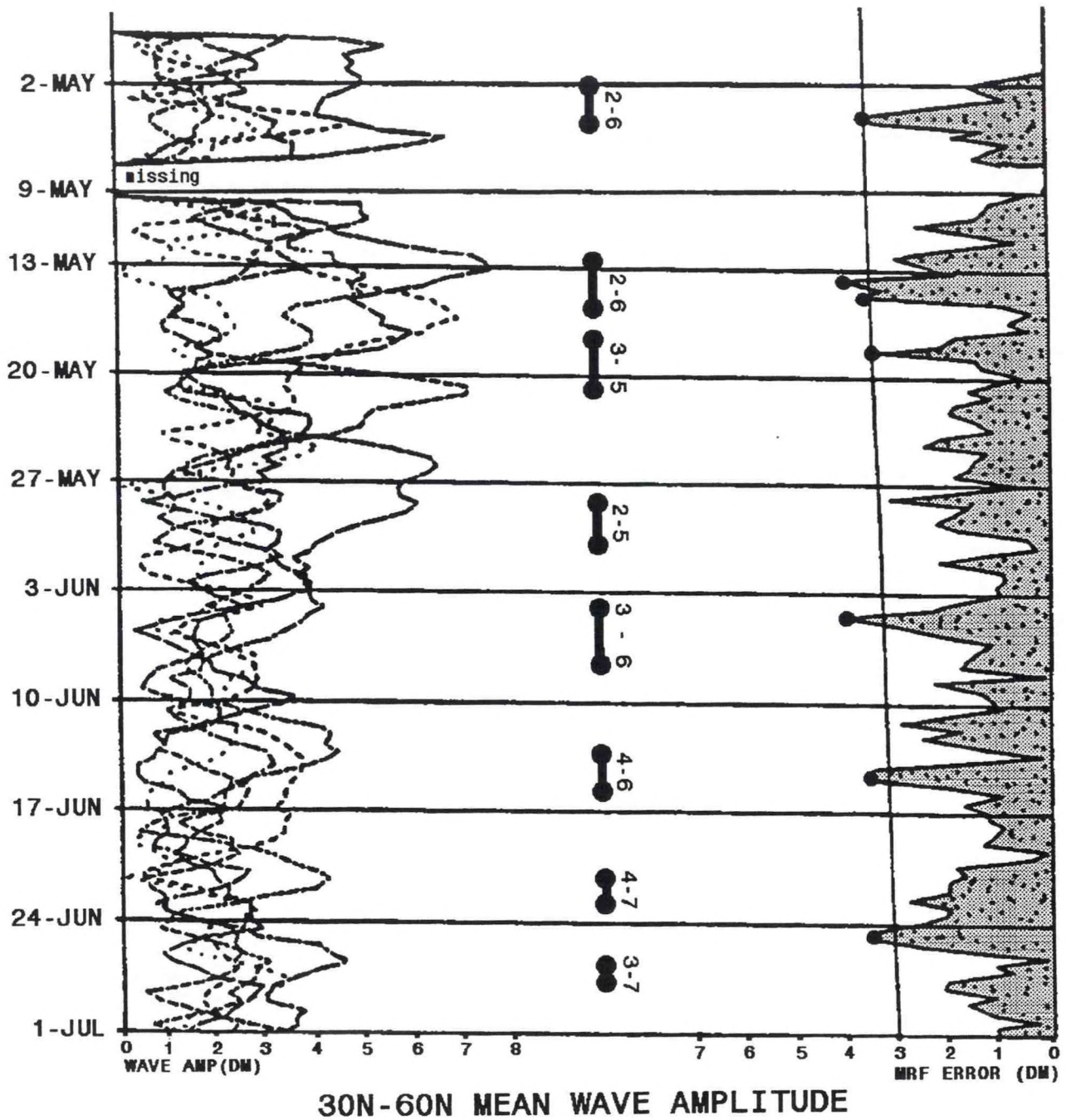

Figure 26. Time series representation of the MRF forecast error. Time is on the ordinate, while wave amplitude (gpdm) and MRF errors (gpdm) are depicted on the abscissa. This is over the latitude band of 30° to 60° N. Wave numbers are indicated on the legends. Wave number transition events are indicated by the "dumbbells". See text for further detail.

Table 1 indicates the results of comparing breakdown periods with significant error events. Computations indicated a correlation of .27 and a reasonably high POD (assuming the breakdown event is a predictor of model error peak). However, while breakdown is related to model error, a significant number of events are uncorrelated.

TABLE 1

CONTINGENCY TABLE REPRESENTATION OF SIGNIFICANT MRF ERROR AND LOW TO HIGH WAVE NUMBER TRANSITIONS
(See text for further detail.)

RELATIONSHIP BETWEEN BREAKDOWN EVENTS AND SIGNIFICANT MRF ERROR

- Breakdown defined by decrease of long wave (wave 2-4) amplitude, followed by increase in medium wave amplitude (waves 4-7), within a 2-5 day period.
- MRF error computed by summing mean height error for 72-hour forecasts between 30 -60N at wave numbers 1 to 8. Significant error defined by those points greater than 1 standard deviation above the 4.5 month trend in mean error.
- Contingency table - 12 Feb to 1 Jul 1993

Breakdown Period Observed	Significant MRF Error: N	Significant MRF Error: Y
N	13	6
Y	7	10

POD = 0.59; FAR = 0.32; CSI = 0.44; TSS = 0.27

5. CONCLUSION

The purpose of this report was to present an observationally formulated conceptual model of northern hemispheric-scale low wave number to high zonal wave number transition events, and illustrate the errors in the operational numerical models that often accompany them. For this study, statistical results were given to verify the correlations between MRF forecast error and transition events. Other models were not available at the time of this work.

Wave number transitions are a very significant forecast problem, and often result in a great deal of baroclinic development. Three cases of these events were shown.

For the northern hemisphere, there can be simultaneous storminess near the trough positions (Figure 4). In the lower 48 states of the U.S., there is often a geopotential height trough from the Rockies to the Great Plains. In turn, these breakdowns are frequently accompanied by severe convective weather (including tornadoes), blizzards, floods, etc. in the mid section of the U.S.

An enumerated summary of features, for low to high zonal wave number transitions, which forecasters can look for, was given at the end of Section 2. A brief restatement follows.

1. Using full-disk satellite imagery, look for persistent (5-7 days) widespread deep-moist tropical convection, especially along and just to the west of the Dateline. If that convection is moving eastward, watch for longitudinal expansion of the extratropical northern hemispheric westerlies across the central Pacific Ocean Basin.

2. If the westerlies do expand, and a configuration similar to Figure 3 appears, beware of a transition.

3. Using water vapor imagery, look for deepening of a trough in the mid Pacific, and enhancement of deep moist convection just southeast of it. If that occurs, a wave number transition is likely in progress. Result, trough in the mid and upper tropospheric height field across the western U.S., like shown in Figure 4.

A point that should be made is the above scenario is ideal. No attempt is being made to say "the tropics always force the mid-latitudes". However, this enumerated summary may help operational forecasters recognize real-time signals to anticipate relatively poor performance of the operational global models.

It was not the intent of this report to get into too involved with planetary wave theory and the causes of model forecast errors during breakdowns. However, there are some tools suitable for monitoring and understanding low to high wave number transitions. Formulating these tools, and a better understanding of the dynamics of wave number transitions, including predicting them, are topics of ongoing and future work. A climatology of wave number transitions must also be included in any future efforts.

In brief, some diagnostic tools might be applying Rossby ray tracing theory to isentropic potential vorticity analyses of the northern hemispheric extratropics (Hoskins and Karoly 1981, Hoskins et al. 1985, Hoskins 1983), transformed Eulerian diagnostics (Pfeffer 1992), calculating atmospheric angular momentum and extended Eliassen-Palm flux vectors (Holton 1992, Hoskins et al. 1983). Others could include spectral analysis and energetics packages (example, Chen 1982, and Chen and Shukla 1983, on using spectral energetics as a diagnostic tool) and assessing northern hemispheric-scale static stability (Weng and Barcilon 1988). Any diagnostic package formulated for monitoring wave amplitude and global model error must be configured for real-time use.

Besides diagnostic tools, ensemble forecasting methods are being studied. As stated in the Introduction to this report, ensemble forecasting is a dynamical systems approach designed to maximize utility in all numerical models (references mentioned in the Introduction). With these methods, there is belief there would be greater predictability of wave number transitions. That would be helpful for especially week 1 and week 2 forecasts.

The errors in the operational numerical models that often occur during low to high zonal wave number transitions are believed to be due to model sensitivities in the presence of low-frequency atmospheric variabilities (O'Lenic and Livezey 1989, Nogues-Paegle et al. 1992) and scale interactions (Tracton 1990). In addition, sources of error may be introduced by problematical physical parameterizations, and initialization problems as the result of unresolvable scales of motion involved with deep moist tropical convection (for example, Bengtsson 1990). The latter could play a key role in breakdown events (works done by Weickmann 1983; Weickmann et. al. 1985, 1990; and Kiladis and Weickmann 1992a, 1992b may provide some justification to this hypothesis).

Diagnostic tools and ensemble prediction methods, mentioned above, need to be workstation based for maximum utility, especially for AWIPS in the modernized National Weather Service (NWS). These tools would not only help improve predictability of low to high wave number transitions, but also aid in understanding the dynamics of planetary-scale circulation in real-time, and the cascading effects down to the mesoscale. Result, improved NWS products and services to the users (including the public).

6. ACKNOWLEDGMENTS

The authors wish to thank the COMET (CO-operative Meteorology Education and Training) group, part of UCAR (University Corporation for Atmospheric Research), located in Boulder Colorado, for the support given to us through their "mentor" program. Appreciation is also extended to Dr. Klaus Weickmann, affiliated with the Climate and Diagnostics Center (CDC) Group of ERL, for his ideas related to our work. Dr. John Brown at NOAA/ERL, and Dr. M. Steven Tracton at NOAA/NCEP/EMC kindly reviewed earlier versions of this manuscript. Finally, Deborah White and Michael Manker, CRH SSD, prepared the text for publication and provided graphical support, respectively.

7. REFERENCES

Barnston, A.G., and R.E. Livezey, 1987: Classification, seasonality and persistence of low-frequency atmospheric circulation patterns. *Mon. Wea. Rev.*, **115**, 1083-1126.

Bengtsson, L., 1990: *Advances in numerical prediction of the atmospheric circulation in the extratropics.* In Extratropical Cyclones: The Erik Palmen Memorial Volume. C. Newton and E.O. Holopainen eds. AMS, 193-220.

_____, 1985: Medium-range forecasting at the ECMWF. Advances in Geophysics, 28B, 3-54.

Berry, E.K., 1993: Performance of the NGM, AVN, LFM and ETA models during the heavy snow event of April 20-21 1992 across the Central Plains: An observational diagnostic/comparison. Post-prints, 3rd National Heavy Precipitation Workshop. NOAA Tech. Memo. NWS ER-87, 331-346.

_____, J.A. McGinley and P. Schultz, 1993: Global model errors associated with rapid low to high zonal wave number transitions. *Preprints, 13th Conf. on Wea. Anal. and Fcstg. incl. Sym. On Flash Floods.* AMS, 117-120.

Black, R.X., and R.M. Dole, 1993: The dynamics of large-scale cyclogenesis over the North Pacific Ocean. *J. Atmos. Sci.*, **50**, 421-442.

Blackmon, M.L., 1976: A climatological spectral study of the 500 mb geopotential height of the Northern hemisphere. *J. Atmos. Sci.*, **33**, 1607-1623.

Cai, M., 1992: An analytic study of the baroclinic adjustment in a quasi-geostrophic two-layer channel model. *J. Atmos. Sci.*, **49**, 1594-1605.

Chen, T.C., 1982: A further study of spectral energetics in the Winter atmosphere. *Mon. Wea. Rev.*, **110**, 947-961.

Chen, T.C., and J. Shukla, 1983: Diagnostic analysis and spectral energetics of a blocking event in the GLAS climate model simulation. *Mon. Wea. Rev.*, **111**, 3-22.

Clark, J.E.H., 1979: Energy propagation by interacting Rossby waves. *Atmos. Ocean.*, **17(4)**, 321-332.

Glantz, M.H., R.W. Katz and N. Nicholls, 1991: *Teleconnections linking worldwide climate anomalies.* Cambridge University press, 535 pp.

Haines, K., P. Malanotte-Rizzoli and M. Morgan, 1993: Persistent jet stream intensifications: A comparison between theory and data. *J. Atmos. Sci.*, **50**, 145-154.

Hide, R., 1953: Some experiments on thermal convection in a rotating liquid. *Quart. J. Roy. Met. Soc.*, **79**, 161.

Hoke, J.E., N.A. Phillips, G.J. DiMego, J.J. Tuccillo and J.G. Sela: The Regional Analysis and Forecast System of the National Meteorological Center. *Wea and Fcstg.*, **4**, 323-334.

Holton, J.R. ,1992: *An Introduction to Dynamic Meteorology*, 3rd ed., Academic Press, 511 pp.

_____, 1979: *An Introduction to Dynamic Meteorology*, 2nd ed., Academic Press, 391 pp.

Horel, J.D, and J.M. Wallace, 1981: Planetary-scale atmospheric phenomena associated with the Southern Oscillation. *J. Atmos. Sci.*, **109**, 813-829.

Hoskins, B.J., 1990: *Theory of extratropical cyclones. In Extratropical Cyclones: The Erik Palmen Memorial Volume.* C. Newton and E.O. Holopainen eds. AMS, 63-80.

_____, 1983: Dynamical processes in the atmosphere and the use models. *Quart. J. Roy. Met. Soc.*, **109**, 1-21.

_____, I.N. James, and G.H. White, 1983: The shape, propagation and mean-flow interaction of large-scale weather systems. *J. Atmos. Sci.*, **40**, 1595-1612.

_____, and D.J. Karoly, 1981: The steady linear response of a spherical atmosphere to thermal and orographic forcing. *J. Atmos. Sci.*, **38**, 1179-1196.

_____, M.E. McIntyre and A.W. Robertson, 1985: On the use and significance of isentropic potential vorticity maps. *Quart. J. Roy. Met. Soc.*, **111**, 877-946.

Hovmöller, E., 1949: The trough-and-ridge diagram. *Tellus*, **1**, 62-66.

Janic, Z.I., 1990: The step-mountain coordinate: Physical package. *Mon. Wea. Rev.*, **118**, 1429-1443.

Kiladis, G.N., and K.M. Weickmann, 1992(a): Circulation anomalies associated with tropical convection during northern Winter. *Mon. Wea. Rev.*, **120**, 1900-1923.

_____, 1992(b): Extratropical forcing of tropical Pacific convection during northern Winter. *Mon. Wea. Rev.*, **120**, 1924-1938.

Kimoto, M., and M. Ghil, 1993(a): Multiple flow regimes in the northern hemisphere Winter. Part I: Methodology and hemispheric regimes. *J. Atmos. Sci.*, **50**, 2625-2643.

_____, 1992(b): Multiple flow regimes in the northern Winter. Part II: Sectorial regimes and preferred transitions. *J. Atmos. Sci.*, **50**, 2645-2673.

Krishnamurti, T.N., J. Molinari, H-L. Pan, and V. Wong, 1977: Downstream amplification and formation of monsoon disturbances. *Mon. Wea. Rev.*, **105**, 1281-1297.

Lanzante, J.R., 1990: The leading modes of 10-30 day variability in the extratropics of the Northern hemisphere during the cold season. *J. Atmos. Sci.*, **47**, 2115-2140.

Livezey, R.E., and K.C. Mo, 1987: Tropical-extratropical teleconnections during the Northern hemisphere Winter. Part II: Relationships between monthly mean Northern hemisphere circulation patterns and proxies for tropical convection. *Mon. Wea. Rev.*, **115**, 3115-3132.

Lorenz, E.N., 1963: The mechanics of vacillation. *J. Meteor.*, **20**, 448-464.

Lyons, S.W., and B. Hundermark, 1992: Zonal-wind oscillations over the Western Hemisphere during Winter: Further evidence of a zonal-eddy relationship. *Mon. Wea. Rev.*, **120**, 1878-1899.

Madden, R.A., and P.R. Julian, 1972: Description of global-scale circulation cells in the tropics with a 40-50 day period. *J. Atmos. Sci.*, **29**, 1109-1123.

Mesinger, F., Z.I. Janjic, S. Nickovic, D. Gavrilov and D.G. Deavon, 1988: The step-mountain coordinate: Model description and performance for cases of Alpine lee cyclogenesis and for a case of an Appalachian redevelopment. *Mon. Wea. Rev.*, **116**, 1493-1518.

Namias, J., 1950: The index cycle and its role in the general circulation. *J. Meteor.*, **7**, 130-139.

National Severe Storms Forecast Center (NSSFC), 1990: National Weather Summary and the severe weather logs from the Severe Environmental Local Storms (SELS) Unit for the period of March 11-15 1990.

Nogues-Paegle, J., D.A. Rodgers and K.C. Mo, 1992: Low-frequency predictability of the dynamical extended-range forecast experiment. *Mon. Wea. Rev.*, **120**, 2025-2041.

O'Lenic, E.A., and R.E. Livezey, 1989: Relationships between systematic errors in medium range numerical forecasts and some of the principle modes of low-frequency variability of the Northern hemisphere circulation. *Mon. Wea. Rev.*, **117**, 1262-1280.

Palmen, E., and C.W. Newton, 1969: *Atmospheric Circulation Systems*, Academic Press, 603 pp.

Pan, H.L., J. Derber, D. Parrish, W. Gemmill, S-Y Hong, and P. Caplan, 1995: Changes to the 1995 NCEP operational MRF model analysis/forecast system. Technical Procedures Bulletin No. 428, DOC, NOAA, NWS, 28pp.

Pfeffer, R.L., 1992: A study of eddy-induced fluctuations of the zonal-mean wind using conventional and transformed Eulerian diagnostics. *J. Atmos. Sci.*, **49**, 1036-1050.

Philander, S.G., 1989: El Nino, La Nina, and the Southern Oscillation. Academic Press, 293 pp.

Rasmusson, E.M., and T.H. Carpenter, 1982: Variations in tropical sea surface temperature and surface fields associated with the Southern Oscillation/El Nino. *Mon. Wea. Rev.*, **110**, 354-384.

Shapiro, M.A., and D. Keyser, 1990: *Fronts, jet streams and the tropopause. In Extratropical Cyclones: The Erik Palmen Memorial Volume.* C. Newton and E.O. Holopainen eds., AMS, 167-191.

Simmons, A.J., and B.J. Hoskins, 1979: The downstream and upstream development of unstable baroclinic waves. *J. Atmos. Sci.*, **36**, 1239-1254.

Toth, Z, 1993: Preferred and unpreferred circulation types in the northern hemisphere Wintertime phase space. *J. Atmos. Sci.*, **50**, 2868-2888.

_____, and E. Kalnay, 1993: Ensemble forecasting at NMC: The generation of perturbations. *Bull. Amer. Meteor.*, **74**, 2317-2330.

Tracton, M.S., 1990: Predictability and its relationship to scale interaction processes in blocking. *Mon. Wea. Rev.*, **118**, 1666-1695.

_____, and E. Kalnay, 1993: Operational ensemble prediction the National Meteorological Center: Practical aspects. *Wea and Fcstg.*, **8**, 379-398.

Trenberth, K.E., 1991: *General characteristics of El Nino-Southern Oscillation. In Teleconnections Linking Worldwide Climate Anomalies.* M.H. Glantz, R.W. Katz and N. Nicholls eds.. Cambridge University Press, 535 pp..

Wallace, J.M., and M.L. Blackmon, 1983: Observations of low-frequency atmospheric variability. In Large-Scale *Dynamical Processes in the Atmosphere.* B.J. Hoskins and R.P. Pearce eds.. Academic Press, 397 pp.

_____, and D.S. Gutzler, 1981: Teleconnections in the geopotential height field during the Northern hemisphere Winter. *Mon. Wea. Rev.*, **109**, 784-812.

Weickmann, K.M., 1983: Intraseasonal circulation and outgoing longwave radiation modes during northern hemisphere winter. *Mon. Wea. Rev.*, **111**, 1838-1858.

_____, G.R. Lussky, and J.E. Kutzbach, 1985: Intraseasonal (30-60 day) fluctuations of outgoing longwave radiation and 250 mb stream function during northern winter. *Mon. Wea. Rev.*, **113**, 941-961.

_____ ,and S.J.S. Khalsa, 1990: The shift of convection from the Indian Ocean to the western Pacific Ocean during a 30-60 day oscillation. *Mon. Wea. Rev.*, **118**, 964-978.

Weng, H. Y., and A. Barcilon, 1988: Wave number transition and wave number vacillation in Eady-type baroclinic flows. *Quart. J. Roy. Met. Soc.*, **114**, 1253-1269.

White, G.H.,1988a: Systematic performance of NMC medium-range forecasts 1985-1988. *Eighth Conf. on Numerical Weather Prediction,* Baltimore, AMS (Boston), , 466-471.

_____, 1988b: On the performance of the NMC medium range forecast model in Midlatitudes. *Palmen Memorial Symposium on Extratropical Cyclones,* Helsinki, Finland, AMS (Boston), 305-308.

Wobus, R.L., and E. Kalnay 1993: Two years of operational prediction of forecast skill at NMC. NMC Office Note 403. Available from NMC Development Division, NCEP, Washington DC, 20233.

NWS CR 47 Practical Application of a Graphical Method of Geostrophic Wind Determination. C.B. Johnson, November 1971 (COM 71-01084).

NWS CR 48 Manual of Great Lakes Ice Forecasting. C. Robert Snider, December 1971 (COM 72-10143).

NWS CR 49 A Preliminary Transport Wind and Mixing Height Climatology, St. Louis, Missouri. Donald E. Wuerch, Albert J. Courtois, Carl Ewald, Gary Ernst, June 1972 (COM 72-10859).

NWS CR 50 An Objective Forecast Technique for Colorado Downslope Winds. Wayne E. Sangster, December 1972 (COM 73-10280).

NWS CR 51 Effect on Temperature and Precipitation of Observation Site Change at Columbia, Missouri. Warren M. Wisner, March 1973 (COM 73-10734).

NWS CR 52 Cold Air Funnel Clouds. Jack R. Cooley and Marshall E. Soderberg, September 1973, (COM 73-11753/AS).

NWS CR 53 The Frequency of Potentially Unfavorable Temperature Conditions in St. Louis, Missouri. Warren M. Wisner,October 1973.

NWS CR 54 Objective Probabilities of Severe Thunderstorms Using Predictors from FOUS and Observed Surface Data. Clarence A. David, May 1974 (COM 74-11258/AS).

NWS CR 55 Detecting and Predicting Severe Thunderstorms Using Radar and Sferics. John V. Graff and Duane C. O'Malley June 1974 (COM 74-11335/AS).

NWS CR 56 The Prediction of Daily Drying Rates. Jerry D. Hill, November 1974 (COM 74-11806/AS).

NWS CR 57 Summer Radar Echo Distribution Around Limon, Colorado. Thomas D. Karr and Ronald L. Wooten, November 1974 (COM 75-10076/AS).

NWS CR 58 Guidelines for Flash Flood and Small Tributary Flood Prediction. Lawrence A. Hughes and Lawrence L. Longsdorf, October 1975 (PB247569/AS)

NWS CR 58 (Revised) March 1978 (PB281461/AS)

NWS CR 59 Hourly Cumulative Totals of Rainfall - Black Hills Flash Flood June 9-10, 1972. Don K. Halligan and Lawrence L. Longsdorf, April 1976 (PB256087).

NWS CR 60 Meteorological Effects on the Drift of Chemical Sprays. Jerry D. Hill, July 1976 (PB259593).

NWS CR 61 An Updated Objective Forecast Technique for Colorado Downslope Winds. Wayne E. Sangster, March 1977 (PB266966/AS).

NWS CR 62 Design Weather Conditions for Prescribed Burning. Ronald E. Haug, April 1977 (PB268034).

NWS CR 63 A Program of Chart Analysis (With Some Diagnostic and Forecast Implications). Lawrence A. Hughes, December 1977 (PB279866/AS).

NWS CR 64 Warm Season Nocturnal Quantitative Precipitation Forecasting for Eastern Kansas Using the Surface Geostrophic Wind Chart. Wayne E. Sangster, April 1979 (PB295982/AS).

NWS CR 65 The Utilization of Long Term Temperature Data in the Description of Forecast Temperatures. Arno Perlow,November 1981 (PB82 163064).

NWS CR 66 The Effect of Diurnal Heating on the Movement of Cold Fronts Through Eastern Colorado. James L. Wiesmueller, August 1982 (PB83 118463).

NWS CR 67 An Explanation of the Standard Hydrologic Exchange Format (SHEF) and Its Implementation in the Central Region. Geoffrey M. Bonnin and Robert S. Cox, April 1983 (PB83 193623).

NWS CR 68 The Posting of SHEF Data to the RFC Gateway Database. Geoffrey M. Bonnin, April 1983 (PB83 222554).

NWS CR 69 Some Basic Elements of Thunderstorm Forecasting. Richard P. McNulty, May 1983 (PB83 222604).

NWS CR 70 Automatic Distribution of AFOS Products Created at the NOAA Central Computer Facility via Hamlet (RJE) Punch Stream. Billy G. Olsen and Dale G. Lillie, November 1983 (PB84 122605).

NWS CR 71 An Investigation of Summertime Convection Over the Upper Current River Valley of Southeast Missouri. Bartlett C. Hagemeyer, July 1984 (PB84 222389).

NWS CR 72 The Standard SHEF Decoder Version 1.1. Geoffrey M. Bonnin, August 1984 (PB85 106508).

NWS CR 73 The Blizzard of February 4-5, 1984 Over the Eastern Dakotas and Western Minnesota. Michael Weiland, October 1984 (PB85 120087).

NWS CR 74 On the Observation and Modeling of the Slope Winds of the Upper Current River Valley of Southeast Missouri and Their Relationship to Air-Mass Thunderstorm Formation. Bartlett C. Hagemeyer, June 1985 (PB85 226926/AS).

NWS CR 75 Complete Guide to Canadian Products in AFOS. Craig Sanders, July 1985 (PB85 228153/AS).

NWS CR 76 The Reliability of the Bow Echo as an Important Severe Weather Signature. Ron W. Przybylinski and William J. Gery, September 1985 (PB86 102340).

NWS CR 77 Observation of Bow Echoes with the Marseilles Radar System. John E. Wright, Jr., September 1985 (PB86 102340).

NWS CR 78 Statistical Analysis of SHEF Coding Errors. Robert S. Cox, Jr., January 1986 (PB86 145141).

NWS CR 79 On the Midwestern Diurnal Convergence Zone on the West Side of the Warm Season Bermuda High. Bartlett C. Hagemeyer, March 1986 (PB86 171378).

NWS CR 80 Some Characteristics of Northeast Kansas Severe Weather 1963-1984. Larry W. Schultz, March 1986 (PB86 173952/AS).

NWS CR 81 The Severe Thunderstorm Outbreak of July 6, 1983 in Southeast Idaho, Western Wyoming and Southwest Montana. Gary L. Cox, April 1986 (PB86 184322/AS).

NWS CR 82 Some Proposals for Modifying the Probability of Precipitation Program of the National Weather Service. Wayne E. Sangster and Michael D. Manker, July 1986 (PB86 226636/AS).

NWS CR 83 Deformation Zones and Heavy Precipitation. Henry Steigerwaldt, August 1986 (PB86 229085/AS).

NWS CR 84 An Overview of the June 7, 1984 Iowa Tornado Outbreak. Charles H. Myers, August 1987.

NWS CR 85 Operational Detection of Hail by Radar Using Heights of VIP-5 Reflectivity Echoes. Richard B. Wagenmaker, September 1987.

NWS CR 86 Fire Weather Verification: The Forecaster Does Make a Difference. Therese Z. Pierce and Scott A. Mentzer, December 1987 (PB88 140744).

NWS CR 87 Operational Use of Water Vapor Imagery. Samuel K. Beckman, December 1987 (PB88 140751).

NWS CR 88 Central Region Applied Research Papers 88-1 Through 88-7. NWS Central Region, Scientific Services Division, May 1988 (PB88-210836).

NWS CR 89 Compendiums of Information for the Missouri Basin River Forecast Center and the North Central River Forecast Center. NWS Central Region, Scientific Services Division, June 1988 (PB88-226204).

NWS CR 90 Synoptic-Scale Regimes Most Conducive to Tornadoes in Eastern Wyoming - A Link Between the Northern Hemispheric Scale Circulation and Convective-Scale Dynamics. William T. Parker and Edward K. Berry, July 1988 (PB88-231337).

Continued on Back Cover.

NWS CR 91 Heavy Snowfall in Northwest Wyoming. Michael S. Weiland, September 1988 (PB89 109524).

NWS CR 92 On the Utility of a Geographic Information System in Modelling Climatic Suitability. Bartlett C. Hagemeyer, September 1988 (PB89 109516).

NWS CR 93 The Synoptic and Meso-Alpha Scale Meteorology of Wyoming Flash Floods. Joseph A. Rogash, October 1988 (PB89 117709)

NWS CR 94 The Removal of Stagnant Winter Air Masses From Wyomings Wind River Basin. Gary L. Cox and Jeffrey M. Graham, November 1988 (PB89 128664).

NWS CR 95 Floods Along Des Plaines and Fox Rivers: September-October 1986. Thomas L. Dietrich, February 1989 (PB89 152797/AS)

NWS CR 96 A Case Study Evaluation of Satellite-Derived Rainfall Estimates and Their Application to Numerical Model Precipitation Forecast Verification. Glenn A. Field, May 1989 (PB89 194591).

NWS CR 97 Central Region Applied Research Papers 97-1 through 97-6. NWS Central Region, Scientific Services Division, July 1989 (PB89 213375/AS).

NWS CR 98 The Record Rainfall of August 13-14, 1987 at Chicago, Illinois. Paul Merzlock, November 1989.

NWS CR 99 Central Region Applied Research Papers 99-1 through 99-7. NWS Central Region, Scientific Services Division, November 1989 (PB90 151325).

NWS CR 100 A Guide to Forecasters in Judging Weather Impact on Growth Environments and Farm Operations in the Midwest. John W. Kottke, December 1989 (PB90 141011).

NWS CR 101 Numerical Solutions to the Shallow Water Equations as Applied to a Local Meteorological Forecast Problem. Eric R. Thaler, March 1990 (PB90 191230).

NWS CR 102 Postprint Volume National Weather Service Aviation Workshop Kansas City, Missouri, December 10-13, 1991. NWS Central Region, Scientific Services Division, March 1992 (PB92-176148).

NWS CR 103 An Investigation of Two Microburst Producing Storms Using A Microburst Recognition Algorithm. David Eversole, January 1994 (PB94-156577).

NWS CR 104 Lincoln ASOS Temperature Test January 13-15, 1993, Gregory Grosshans and Phil Clark, March 1994 (PB94-159993).

NWS CR 105 Forecasting Snowfall Using Mixing Ratios on an Isentropic Surface "An Empirical Study", Crispin Garcia, Jr, May 1994 (PB94-188760).

NWS CR 106 The Use of Profiler Data for Analysis and Nowcasting of a Winter Season Extratropical Cyclone, Bradley S. Small, June 1994 (PB94-187804).

NWS CR 107 Flood Forecasting for the Lower Missouri River Basin: June - September, 1993, John F. Pescatore, September 1994 (PB95-123568).

NWS CR 108 Heterogeneous Nucleation and its Relationship to Precipitation Type, Gregory Smith, April 1995 (PB95-217170).

NWS CR 109 Synoptic, Mesoscale and Radar Aspects of the Northeast Kansas Supercell of September 21, 1993, Kenneth Labas and Brian Walawender, October 1995 (PB96-125075).

NWS CR-110 The Effect of Quantitative Precipitation Forecasts on River Forecasts, Noreen O. Schwein, January 1996 (PB96-)

NOAA SCIENTIFIC AND TECHNICAL PUBLICATIONS

The National Oceanic and Atmospheric Administration was established as part of the Department of Commerce on October 3, 1970. The mission responsibilities of NOAA are to assess the socioeconomic impact of natural and technological changes in the environment and to monitor and predict the state of tha solid Earth, the oceans and their living resources, the atmosphere, and the space environment of the Earth.

The major components of NOAA regularly produce various types of scientific and technical information in the following kinds of publications.:

PROFESSIONAL PAPERS--Important definitive research results, major techniques, and special investigations.

CONTRACT AND GRANT REPORTS--Reports prepared by contractors or grantees under NOAA sponsorship.

ATLAS--Presentation of analyzed data generally in the form of maps showing distribution of rainfall, chemical and physical conditions of oceans and atmosphere, distribution of fishes and marine mammals, ionospheric conditions,etc.

TECHNICAL SERVICE PUBLICATION--Reports containing data, observations, instructions, etc. A partial listing includes data serials; prediction and outlook periodicals; technical manuals, training papers, planning reports, and information serials; and miscellaneous technical publications.

TECHINCAL REPORTS--Journal quality with extensive details, mathematical developments, or data listings.

TECHNICAL MEMORANDUMS--Reports of preliminary, partial, or negative research or technology results, interim instructions, and the like.

Information on availability of NOAA publication can be obtained from:

NATIONAL TECHNICAL INFORMATIN SERVICE
U.S. DEPARTMENT OF COMMERCE
5285 PORT ROYAL ROAD
SPRINGFIELD, VA 22161